

THE ROLE OF TRANSCRIPTION FACTOR STOX1A
IN TRANSCRIPTIONAL NETWORKS ASSOCIATED
WITH NEURODEGENERATION

Daan van Abel

The studies described in this thesis were carried out at the Department of Clinical Chemistry, Pathology and Molecular Biology Laboratory (MBL), VU University Medical Center, Amsterdam, The Netherlands.

Printing of this thesis was kindly supported by:

Alzheimer Nederland (Bunnik)



Internationale Stichting Alzheimer Onderzoek



Clinical Chemistry Department VUMC, Amsterdam, The Netherlands

ISBN:

Layout: Daan van Abel; Cover Design: Bas van Abel

Printing: Ipskamp Drukkers

Copyright © 2012 Daan van Abel. All rights reserved

VRIJE UNIVERSITEIT

THE ROLE OF TRANSCRIPTION FACTOR STOX1A
IN TRANSCRIPTIONAL NETWORKS ASSOCIATED
WITH NEURODEGENERATION

ACADEMISCH PROEFSCHRIFT

ter verkrijging van de graad Doctor aan
de Vrije Universiteit Amsterdam,
op gezag van rector magnificus
prof.dr. L.M. Bouter,
in het openbaar te verdedigen
ten overstaan van de promotiecommissie
van de Faculteit der Geneeskunde
op woensdag 19 september 2012 om 15.45 uur
in de aula van de universiteit,
de Boelelaan 1105

door

Daan van Abel

geboren te Nijmegen

promotor: prof.dr. C.B.M. Oudejans

copromotor: dr. M. van Dijk

reading committee:

dr. N.Ameziane
prof.dr. M.A. Blankenstein
prof.dr. A.J Rozemuller
dr. W. Scheper
prof.dr. J.C van Swieten
dr. R.M.F. Wolthuis

Vaak hebben invalletjes van één regel weinig om het lijf

Van Kooten & De Bie

Contents

Chapter 1	General Introduction Aims and Outline	11 22
Chapter 2	Direct downregulation of CNTNAP2 by STOX1A is associated with Alzheimer's disease. <i>Journal of Alzheimer's Disease (Accepted), 2012</i>	33
Chapter 3	SFRS7-mediated splicing of tau exon 10 is directly regulated by STOX1A in glial cells. <i>PLoS ONE, 2011</i>	55
Chapter 4	Transcription factor STOX1A promotes mitotic entry by binding to the CCNB1 promoter. <i>PLoS ONE, 2012</i>	75
Chapter 5	STOX1A induces phosphorylation of tau proteins at epitopes hyperphosphorylated in Alzheimer's disease. <i>Submitted</i>	91
Chapter 6	RNA-seq transcriptome analysis of STOX1A induced differential expression in neuronal cells. <i>In Preparation</i>	105
Chapter 7	Summarizing Discussion Directions for Future Work	127 130
Appendices	Nederlandse Samenvatting List of Publications Curriculum Vitae Dankwoord	140 145 147 148



Chapter 1

General Introduction
Aims and Outline

Alzheimer's disease

Alzheimer's disease (AD) is the most common form of dementia with an estimated prevalence ranging from 4.4% in persons aged 65 years to 22% at ages 90 and older [1]. Age is the most important risk factor for AD but also other factors like genetic factors (see below) play an important role. AD is clinically characterized by insidious onset and progressive impairment of memory and other cognitive functions [2]. Classically, abundant neurofibrillary tangles (NFT) (Fig. 1), composed of the hyperphosphorylated microtubule-associated protein (MAP) tau and accumulation of extracellular senile plaques made out of β -amyloid deposition ($A\beta$) (Fig. 1), are known as the key neuropathological features of AD [3].

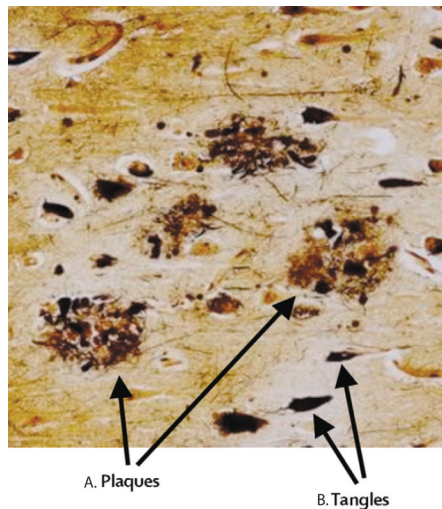


Figure 1. Image shows the two main pathological hallmarks in Alzheimer's disease. (A), Extracellular deposits of $A\beta$ plaques and (B) tangles, the intracellular aggregates composed of a hyperphosphorylated form of the microtubule-associated protein tau. Figure adapted from Blennow et al. [114].

Accumulation of extracellular senile plaques made out of $A\beta$ as a central event in AD is formulated as 'the amyloid hypothesis'. The basis of this theory originates from genetic studies where it has been found that mutations in the amyloid precursor protein (APP) and presenilin 1 and 2 (PS1, PS2) cause rare, early onset (before the age of 60 to 65) autosomal-dominant inherited familial AD (FAD) [4-7]. Mutations in all of these three genes can cause altered production of $A\beta$ via the amyloidogenic pathway (Fig. 2) [8] and therefore have provided insight into the underlying molecular mechanisms operating in AD. In the amyloidogenic pathway proteolytic processing of APP by β -site APP cleaving enzyme (BACE1) followed by γ -secretase (which includes PS1, PS2, Nicastrin, anterior pharynx-defective 1 (APH-1), and presenilin enhancer 2 (PEN2) [9] generates an APP intracellular domain (AICD) [10] and $A\beta$ peptides which accumulate into senile plaques as seen in AD [11] (Fig. 2). Multiple studies have shown that deposition of $A\beta$ is neurotoxic and/or neuroinflammatory and

is therefore believed to be one of the causes of synaptic dysfunction and subsequent neuronal cell death, thereby contributing to memory loss and other symptoms [12]. However, paradoxically, a neuroprotective role for $A\beta$ is also currently debated and compatible with a promising new theory: the “two hit hypothesis”, which will be discussed later.

While the fully penetrant mutations in *APP*, *PS1*, and *PS2* were identified as causal factors in FAD, late-onset Alzheimer's disease (LOAD, above the age of 65) shows less-obvious or no apparent familial aggregation. Therefore, susceptibility for LOAD is likely caused by an array of risk alleles and/or environmental factors, which may act through various pathways eventually leading to e.g. defects in the production, deposition, and removal of $A\beta$ (Fig 3). Understanding of how these risk alleles,

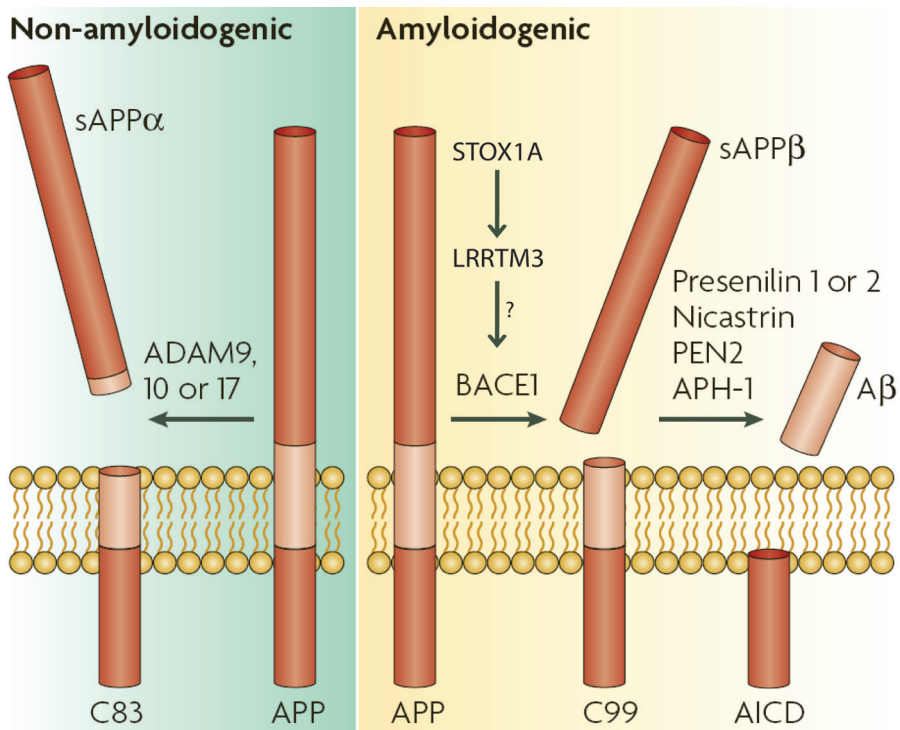


Figure 2. Amyloidogenic and the non-amyloidogenic pathway. In the non-amyloidogenic pathway, APP is cleaved within the $A\beta$ domain (light pink) by the γ -secretases ADAM9, 10 or 17. Two fragments are released, the larger ectodomain (sAPP α) and the smaller carboxy-terminal fragment (C83). APP molecules that are not cleaved by the non-amyloidogenic pathway become a substrate for γ -secretase (β -site APP cleaving enzyme 1; BACE1), releasing an ectodomain (sAPP β), and retaining the last 99 amino acids of APP (known as C99) within the membrane. The first amino acid of C99 is the first amino acid of $A\beta$. C99 is subsequently cleaved 38–43 amino acids from the amino terminus to release $A\beta$, by the γ -secretase complex, which is made up of presenilin 1 or 2, nicastrin, anterior pharynx defective and presenilin enhancer 2. LRRTM3 promotes APP processing via BACE1 through a mechanism currently unknown. STOX1A has been shown to operate upstream of LRRTM3. AICD, APP intracellular domain; APH-1, anterior pharynx defective; PEN2, presenilin enhancer 2; LRRTM3, Leucine-rich repeat transmembrane 3; STOX1A, Storkheadbox 1A. Figure adapted from Laferla et al. [115]

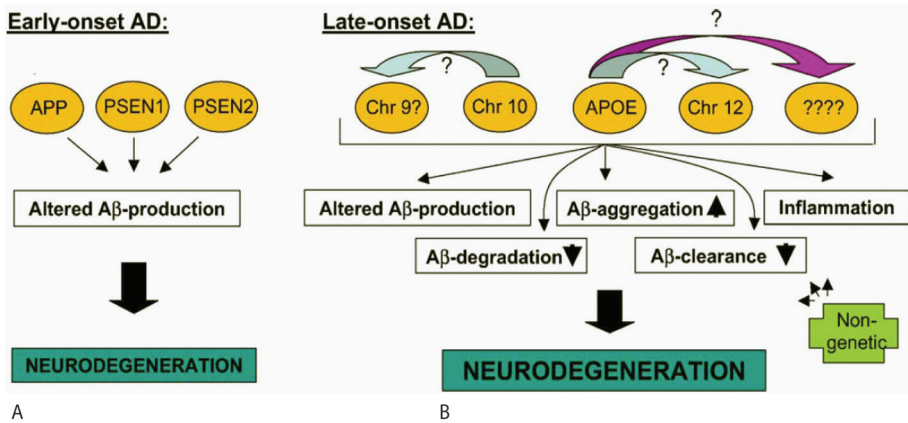


Figure 3. Scheme of contribution and interaction pattern of known and putative AD genes. (A) Known early onset risk AD genes where mutations lead to altered production of A β . (B) Simplified model showing an array of risk alleles and/or non-genetic environmental factors which may act through various pathways eventually leading to e.g. defects in the production, deposition and removal of A β . Figure adapted from Bertram et al. [102].

environmental factors and their underlying pathways operate in LOAD could also help explain the presence of the second key hallmark in LOAD, the NFT. Interestingly, as for A β , the “two hit hypothesis”, which will be discussed later, has also provided insight in a possible underlying mechanism, which explains NFT formation in LOAD.

In conclusion, research has been primarily focusing on the understanding of the genetic etiology of LOAD, such as Apolipoprotein E gene (*APOE*), and its pathological hallmarks; A β deposition and the NFT. In the next chapter is it discussed how hyperphosphorylated tau proteins, the main constituents of NFT, also play a central role in AD and other neurodegenerative diseases.

Tau protein and neurodegeneration

Senile plaques composed of A β are not the only pathological features found in early onset FAD and LOAD. A second key pathological feature in AD (but also in several other neurodegenerative diseases as shown below) are paired helical filaments (PHF) and straight filaments (SF) accumulated as intra-neuronal NFT (Fig. 1) and as neuropil threads or dystrophic neurites in dendrites and axons. Eventually these neurons die, leaving behind extracellular NFTs or so called “ghost tangles” [13, 14].

The number of NFT directly correlates with the presence and the degree of dementia in AD [15-17] and therefore NFT count is also used to diagnose the progression of AD. According to the Braak-staging system six histopathological stages can be discriminated [18]. The transentorhinal stages I-II: clinically silent cases; limbic stages III-IV: incipient Alzheimer's disease; neocortical stages V-VI: fully developed Alzheimer's disease [18].

The major component of NFT consists of the hyper-phosphorylated microtubule-associated protein (MAP) tau [19-22]. The main importance of normal tau protein in the binding and stabilization of microtubules was first described in the mid 1970s [23,

24] but new functions of tau in maintaining neuronal cell shape and axonal transport are emerging rapidly [25]. Tau is a phospho-protein and therefore its activity is regulated through phosphorylation. However, when hyper-phosphorylated as seen in NFT, tau has been shown to reduce its ability to promote microtubule assembly [26], a process, which has also been found to be impaired in brain extracts from AD cases [27]. Furthermore, studies in transgenic mouse models have shown that the abnormal hyper-phosphorylation of tau is an early change that precedes neuronal cell loss and the formation of NFT inclusions [28, 29]. Therefore, for the last decades there has been a tremendous increase of interest in the physiological and pathological role of tau and its hyper-phosphorylation in neurodegenerative diseases, in particular the activities of protein kinases and protein phosphatases, which regulate the phosphorylation status of tau protein.

NFT are not exclusively found in AD but also in other neurodegenerative disorders including Pick's disease, progressive supranuclear palsy (PSP), corticobasal degeneration, argyrophilic grain disease, and hereditary frontotemporal dementia and parkinsonism linked to chromosome 17 (FTDP-17), collectively referred as tauopathies [30]. In the latter group of disorders NFT are not exclusively neuronal, but are also found in glial cells such as oligodendrocytes and astrocytes [30-32].

The relevance of tau in neurodegeneration is emphasized by studies where multiple mutations in the tau gene identified from FTDP-17 patients have provided evidence that tau abnormalities alone are sufficient to cause neurodegeneration [33-35]. Subsequently, today more than 35 pathogenic mutations in the tau gene have been identified from FTDP-17 patients and related neurodegenerative diseases [36-40]. These mutations can be classified into two groups. The first group consists of mutations, which are associated with the direct impairment in the ability of tau to bind and promote the polymerization and stability of microtubules [41]. The second group of mutations have been shown to affect alternative splicing of tau exon 10 via splicing cis-elements, splicing enhancers, or via destabilization of the stem loop structure of tau pre-mRNA [42]. The loss in binding ability of tau to microtubules is shared in both groups and is believed to produce an increase in the levels of free tau proteins in the neuronal cytoplasm. Subsequently, the free tau proteins are hyper-phosphorylated at residues that make tau more fibrillogenic, which increases NFT formation and consequently leads to neurodegeneration [30, 43]. While the second group of mutations by itself are sufficient to trigger neurodegeneration in FTDP-17 patients, there is an increasing interest in understanding the underlying mechanisms that regulate alternative splicing of tau exon 10.

Tau exon 10 splicing

Molecular cloning has identified six tau isoforms in human brain tissue that are produced from the tau gene by alternative mRNA splicing [44]. They differ from each other by the presence of either three (3R-tau) or four (4R-tau) microtubule binding repeat sequences in the carboxy-terminal (C-terminal) part of the molecule and the absence or presence of one or two inserts (29 or 58 amino acids) in the amino-terminal (N-terminal) part [45]. Not surprisingly, it has been shown that 4R-tau has a

greater microtubule binding affinity than 3R-tau and therefore promotes microtubule assembly better [46, 47]. The presence of 3R-tau or 4R-tau depends on exclusion (3R-tau) or inclusion (4R-tau) of tau exon 10 and is developmentally (and cell type-specifically) regulated. In fetal brain >95% of tau mRNA consists of 3R-tau and in adult human brain, the ratio of 3R-tau to 4R-tau isoforms is about 1 [46, 48]. The shift from abundant 3R tau to an equal ratio between 3R and 4R tau isoforms is potentially associated with a switch from a more dynamic to a more stable microtubule network necessary for the development of the brain [49, 50]. Several tauopathies show de-regulation of 3R-tau and 4R-tau isoform expression altering the 3R/4R tau ratio. This includes corticobasal degeneration and progressive supranuclear palsy (PSP) which mainly show 4R-tau pathology [51], while in Pick's disease there is abundant 3R-tau pathology [52-54]. There is still a debate on whether tau isoform patterns are specific for LOAD. Currently, several studies have failed to show a direct correlation between the 4R/3R ratio and tau pathology in LOAD patients [55-57], yet another study demonstrated that in the temporal cortex of many LOAD brains, production of 4R-tau is significantly elevated [58]. Nevertheless, it is becoming clear that abnormal splicing of tau exon 10, is probably one of the mechanisms by which tau accumulates and aggregates into NFT in tauopathic brains.

Summarized, a combination of two major hallmarks (A β and NFT) characterizes LOAD pathology. In the last decade it became clear that these hallmarks are the result of other pathological changes, which occurred very early in the disease progression of LOAD [59]. Specifically, both oxidative stress [60, 61] and cell cycle markers [62] in LOAD neurons are found to precede A β and NFT pathology. Together these findings have led to a very promising new hypothesis which can be seen as a cause rather than a consequence for the typical hallmarks seen (A β and tau) LOAD pathology [60, 63, 64]. The next chapters will discuss this theory, which is based on abnormal neuronal cell cycle re-entry.

The cell cycle and Alzheimer's disease

The eukaryotic cell cycle can be distinguished into two main stages, the interphase and M (mitotic) stage. Additionally, when cells are in a non-dividing quiescent state, they reside in the G₀ phase of the cell cycle. The interphase consists of 3 major phases (the G₁, S, and G₂ phase) where the cells are prepared for cell division. The M phase sequentially progresses into the prophase, metaphase, anaphase, and telophase, immediately followed by cytokinesis which eventually results in two identical daughter cells [65]. The transition into each of the G₁, S and G₂/M phases is driven by the tightly regulated activation of cyclin dependant kinases (CDKs) upon phosphorylation at specific residues. The phosphorylation of CDKs induces conformational changes which enhances the binding towards their activating binding partners cyclins [65-67]. In general, during the G₁ phase, the start of the cell cycle is initiated by activation of CDK4/CDK6 bound to cyclin D by mitogenic signals, such as extracellular growth factors or intercellular contacts. Furthermore, the activated CDK4/CDK6/cyclinD complex also controls re-entry of resting (G₀) cells into the G₁ phase of the cell cycle [68]. G₁ to S phase progression is then controlled by CDK2 bound to S-phase cyclins

[69] (E- and A-type) and G2 to M phase is triggered by CDK1 associated with mitotic cyclins [70] (A- and B-type). Only in complex with these cyclins, the CDKs can form an active kinase.

Cyclins, in contrast to fairly stable protein expression levels of CDKs, are differentially expressed throughout the cell cycle and degraded at specific phases by ubiquitin-mediated cyclin proteolysis. Reversely, in G1 phase, CDK activity is negatively regulated by specific CDK inhibitors (CDKIs). These CDKIs consists of two groups, the INK4 family which includes p15 (INK4b), p16 (INK4a), p18 (INK4c), p19 (INK4d), and the Cip/Kip family which includes p21 (Waf1, Cip1), p27 (Cip2), and p57 (Kip2) [65, 66]. During S and G2 phase, CDK1, which is less sensitive to CDK inhibitors (CDKIs), is kept inactive by Wee1/Myt kinases [71-73].

When CDKs are active they are capable of phosphorylating target proteins on CDK consensus sites which in turn may regulate expression of cell cycle associated genes such as cyclins [65, 66]. Three CDKs target proteins have been shown to be forkhead transcription factors, FOXM1 [74], FOXO1 [75], and FOXK2 [76], all shown to be regulated by CDK1 [74-76].

Cell division in most of our body cells is driven by the repeated cycling of G1, S, G2, and the M phase, this in contrast to most neurons in the adult brain, which in general are thought to reside in the quiescent state of the cell cycle (G0). However, during early development of the central nervous system (CNS) there is a well-regulated pattern of regular cell division. The process begins with a few hundred of ectodermal cells, which rapidly develop into as many as hundred billion of neurons in the adult CNS. This process of neurogenesis has been shown to take place in a tightly packed layer of nuclei lining the lumen of the neural tube (the ventricular zone, VZ) and later in the closely opposed region known as the subventricular zone (SVZ) [77]. When the neurons emigrate from the VZ and SVZ they lose their capacity to divide and become mature differentiated non-dividing cells (G0) not capable of re-entering the cell cycle [77]. However, as increasing evidence indicates, neurons in AD patients appear to have emerged from this post-mitotic state showing an activated cell cycle phenotype rather than a silent one [64].

Interestingly, while markers of each stage of the cell cycle (G1, S, G2, and M –phase) are found in AD neurons, there is no actual evidence which has shown the completion of a successful mitosis [64]. Furthermore, in contrast to the highly organized nature of a regular cell cycle, a highly un-organized nature of the cell cycle is observed in affected neurons in AD [64]. A prominent example is that the expression of most of these cell cycle markers are found in the cytoplasm rather than in the nucleus where they act [78]. In conclusion, it seems that post-mitotic neuronal cells in AD can re-enter the cell cycle, however, being an abortive and de-regulated cell cycle [64].

Recently, a hypothesis has been developed explaining why neuronal cell cycle re-entry in LOAD avoids apoptosis to gain an “immortality” analogous to tumor cells [60, 63]. Normally, a mitotic stimulus in post-mitotic neurons leads to cell cycle re-entry resulting in apoptosis and cell death before mitosis can even occur. In contrast, the hypothesis explains why a neuronal cell cycle re-entry in LOAD initially avoids apoptosis to gain an “immortality” analogous to tumor cells [60, 63]. This steady state of “immortal” LOAD neurons mirrors the pathological hallmarks seen in AD (A β

and NFT).

The above hypothesis, the “two hit hypothesis”, was proposed [60] by its similarities with the “two hit hypothesis” in cancer [79] and helps explain why a healthy neuron becomes a LOAD neuron. The reason for the differences in pathological outcomes between cancer and LOAD has been suggested to lie in their alternative usage of the MAPK pathway [80].

The “two hit hypothesis” in LOAD

In the “two hit hypothesis” it is suggested that a combination of both oxidative stress and cell cycle aberration is necessary for a normal neuron to become a LOAD neuron [60, 63, 64]. The sequence of events can begin with either one, leading to the other. This results in an “immortal” neuronal cell that can survive for decades. This “immortality” of a LOAD neuron compared to a normal neuron can be explained by the findings that excessive oxidative stress inhibits downstream propagation of caspase-mediated apoptotic signals [81]. Also, evidence for deregulated apoptotic signalling in LOAD has been found by Raina et al. [82, 83]. Together, this suggests that a combination of the two hits might produce a neuron, which has activated its cell cycle machinery but fails to progress through the cell cycle or divide. While such cell may normally die, the avoidance of apoptosis would initially prevent cell death and causes the neuron to remain in a “steady state” of partial cell cycle progression. This “steady state” of partial cell cycle progression in which neurons can remain for decades, could result in the excessive phosphorylation of tau proteins by e.g. activated mitotic kinases and therefore initiate the formation of NFT. Accordingly, overexpression of the myc oncogene, which forces post-mitotic neurons to re-enter the cell cycle, results in tau changes similar to those seen in LOAD neurons [84, 85].

The “two hit hypothesis” also gives a new meaning to the role for A β in LOAD pathology. While it is generally believed that A β aggregation and deposition is toxic and therefore causes neuronal cell death, there is currently a debate on whether this is actually true. This debate has arisen from the finding that A β has anti-oxidative properties [86, 87]. Because of this feature it has been suggested that A β actually has a protective effect shielding neurons from oxidative damage [88, 89]. In the view of the “two hit hypothesis” this would mean that in response to the accumulation of oxidative damage in LOAD neurons, production of A β could be induced to neutralize future free radicals and therefore actually tries to protect the neuron from oxidative damage. Taking into account that A β itself has been found to be mitogenic [90], the production of A β in response to excessive oxidative damage could initiate neuronal cell cycle re-entry. Furthermore, A β itself and/or the excessive amounts of oxidative damage can also cause deregulated expression of transcription factors. An example for this is the transcription factor SP1 which was found to be regulated by oxidative stress [91]. Upregulation of SP1 can regulate the expression of several AD-related proteins, including APP [92].

The induction of cell cycle proteins itself can in turn also control expression of transcription factors. E.g. aberrant expression of the mitotic kinase CDK1 and its binding partner cyclin B1 have been found in degenerating neurons of AD [78].

Active CDK1 has been shown to regulate transcription factor activity [74-76]. CDK1 dependent activation of brain specific transcription factors could initiate transcriptional programs, which drive the cell cycle machinery itself and therefore could result in a positive feedback loop. Large amounts of cell cycle dependent kinases could then phosphorylate tau resulting in NFT formation.

Together, eventually, after several of the above events, the accumulation of excessive A β deposition and hyperphosphorylation of tau (as a result of accumulated active mitotic kinases) does become toxic to the cells and finally leads to successful apoptosis and neuronal death.

In conclusion, the “two hit hypothesis” explains why a combination of oxidative stress and neuronal cell cycle abnormalities can result in the typical pathological hallmarks seen in LOAD. Because these events seem to appear very early in the disease progression of LOAD [59] and precede formation of A β and NFT’s, insight into exact mechanisms that induce and mediate these cell cycle events might eventually enable the prevention or even reversal of the disease.

***STOX1*, a transcription factor related to the family of forkhead transcription factors**

Shown above, one of the factors that may contribute to the production of A β is the abnormal regulation of gene transcription. This may be the result of oxidative damage, which induces the expression of transcription factors, as shown for SP1. The cell cycle machinery itself is also capable of regulating the activity of transcription factors, and when activated can drive expression of cell cycle regulatory proteins itself [74-76]. Abnormal activation of transcription factors may therefore potentially cause transcription of genes that are directly or indirectly involved in the production of A β and formation of NFT. This feature makes them interesting targets for therapeutic intervention.

Recently, transcription factor *STOX1* has been found to be associated with LOAD. Paradoxically, *STOX1* was initially discovered as a gene associated with Pre-eclampsia which is a pregnancy-associated disease occurring in 5–8% of pregnancies which threatens the lives of both mother and fetus [93]. Genome wide linkage studies have shown that linkage for pre-eclampsia in Dutch females resides in a region on

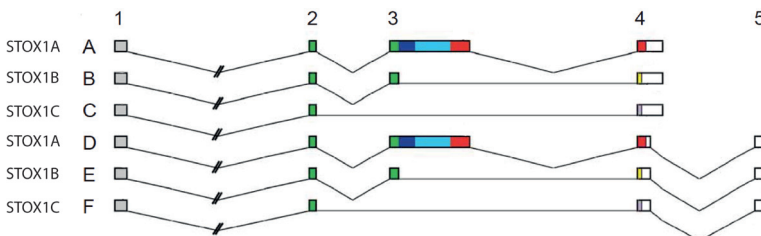


Figure 4. Transcriptional organization of *STOX1*. By differential donor splice site use, exon 3 skipping and alternative use of exon 5, six different transcripts are generated (A–F) that encode three different proteins; *STOX1A*, *STOX1B* and *STOX1C*. Identical colors in exons indicate identical protein sequences. Exon 1 contains the bihelical NLS (gray). Exon 2 and first part of exon 3 contain the DNA-binding winged helix domain (green). The blue box in exon 3 contains the nuclear export sequence. Figure adapted from van Dijk et al. [95].

chromosome 10q22 [94, 95]. In-depth analysis of this region resulted in the discovery of *STOX1*, the Dutch pre-eclampsia susceptibility gene [95].

The *STOX1* gene contains a winged helix domain structurally and functionally similar to that of the forkhead family of transcription factors and expresses 3 isoforms; *STOX1A*, *STOX1B*, and *STOX1C*. *STOX1A* (the full length isoform) and *STOX1B* express the complete winged helix domain while *STOX1C* expresses only part of it (Fig. 4). Furthermore, only *STOX1A* contains both a nuclear localization (NLS) and a nuclear export signal (NES, Fig. 4). In the forkhead family of transcription factors, these dual control sequences, among other factors, regulate nuclear-cytoplasmic shuttling [96]. Therefore the main focus of research lies with *STOX1A* as this isoform contains all the regulatory domains for its functioning. For several transcription factors of the forkhead family nucleo-cytoplasmic shuttling is regulated by Akt (also known as Protein Kinase B, PKB) phosphorylation, in turn influencing their activity [97-100]. A recent study elucidates the functional similarities of *STOX1A* with members of the forkhead transcription factor family [101]. In this study it was shown that *STOX1A*, when phosphorylated by Akt, is inhibited from entering the nucleus and is subsequently degraded by ubiquitin-mediated proteolysis [101]. Besides the inactivation of *STOX1A* through degradation, exclusion from the nucleus prevents the ability of *STOX1A* to bind to DNA and therefore loses its transcriptional activity. In contrast, when *STOX1A* is located in the nucleus it can perform its transcriptional activity through specific binding to target genes, which in turn can be expressed or suppressed. In conclusion, *STOX1A*, identified as a susceptibility gene for pre-eclampsia, shows several similarities with members of the family of forkhead transcription factors. Interestingly, one of its target genes *LRRTM3* is involved in LOAD pathology.

STOX1A and Alzheimer's disease

It becomes clear that LOAD is a multi-factorial and heterogeneous disease which involves many potential risk genes. With the exception of APOE as a confirmed risk gene for LOAD, there are several hundreds of other potential risk genes described [102]. These genes reside on several different chromosomal loci with potential linkage for LOAD as discovered by genomic screening. These include loci on chromosomes 9 [103], 10 [103-106], and 12 [103, 107] (Fig. 3B). The leucine-rich repeat transmembrane 3 (*LRRTM3*) gene mapping to the locus on chromosome 10 (10q22) has previously been shown to be linked to LOAD [104, 105, 108]. A detailed study of this gene showed that *LRRTM3* promotes APP processing via BACE1 and therefore increases the production of A β via the amyloidogenic pathway [108] (Fig 2). In a recent study it was found that *STOX1A* is expressed abundantly in the brain and the expression level correlates with the severity of LOAD [109]. Interestingly, it was also shown that *LRRTM3* is selectively transactivated by *STOX1A*. This resulted in increased APP processing via BACE1, thereby enhancing the production of the A β peptide. Together, it was shown for the first time that *STOX1A* is functionally involved in LOAD by acting upstream in the amyloidogenic pathway consequently

effecting the production of A β [109].

However, A β depositions in the brain without a second key pathological hallmark (the NFT as mentioned above) are not sufficient to produce LOAD clinically. In fact, several normal aged individuals have been shown to have similar amounts of A β plaques in the brain as typical cases of AD [15, 16, 110-112]. This elucidates the importance of the simultaneous deregulation and interplay between different pathways, their associated risk genes and their outcomes, which results in the typical LOAD pathology (A β deposition and NFT).

Aims and outline

Previous studies have established a direct link between STOX1A, LRRTM3 and the amyloidogenic pathway, which plays a central role in LOAD pathology [3], [109]. However LRRTM3 alone cannot account for all the aspects associated with LOAD. It becomes clear that LOAD is a multi-factorial and heterogeneous disease, which involves many potential risk genes. These genes may act through a variety of transcriptional networks, which results in its classical pathological outcomes (NFT and A β). Most likely these changes are preceded by a combination of oxidative stress, which increases with age, and cell cycle aberration as explained by the “two hit hypothesis”.

While transcription factors like STOX1A regulate several hundreds of target genes and STOX1A is expressed abundantly in the brain and is associated with LOAD, the main objective of this thesis is the search and exploration of target genes that STOX1A directly or indirectly regulates. Discovery of such genes, pathways, and their associated biological functions could further unravel how STOX1A operates in transcriptional networks in the normal brain as well as in neurodegenerative diseases like LOAD.

In the future, better knowledge of these transcriptional networks could elucidate the molecular mechanisms involved in LOAD, and may help design disease-modifying drugs.

In an initial study to search for direct STOX1A target genes we used chromatin immunoprecipitation shotgun cloning (ChIP-shotgun cloning) in a neuronal cell model overexpressing STOX1A. With the use of this procedure it is described in **Chapter 2** how this resulted in the discovery of contactin-associated protein-like 2 (*CNTNAP2*) as a direct gene target of STOX1A. Additionally, we used a relatively new technique called ChIP-sequencing (ChIP-Seq) to discover direct STOX1A target genes on a genome-wide scale. This technique, which involves Massively Parallel Sequencing (MPS), led to the discovery of several other potential directly regulated STOX1A target genes. One of the validated target genes was found to be transactivated by STOX1A in a cell type specific manner. This gene, serine/arginine-rich splicing factor 7 (*SFRS7*), has previously been shown to modulate splicing of tau at exon 10. The in-depth functional and pathological consequences for STOX1A as an upstream target gene for *SFRS7* are discussed in **Chapter 3**.

While previous results already suggested a potential link between STOX1A and regulation of the cell cycle [109] and STOX1A is structurally and functionally similar to the family of forkhead transcription factors, of which several have been described to function in the cell cycle, we investigated a potential role for STOX1A in cell cycle regulation. The involvement of STOX1A in cell cycle events is explored in **Chapter 4**. NFT, the second key hallmark of LOAD consists of hyper-phosphorylated tau protein. Interestingly, a near identical tau phosphorylation pattern, as found in NFT of LOAD, is suggested to be driven by kinases associated with the cell cycle machinery [62]. More specifically, Okadaic acid induced overexpression of cyclin B1 (CCNB1) has been shown to induce tau phosphorylation *in vivo* [113]. Therefore, with the

knowledge that STOX1A directly regulates CCNB1 expression during the cell cycle (**Chapter 4**), we speculated that STOX1A might, at least through activation of cell cycle related kinases, induce phosphorylation of tau proteins. A correlation between STOX1A expression and tau phosphorylation was tested and described in **Chapter 5**. Together, these results have provided evidence for several direct (*SFRS7*, *CNTNAP2*, Integrin alpha-9 (*ITGA9*), *CCNB1*) and (in)direct (cyclin A1 (*CCNA1*), cyclin C1 (*CCNC1*), cyclin E (*CCNE*), *MAPT*) downstream STOX1A target genes. The study of these STOX1A target genes has resulted in better understanding of its potential biological function. To expand this knowledge and to see how STOX1A operates on a genome wide level we also performed a transcriptome analysis with the use of MPS. In this study, genome-wide differential RNA expression effectuated by STOX1A overexpression in neuronal cells was investigated. The applied technique (RNA-seq) and its outcomes are described in **Chapter 6**.

References

- 1 Lobo A, Launer LJ, Fratiglioni L, Andersen K, Di Carlo A, Breteler MM, Copeland JR, Dartigues JF, Jagger C, Martinez-Lage J et al: Prevalence of dementia and major subtypes in Europe: A collaborative study of population-based cohorts. *Neurologic Diseases in the Elderly Research Group. Neurology* 2000, 54(11 Suppl 5):S4-9.
- 2 McKhann G, Drachman D, Folstein M, Katzman R, Price D, Stadlan EM: Clinical diagnosis of Alzheimer's disease: report of the NINCDS-ADRDA Work Group under the auspices of Department of Health and Human Services Task Force on Alzheimer's Disease. *Neurology* 1984, 34(7):939-944.
- 3 Castellani RJ, Rolston RK, Smith MA: Alzheimer disease. *Dis Mon* 2010, 56(9):484-546.
- 4 Citron M, Oltersdorf T, Haass C, McConlogue L, Hung AY, Seubert P, Vigo-Pelfrey C, Lieberburg I, Selkoe DJ: Mutation of the beta-amyloid precursor protein in familial Alzheimer's disease increases beta-protein production. *Nature* 1992, 360(6405):672-674.
- 5 Cai XD, Golde TE, Younkin SG: Release of excess amyloid beta protein from a mutant amyloid beta protein precursor. *Science (New York, NY)* 1993, 259(5094):514-516.
- 6 Scheuner D, Eckman C, Jensen M, Song X, Citron M, Suzuki N, Bird TD, Hardy J, Hutton M, Kukull W et al: Secreted amyloid beta-protein similar to that in the senile plaques of Alzheimer's disease is increased in vivo by the presenilin 1 and 2 and APP mutations linked to familial Alzheimer's disease. *Nature medicine* 1996, 2(8):864-870.
- 7 Duff K, Eckman C, Zehr C, Yu X, Prada CM, Perez-tur J, Hutton M, Buee L, Harigaya Y, Yager D et al: Increased amyloid-beta42(43) in brains of mice expressing mutant presenilin 1. *Nature* 1996, 383(6602):710-713.
- 8 Tanzi RE, Bertram L: Twenty years of the Alzheimer's disease amyloid hypothesis: a genetic perspective. *Cell* 2005, 120(4):545-555.
- 9 Kaether C, Haass C, Steiner H: Assembly, trafficking and function of gamma-secretase. *Neuro-degenerative diseases* 2006, 3(4-5):275-283.
- 10 Passer B, Pellegrini L, Russo C, Siegel RM, Lenardo MJ, Schettini G, Bachmann M, Tabaton M, D'Adamio L: Generation of an apoptotic intracellular peptide by gamma-secretase cleavage of Alzheimer's amyloid beta protein precursor. *J Alzheimers Dis* 2000, 2(3-4):289-301.
- 11 Haass C, Steiner H: Alzheimer disease gamma-secretase: a complex story of GxGD-type presenilin proteases. *Trends in cell biology* 2002, 12(12):556-562.
- 12 Selkoe DJ: Alzheimer's disease is a synaptic failure. *Science (New York, NY)* 2002, 298(5594):789-791.
- 13 Bondareff W, Harrington C, Wischik CM, Hauser DL, Roth M: Immunohistochemical staging of neurofibrillary degeneration in Alzheimer's disease. *Journal of neuropathology and experimental neurology* 1994, 53(2):158-164.
- 14 Braak E, Braak H, Mandelkow EM: A sequence of cytoskeleton changes related to the formation of neurofibrillary tangles and neuropil threads. *Acta neuropathologica* 1994, 87(6):554-567.
- 15 Alafuzoff I, Iqbal K, Friden H, Adolfsson R, Winblad B: Histopathological criteria for progressive dementia disorders: clinical-pathological correlation and classification by multivariate data analysis. *Acta neuropathologica* 1987, 74(3):209-225.
- 16 Arriagada PV, Growdon JH, Hedley-Whyte ET, Hyman BT: Neurofibrillary tangles but not senile plaques parallel duration and severity of Alzheimer's disease. *Neurology* 1992, 42(3 Pt 1):631-639.

- 17 Tomlinson BE, Blessed G, Roth M: Observations on the brains of demented old people. *Journal of the neurological sciences* 1970, 11(3):205-242.
- 18 Braak H, Braak E: Neuropathological staging of Alzheimer-related changes. *Acta neuropathologica* 1991, 82(4):239-259.
- 19 Grundke-Iqbal I, Iqbal K, Quinlan M, Tung YC, Zaidi MS, Wisniewski HM: Microtubule-associated protein tau. A component of Alzheimer paired helical filaments. *The Journal of biological chemistry* 1986, 261(13):6084-6089.
- 20 Grundke-Iqbal I, Iqbal K, Tung YC, Quinlan M, Wisniewski HM, Binder LI: Abnormal phosphorylation of the microtubule-associated protein tau (tau) in Alzheimer cytoskeletal pathology. *Proceedings of the National Academy of Sciences of the United States of America* 1986, 83(13):4913-4917.
- 21 Kosik KS, Joachim CL, Selkoe DJ: Microtubule-associated protein tau (tau) is a major antigenic component of paired helical filaments in Alzheimer disease. *Proceedings of the National Academy of Sciences of the United States of America* 1986, 83(11):4044-4048.
- 22 Wood JG, Mirra SS, Pollock NJ, Binder LI: Neurofibrillary tangles of Alzheimer disease share antigenic determinants with the axonal microtubule-associated protein tau (tau). *Proceedings of the National Academy of Sciences of the United States of America* 1986, 83(11):4040-4043.
- 23 Weingarten MD, Lockwood AH, Hwo SY, Kirschner MW: A protein factor essential for microtubule assembly. *Proceedings of the National Academy of Sciences of the United States of America* 1975, 72(5):1858-1862.
- 24 Cleveland DW, Hwo SY, Kirschner MW: Physical and chemical properties of purified tau factor and the role of tau in microtubule assembly. *Journal of molecular biology* 1977, 116(2):227-247.
- 25 Morris M, Maeda S, Vossel K, Mucke L: The many faces of tau. *Neuron* 2011, 70(3):410-426.
- 26 Yoshida H, Ihara Y: Tau in paired helical filaments is functionally distinct from fetal tau: assembly incompetence of paired helical filament-tau. *Journal of neurochemistry* 1993, 61(3):1183-1186.
- 27 Iqbal K, Grundke-Iqbal I, Zaidi T, Merz PA, Wen GY, Shaikh SS, Wisniewski HM, Alafuzoff I, Winblad B: Defective brain microtubule assembly in Alzheimer's disease. *Lancet* 1986, 2(8504):421-426.
- 28 Lewis J, McGowan E, Rockwood J, Melrose H, Nacharaju P, Van Slegtenhorst M, Gwinn-Hardy K, Paul Murphy M, Baker M, Yu X et al: Neurofibrillary tangles, amyotrophy and progressive motor disturbance in mice expressing mutant (P301L) tau protein. *Nature genetics* 2000, 25(4):402-405.
- 29 Allen B, Ingram E, Takao M, Smith MJ, Jakes R, Virdee K, Yoshida H, Holzer M, Craxton M, Emson PC et al: Abundant tau filaments and nonapoptotic neurodegeneration in transgenic mice expressing human P301S tau protein. *J Neurosci* 2002, 22(21):9340-9351.
- 30 Lee VM, Goedert M, Trojanowski JQ: Neurodegenerative tauopathies. *Annual review of neuroscience* 2001, 24:1121-1159.
- 31 Higuchi M, Zhang B, Forman MS, Yoshiyama Y, Trojanowski JQ, Lee VM: Axonal degeneration induced by targeted expression of mutant human tau in oligodendrocytes of transgenic mice that model glial tauopathies. *J Neurosci* 2005, 25(41):9434-9443.
- 32 Forman MS, Lal D, Zhang B, Dabir DV, Swanson E, Lee VM, Trojanowski JQ: Transgenic mouse model of tau pathology in astrocytes leading to nervous system

- 1
- degeneration. *J Neurosci* 2005, 25(14):3539-3550.
- 33 Hutton M, Lendon CL, Rizzu P, Baker M, Froelich S, Houlden H, Pickering-Brown S, Chakraverty S, Isaacs A, Grover A et al: Association of missense and 5'-splice-site mutations in tau with the inherited dementia FTDP-17. *Nature* 1998, 393(6686):702-705.
- 34 Poorkaj P, Bird TD, Wijsman E, Nemens E, Garruto RM, Anderson L, Andreadis A, Wiederholt WC, Raskind M, Schellenberg GD: Tau is a candidate gene for chromosome 17 frontotemporal dementia. *Annals of neurology* 1998, 43(6):815-825.
- 35 Spillantini MG, Murrell JR, Goedert M, Farlow MR, Klug A, Ghetti B: Mutation in the tau gene in familial multiple system tauopathy with presenile dementia. *Proceedings of the National Academy of Sciences of the United States of America* 1998, 95(13):7737-7741.
- 36 Wilhelmsen KC, Lynch T, Pavlou E, Higgins M, Nygaard TG: Localization of disinhibition-dementia-parkinsonism-amyotrophy complex to 17q21-22. *American journal of human genetics* 1994, 55(6):1159-1165.
- 37 Wijker M, Wszolek ZK, Wolters EC, Rooimans MA, Pals G, Pfeiffer RF, Lynch T, Rodnitzky RL, Wilhelmsen KC, Arwert F: Localization of the gene for rapidly progressive autosomal dominant parkinsonism and dementia with pallido-ponto-nigral degeneration to chromosome 17q21. *Human molecular genetics* 1996, 5(1):151-154.
- 38 Foster NL, Wilhelmsen K, Sima AA, Jones MZ, D'Amato CJ, Gilman S: Frontotemporal dementia and parkinsonism linked to chromosome 17: a consensus conference. Conference Participants. *Annals of neurology* 1997, 41(6):706-715.
- 39 Lendon CL, Lynch T, Norton J, McKeel DW, Jr., Busfield F, Craddock N, Chakraverty S, Gopalakrishnan G, Shears SD, Grimmett W et al: Hereditary dysphasic disinhibition dementia: a frontotemporal dementia linked to 17q21-22. *Neurology* 1998, 50(6):1546-1555.
- 40 Bird TD, Wijsman EM, Nochlin D, Leehey M, Sumi SM, Payami H, Poorkaj P, Nemens E, Raskind M, Schellenberg GD: Chromosome 17 and hereditary dementia: linkage studies in three non-Alzheimer families and kindreds with late-onset FAD. *Neurology* 1997, 48(4):949-954.
- 41 Delobel P, Flament S, Hamdane M, Jakes R, Rousseau A, Delacourte A, Vilain JP, Goedert M, Buee L: Functional characterization of FTDP-17 tau gene mutations through their effects on *Xenopus* oocyte maturation. *The Journal of biological chemistry* 2002, 277(11):9199-9205.
- 42 Zhou J, Yu Q, Zou T: Alternative splicing of exon 10 in the tau gene as a target for treatment of tauopathies. *BMC neuroscience* 2008, 9 Suppl 2:S10.
- 43 Buee L, Bussiere T, Buee-Scherer V, Delacourte A, Hof PR: Tau protein isoforms, phosphorylation and role in neurodegenerative disorders. *Brain research* 2000, 33(1):95-130.
- 44 Goedert M, Spillantini MG, Crowther RA: Tau proteins and neurofibrillary degeneration. *Brain pathology (Zurich, Switzerland)* 1991, 1(4):279-286.
- 45 Goedert M, Spillantini MG, Jakes R, Rutherford D, Crowther RA: Multiple isoforms of human microtubule-associated protein tau: sequences and localization in neurofibrillary tangles of Alzheimer's disease. *Neuron* 1989, 3(4):519-526.
- 46 Goedert M, Jakes R: Expression of separate isoforms of human tau protein: correlation with the tau pattern in brain and effects on tubulin polymerization. *The EMBO journal* 1990, 9(13):4225-4230.
- 47 Butner KA, Kirschner MW: Tau protein binds to microtubules through a flexible array of distributed weak sites. *The Journal of cell biology* 1991, 115(3):717-730.

-
- 48 Gao QS, Memmott J, Lafyatis R, Stamm S, Sreaton G, Andreadis A: Complex regulation of tau exon 10, whose missplicing causes frontotemporal dementia. *Journal of neurochemistry* 2000, 74(2):490-500.
- 49 Goode BL, Feinstein SC: Identification of a novel microtubule binding and assembly domain in the developmentally regulated inter-repeat region of tau. *The Journal of cell biology* 1994, 124(5):769-782.
- 50 Bullmann T, de Silva R, Holzer M, Mori H, Arendt T: Expression of embryonic tau protein isoforms persist during adult neurogenesis in the hippocampus. *Hippocampus* 2007, 17(2):98-102.
- 51 Sergeant N, Wattez A, Delacourte A: Neurofibrillary degeneration in progressive supranuclear palsy and corticobasal degeneration: tau pathologies with exclusively "exon 10" isoforms. *Journal of neurochemistry* 1999, 72(3):1243-1249.
- 52 Delacourte A, Robitaille Y, Sergeant N, Buee L, Hof PR, Wattez A, Laroche-Cholette A, Mathieu J, Chagnon P, Gauvreau D: Specific pathological Tau protein variants characterize Pick's disease. *Journal of neuropathology and experimental neurology* 1996, 55(2):159-168.
- 53 Sergeant N, David JP, Lefranc D, Vermersch P, Wattez A, Delacourte A: Different distribution of phosphorylated tau protein isoforms in Alzheimer's and Pick's diseases. *FEBS letters* 1997, 412(3):578-582.
- 54 Chambers CB, Lee JM, Troncoso JC, Reich S, Muma NA: Overexpression of four-repeat tau mRNA isoforms in progressive supranuclear palsy but not in Alzheimer's disease. *Annals of neurology* 1999, 46(3):325-332.
- 55 Connell JW, Rodriguez-Martin T, Gibb GM, Kahn NM, Grierson AJ, Hanger DP, Revesz T, Lantos PL, Anderton BH, Gallo JM: Quantitative analysis of tau isoform transcripts in sporadic tauopathies. *Brain Res Mol Brain Res* 2005, 137(1-2):104-109.
- 56 Boutajangout A, Boom A, Leroy K, Brion JP: Expression of tau mRNA and soluble tau isoforms in affected and non-affected brain areas in Alzheimer's disease. *FEBS letters* 2004, 576(1-2):183-189.
- 57 Ingelsson M, Ramasamy K, Cantuti-Castelvetri I, Skoglund L, Matsui T, Orne J, Kowa H, Raju S, Vanderburg CR, Augustinack JC et al: No alteration in tau exon 10 alternative splicing in tangle-bearing neurons of the Alzheimer's disease brain. *Acta neuropathologica* 2006, 112(4):439-449.
- 58 Glatz DC, Rujescu D, Tang Y, Berendt FJ, Hartmann AM, Faltraco F, Rosenberg C, Hulette C, Jellinger K, Hampel H et al: The alternative splicing of tau exon 10 and its regulatory proteins CLK2 and TRA2-BETA1 changes in sporadic Alzheimer's disease. *Journal of neurochemistry* 2006, 96(3):635-644.
- 59 Yang Y, Varvel NH, Lamb BT, Herrup K: Ectopic cell cycle events link human Alzheimer's disease and amyloid precursor protein transgenic mouse models. *J Neurosci* 2006, 26(3):775-784.
- 60 Zhu X, Lee HG, Perry G, Smith MA: Alzheimer disease, the two-hit hypothesis: an update. *Biochimica et biophysica acta* 2007, 1772(4):494-502.
- 61 Nunomura A, Perry G, Pappolla MA, Friedland RP, Hirai K, Chiba S, Smith MA: Neuronal oxidative stress precedes amyloid-beta deposition in Down syndrome. *Journal of neuropathology and experimental neurology* 2000, 59(11):1011-1017.
- 62 Vincent I, Zheng JH, Dickson DW, Kress Y, Davies P: Mitotic phosphoepitopes precede paired helical filaments in Alzheimer's disease. *Neurobiology of aging* 1998, 19(4):287-296.
- 63 Zhu X, Raina AK, Perry G, Smith MA: Alzheimer's disease: the two-hit hypothesis. *Lancet neurology* 2004, 3(4):219-226.
-

- 64 Bonda DJ, Lee HP, Kudo W, Zhu X, Smith MA, Lee HG: Pathological implications of cell cycle re-entry in Alzheimer disease. *Expert reviews in molecular medicine* 2010, 12:e19.
- 65 Vermeulen K, Van Bockstaele DR, Berneman ZN: The cell cycle: a review of regulation, deregulation and therapeutic targets in cancer. *Cell proliferation* 2003, 36(3):131-149.
- 66 Hochegger H, Takeda S, Hunt T: Cyclin-dependent kinases and cell-cycle transitions: does one fit all? *Nature reviews* 2008, 9(11):910-916.
- 67 Jeffrey PD, Russo AA, Polyak K, Gibbs E, Hurwitz J, Massague J, Pavletich NP: Mechanism of CDK activation revealed by the structure of a cyclinA-CDK2 complex. *Nature* 1995, 376(6538):313-320.
- 68 Sherr CJ: G1 phase progression: cycling on cue. *Cell* 1994, 79(4):551-555.
- 69 Woo RA, Poon RY: Cyclin-dependent kinases and S phase control in mammalian cells. *Cell cycle (Georgetown, Tex)* 2003, 2(4):316-324.
- 70 Porter LA, Donoghue DJ: Cyclin B1 and CDK1: nuclear localization and upstream regulators. *Progress in cell cycle research* 2003, 5:335-347.
- 71 L L Parker, P J Sylvestre, M J Byrnes, 3rd, F Liu, H Piwnica-Worms. Identification of a 95-kDa WEE1-like tyrosine kinase in HeLa cells. *Proc Natl Acad Sci U S A*. 1995 October 10; 92(21): 9638-9642.
- 72 Mueller PR, Coleman TR, Kumagai A, Dunphy WG. Myt1: a membrane-associated inhibitory kinase that phosphorylates Cdc2 on both threonine-14 and tyrosine-15. *Science*. 1995 Oct 6;270(5233):86-90.
- 73 King RW, Deshaies RJ, Peters JM, Kirschner MW: How proteolysis drives the cell cycle. *Science (New York, NY)* 1996, 274(5293):1652-1659.
- 74 Major ML, Lepe R, Costa RH: Forkhead box M1B transcriptional activity requires binding of Cdk-cyclin complexes for phosphorylation-dependent recruitment of p300/CBP coactivators. *Molecular and cellular biology* 2004, 24(7):2649-2661.
- 75 Yuan Z, Becker EB, Merlo P, Yamada T, DiBacco S, Konishi Y, Schaefer EM, Bonni A: Activation of FOXO1 by Cdk1 in cycling cells and postmitotic neurons. *Science (New York, NY)* 2008, 319(5870):1665-1668.
- 76 Marais A, Ji Z, Child ES, Krause E, Mann DJ, Sharrocks AD: Cell cycle-dependent regulation of the forkhead transcription factor FOXK2 by CDK.cyclin complexes. *The Journal of biological chemistry* 2010, 285(46):35728-35739.
- 77 Dehay C, Kennedy H: Cell-cycle control and cortical development. *Nat Rev Neurosci* 2007, 8(6):438-450.
- 78 Vincent I, Jicha G, Rosado M, Dickson DW: Aberrant expression of mitotic cdc2/cyclin B1 kinase in degenerating neurons of Alzheimer's disease brain. *J Neurosci* 1997, 17(10):3588-3598.
- 79 Knudson AG, Jr: Mutation and cancer: statistical study of retinoblastoma. *Proceedings of the National Academy of Sciences of the United States of America* 1971, 68(4):820-823.
- 80 Kim EK, Choi EJ: Pathological roles of MAPK signaling pathways in human diseases. *Biochimica et biophysica acta* 2010, 1802(4):396-405.
- 81 Hampton MB, Fadeel B, Orrenius S: Redox regulation of the caspases during apoptosis. *Annals of the New York Academy of Sciences* 1998, 854:328-335.
- 82 Raina AK, Zhu X, Rottkamp CA, Monteiro M, Takeda A, Smith MA: Cyclin' toward dementia: cell cycle abnormalities and abortive oncogenesis in Alzheimer disease. *Journal of neuroscience research* 2000, 61(2):128-133.
- 83 Raina AK, Hochman A, Zhu X, Rottkamp CA, Nunomura A, Siedlak SL, Boux H, Castellani RJ, Perry G, Smith MA: Abortive apoptosis in Alzheimer's disease. *Acta*

- neuropathologica 2001, 101(4):305-310.
- 84 Lee HG, Casadesus G, Nunomura A, Zhu X, Castellani RJ, Richardson SL, Perry G, Felsher DW, Petersen RB, Smith MA: The neuronal expression of MYC causes a neurodegenerative phenotype in a novel transgenic mouse. *The American journal of pathology* 2009, 174(3):891-897.
- 85 Repetto E, Yoon IS, Zheng H, Kang DE: Presenilin 1 regulates epidermal growth factor receptor turnover and signaling in the endosomal-lysosomal pathway. *The Journal of biological chemistry* 2007, 282(43):31504-31516.
- 86 Hayashi T, Shishido N, Nakayama K, Nunomura A, Smith MA, Perry G, Nakamura M: Lipid peroxidation and 4-hydroxy-2-nonenal formation by copper ion bound to amyloid-beta peptide. *Free radical biology & medicine* 2007, 43(11):1552-1559.
- 87 Nakamura M, Shishido N, Nunomura A, Smith MA, Perry G, Hayashi Y, Nakayama K, Hayashi T: Three histidine residues of amyloid-beta peptide control the redox activity of copper and iron. *Biochemistry* 2007, 46(44):12737-12743.
- 88 Moreira PI, Santos MS, Oliveira CR, Shenk JC, Nunomura A, Smith MA, Zhu X, Perry G: Alzheimer disease and the role of free radicals in the pathogenesis of the disease. *CNS & neurological disorders drug targets* 2008, 7(1):3-10.
- 89 Castellani RJ, Lee HG, Siedlak SL, Nunomura A, Hayashi T, Nakamura M, Zhu X, Perry G, Smith MA: Reexamining Alzheimer's disease: evidence for a protective role for amyloid-beta protein precursor and amyloid-beta. *J Alzheimers Dis* 2009, 18(2):447-452.
- 90 Schubert D, Cole G, Saitoh T, Oltersdorf T: Amyloid beta protein precursor is a mitogen. *Biochemical and biophysical research communications* 1989, 162(1):83-88.
- 91 Santpere G, Nieto M, Puig B, Ferrer I: Abnormal Sp1 transcription factor expression in Alzheimer disease and tauopathies. *Neuroscience letters* 2006, 397(1-2):30-34.
- 92 Citron BA, Dennis JS, Zeitlin RS, Echeverria V: Transcription factor Sp1 dysregulation in Alzheimer's disease. *Journal of neuroscience research* 2008, 86(11):2499-2504.
- 93 Redman CW, Sargent IL: Latest advances in understanding preeclampsia. *Science (New York, NY)* 2005, 308(5728):1592-1594.
- 94 Lachmeijer AM, Arngrimsson R, Bastiaans EJ, Frigge ML, Pals G, Sigurdardottir S, Stefansson H, Palsson B, Nicolae D, Kong A et al: A genome-wide scan for preeclampsia in the Netherlands. *Eur J Hum Genet* 2001, 9(10):758-764.
- 95 van Dijk M, Mulders J, Poutsma A, Konst AA, Lachmeijer AM, Dekker GA, Blankenstein MA, Oudejans CB: Maternal segregation of the Dutch preeclampsia locus at 10q22 with a new member of the winged helix gene family. *Nature genetics* 2005, 37(5):514-519.
- 96 Zhao X, Gan L, Pan H, Kan D, Majeski M, Adam SA, Unterman TG: Multiple elements regulate nuclear/cytoplasmic shuttling of FOXO1: characterization of phosphorylation- and 14-3-3-dependent and -independent mechanisms. *The Biochemical journal* 2004, 378(Pt 3):839-849.
- 97 Janes SM, Ofstad TA, Campbell DH, Watt FM, Prowse DM: Transient activation of FOXN1 in keratinocytes induces a transcriptional programme that promotes terminal differentiation: contrasting roles of FOXN1 and Akt. *Journal of cell science* 2004, 117(Pt 18):4157-4168.
- 98 Wolfrum C, Besser D, Luca E, Stoffel M: Insulin regulates the activity of forkhead transcription factor Hnf-3beta/Foxa-2 by Akt-mediated phosphorylation and nuclear/cytosolic localization. *Proceedings of the National Academy of Sciences of the United States of America* 2003, 100(20):11624-11629.
- 99 Dahle MK, Gronning LM, Cederberg A, Blomhoff HK, Miura N, Enerback S, Tasken KA, Tasken K: Mechanisms of FOXC2- and FOXD1-mediated regulation

of the RI alpha subunit of cAMP-dependent protein kinase include release of transcriptional repression and activation by protein kinase B alpha and cAMP. *The Journal of biological chemistry* 2002, 277(25):22902-22908.

- 100 Aoki M, Jiang H, Vogt PK: Proteasomal degradation of the FoxO1 transcriptional regulator in cells transformed by the P3k and Akt oncoproteins. *Proceedings of the National Academy of Sciences of the United States of America* 2004, 101(37):13613-13617.
- 101 van Dijk M, van Bezu J, van Abel D, Dunk C, Blankenstein MA, Oudejans CB, Lye SJ: The STOX1 genotype associated with pre-eclampsia leads to a reduction of trophoblast invasion by alpha-T-catenin upregulation. *Human molecular genetics* 2010, 19(13):2658-2667.
- 102 Bertram L, McQueen MB, Mullin K, Blacker D, Tanzi RE: Systematic meta-analyses of Alzheimer disease genetic association studies: the AlzGene database. *Nature genetics* 2007, 39(1):17-23.
- 103 Blacker D, Bertram L, Saunders AJ, Moscarillo TJ, Albert MS, Wiener H, Perry RT, Collins JS, Harrell LE, Go RC et al: Results of a high-resolution genome screen of 437 Alzheimer's disease families. *Human molecular genetics* 2003, 12(1):23-32.
- 104 Myers A, Holmans P, Marshall H, Kwon J, Meyer D, Ramic D, Shears S, Booth J, DeVrieze FW, Crook R et al: Susceptibility locus for Alzheimer's disease on chromosome 10. *Science (New York, NY)* 2000, 290(5500):2304-2305.
- 105 Ertekin-Taner N, Graff-Radford N, Younkin LH, Eckman C, Baker M, Adamson J, Ronald J, Blangero J, Hutton M, Younkin SG: Linkage of plasma Abeta42 to a quantitative locus on chromosome 10 in late-onset Alzheimer's disease pedigrees. *Science (New York, NY)* 2000, 290(5500):2303-2304.
- 106 Myers A, Wavrant De-Vrieze F, Holmans P, Hamshere M, Crook R, Compton D, Marshall H, Meyer D, Shears S, Booth J et al: Full genome screen for Alzheimer disease: stage II analysis. *American journal of medical genetics* 2002, 114(2):235-244.
- 107 Pericak-Vance MA, Bass MP, Yamaoka LH, Gaskell PC, Scott WK, Terwedow HA, Menold MM, Conneally PM, Small GW, Vance JM et al: Complete genomic screen in late-onset familial Alzheimer disease. Evidence for a new locus on chromosome 12. *Jama* 1997, 278(15):1237-1241.
- 108 Majercak J, Ray WJ, Espeseth A, Simon A, Shi XP, Wolffe C, Getty K, Marine S, Stec E, Ferrer M et al: LRRTM3 promotes processing of amyloid-precursor protein by BACE1 and is a positional candidate gene for late-onset Alzheimer's disease. *Proceedings of the National Academy of Sciences of the United States of America* 2006, 103(47):17967-17972.
- 109 van Dijk M, van Bezu J, Poutsma A, Veerhuis R, Rozemuller AJ, Scheper W, Blankenstein MA, Oudejans CB: The pre-eclampsia gene STOX1 controls a conserved pathway in placenta and brain upregulated in late-onset Alzheimer's disease. *J Alzheimers Dis* 2010, 19(2):673-679.
- 110 Dickson DW, Farlo J, Davies P, Crystal H, Fuld P, Yen SH: Alzheimer's disease. A double-labeling immunohistochemical study of senile plaques. *The American journal of pathology* 1988, 132(1):86-101.
- 111 Dickson DW, Crystal HA, Mattiace LA, Masur DM, Blau AD, Davies P, Yen SH, Aronson MK: Identification of normal and pathological aging in prospectively studied nondemented elderly humans. *Neurobiology of aging* 1992, 13(1):179-189.
- 112 Katzman R, Terry R, DeTeresa R, Brown T, Davies P, Fuld P, Renbing X, Peck A: Clinical, pathological, and neurochemical changes in dementia: a subgroup with preserved mental status and numerous neocortical plaques. *Annals of neurology* 1988, 23(2):138-144.

- 113** Chen B, Cheng M, Hong DJ, Sun FY, Zhu CQ: Okadaic acid induced cyclin B1 expression and mitotic catastrophe in rat cortex. *Neuroscience letters* 2006, 406(3):178-182.
- 114** Blennow K, de Leon MJ, Zetterberg H: Alzheimer's disease. *Lancet* 2006, 368(9533):387-403.
- 115** LaFerla FM, Green KN, Oddo S: Intracellular amyloid-beta in Alzheimer's disease. *Nat Rev Neurosci* 2007, 8(7):499-509.

2

Chapter 2

Direct downregulation of CNTNAP2 by STOX1A is associated with Alzheimer's disease

Daan van Abel¹, Omar Michel¹, Rob Veerhuis², Marlies Jacobs³, Marie van Dijk¹, Cees BM Oudejans¹

¹Department of Clinical Chemistry, ²The Alzheimer Center, ³Department of Pathology,
^{1,2,3}VU University Medical Center, Amsterdam, The Netherlands.

Accepted in the Journal of Alzheimer's Disease, 2012

Abstract

STOX1A is a transcription factor which is functionally and structurally similar to the forkhead box protein family. STOX1A has been shown to be associated with pre-eclampsia, a pregnancy associated disease, and to have potential implications in Late Onset Alzheimer's Disease (LOAD). However, the exact function of STOX1A and its target genes are still largely unknown. Therefore, in this study we performed chromatin immunoprecipitation coupled to shotgun cloning to discover novel STOX1A target genes. Our results show that CNTNAP2, a member of the neurexin family, is directly downregulated by STOX1A. Additionally, we show that CNTNAP2 expression is downregulated in the hippocampus of Alzheimer's disease patients where STOX1A expression has been shown to be upregulated.

In conclusion these results further indicate the potential involvement of STOX1A and its target genes in the etiology of Alzheimer's disease.

Introduction

Forkhead box proteins, characterized by a DNA binding motif termed the winged helix domain [1], are a family of transcription factors that play a role in the regulation of genes involved in multiple disease associated pathways [2]. Previously, we found that Storkhead box 1 (*STOX1*), a transcription factor structurally and functionally related to the forkhead box protein family, is a susceptibility gene for pre-eclampsia, a hypertensive disorder of pregnancy [3]. In addition to *STOX1* as a pre-eclampsia susceptibility gene, a recent study performed in our lab showed that *STOX1*, which resides on chromosome 10q22, is also functionally important in Late Onset Alzheimer's Disease (LOAD) [4]. LOAD is a disease with progressive and insidious neurodegeneration of the central nervous system (CNS) resulting in memory loss and impairments in behaviour, language and visual-spatial skills involving elderly patients (> 65 years) of both sexes [5].

Interestingly, while both syndromes (pre-eclampsia and LOAD) lack shared clinical features, both share multiple susceptibility loci which exceed the threshold for significant linkage found on chromosomes 2, 9, 10, and 12 [7-14]. Furthermore, these loci are situated at positions near or at 2p12, 2p25, 9p13, 10q22, and 12q22 for which at least 10q22 is subject to a parent-of-origin effect with maternal segregation in both syndromes [9, 15]. These (epi)genetic similarities led us to suggest that these chromosomal regions are subject to evolutionary conserved, genetic pressures. A recent study performed by us suggests that chromosomal region 10q22 also shares a functional overlap [4]. In the former study, it was found in our lab that *STOX1A* expression in the brain correlates with the severity of LOAD and transactivates the neuronal leucine-rich repeat transmembrane 3 (*LRRTM3*) gene [4]. The *LRRTM3* gene resides within the large intron of the α -T catenin-encoding *CTNNA3* gene on 10q21-22 and has been confirmed as a functional and positional candidate gene for LOAD [6].

LRRTM3 has been shown to promote amyloid- β precursor protein (A β PP) processing via Beta-secretase 1 (BACE1) resulting in enhanced production of amyloid β (A β) [6]. Aggregation of A β in the brain is one of the key pathological hallmarks of LOAD [5]. Transcription factors like *STOX1A* are likely to regulate several hundreds of target genes, but the exact function of *STOX1A* and its target genes is still largely unknown. As *STOX1A* is highly expressed in the brain [4] we started a search for *STOX1A* downstream target genes to further explore the fundamental role of *STOX1A* in neuronal pathways. In this study we used *STOX1A* chromatin immunoprecipitation followed by random shotgun cloning (ChIP-shotgun cloning) in the neuroblastoma cell-line SK-N-SH, a cellular model for neuronal function. This approach resulted in the identification of the neurexin family member Contactin Associated Protein-like 2 (*CNTNAP2*) gene as a direct target for *STOX1A* in SK-N-SH cells. Here we describe that *STOX1A* directly and negatively regulates *CNTNAP2* expression in neuroblastoma SK-N-SH cells. Furthermore, our results show that downregulation of *CNTNAP2* expression in the hippocampus is associated with LOAD pathology. Therefore, this study describes a second *STOX1A* target gene with potential implication in LOAD pathology.

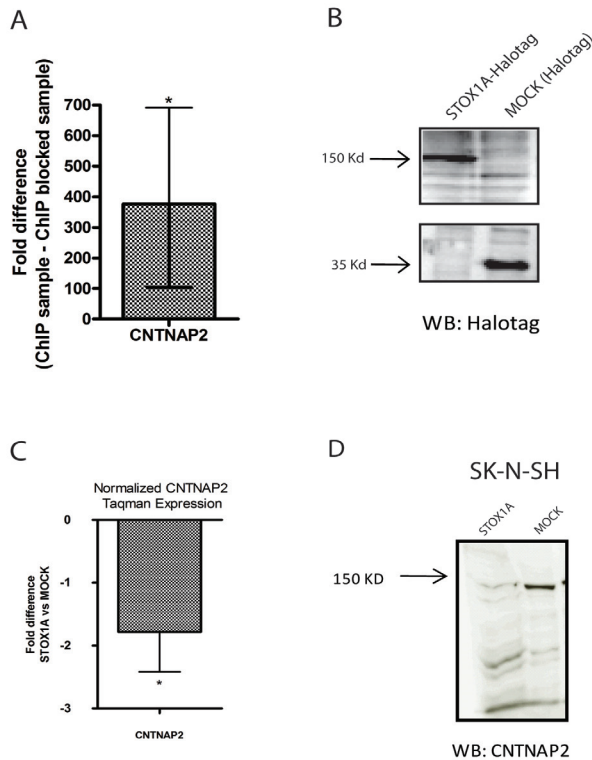


Figure 1. STOX1A binds to a region in intron 1 of the *CNTNAP2* gene resulting in decreased *CNTNAP2* mRNA and protein levels. (A) Results show a mean 376 fold (mean $\Delta\Delta\text{Ct}$ is $-8,56$) enrichment for *CNTNAP2* in STOX1A stimulated ChIP DNA compared with their negative controls (ChIP sample vs ChIP blocked sample). Bar is mean \pm SEM. Asterisks indicates $P < 0.05$ (one sample t-test with theoretical mean 0). (B) Expression of STOX1A protein was confirmed with an anti-Halotag specific antibody by western blot using total cell protein extracts obtained from STOX1A (left lane) and MOCK (right lane) transfected SK-N-SH cells. A specific band representing STOX1A-halotag protein was observed at its expected size of 150 kD. Halotag protein (MOCK) was detected at its expected size of 34 kD. Western blot image is a representative of at least 3 independent experiments. (C) Quantitative RT-PCR data shows a mean 1,78 fold (mean $\Delta\Delta\text{Ct}$ is $0,835$) decreased mRNA expression for *CNTNAP2*. Bars are mean \pm SEM. * indicate $P < 0.05$ (one sample t-test with theoretical mean 0). (D) Endogenous *CNTNAP2* protein was determined with a *CNTNAP2* specific antibody by western blot using total cell protein extracts obtained from STOX1A and MOCK transfected SK-N-SH cells. Western blot image is a representative of at least 3 independent experiments.

Results

ChIP-shotgun cloning identifies a STOX1A DNA binding region associated with CNTNAP2.

By using the ChIP-shotgun cloning procedure 283 potential STOX1A binding regions were found (Supplementary Table 1) and 42 background regions (Supplementary Table 2). We focused on regions for which multiple hits were positioned within a gene (Supplementary Table 1, highlighted in grey). Validation was done using Q-PCR with probes and primers specific for the obtained regions (Supplementary Table 3). Results show significant enrichment for the region located in intron 1 of the *CNTNAP2* gene (Fig. 1A) in STOX1A ChIP DNA compared to the negative controls. A small but

significant enrichment was found for a region associated with the Integrin alpha-9 (*ITGA9*) (Supplementary Fig. 1) gene. No significant enrichment was found for the other obtained regions (Data not shown).

To test the effect of *STOX1A* on *CNTNAP2* mRNA levels we transiently transfected SK-N-SH cells with *STOX1A* or MOCK (negative control) constructs. Transient overexpression of *STOX1A* and MOCK (Halotag) protein was confirmed on western blot (Fig. 1B) and significantly decreased levels of both mRNA (Fig. 1C) and protein levels (Fig. 1D) were seen for *CNTNAP2* in *STOX1A* compared to MOCK transfected SK-N-SH cells.

Knockdown of endogenous *STOX1A* resulted in a significant increase in *CNTNAP2* mRNA expression (Supplementary Fig. 2). However, this effect was not seen on a protein level (Data not shown).

CNTNAP2 expression levels are altered in LOAD patients versus non-demented controls

As our results show that *CNTNAP2* is directly downregulated by *STOX1A* and given that *STOX1A* expression correlates with the severity of LOAD, we speculated that *CNTNAP2* expression levels in affected brain regions are reduced in LOAD. First, we tested *STOX1A* mRNA expression levels in hippocampus tissue of LOAD patients (Table 1). Consistent with previous results from our lab [4] *STOX1A* mRNA levels were significantly increased in the hippocampus of LOAD (Braak stage 5/6) compared to non-demented controls (Braak 0/1, Fig. 2A). As hypothesized, *CNTNAP2* mRNA levels were significantly decreased in the LOAD samples compared to non-demented controls (Fig. 2B). Furthermore, we tested mRNA expression levels of *FOXP2*, a member of the forkhead transcription factor family previously shown to directly downregulate *CNTNAP2* expression [18]. However, we did not find a significant increase of *FOXP2* mRNA expression in the hippocampus of LOAD (Braak stage 5/6) compared to non-demented controls (Braak 0/1, Fig. 2C).

Table 1. Demographics of the cases included in this study.

Diagnosis ¹	Patient ID	Gender	Age (Years)	Braak score	Brain weight (grams)	PMD (hrs:min) ²
Non demented control	08/83	Female	80	1A	1227	6:58
Non demented control	08/315	Male	80	1A	1350	8:10
Non demented control	04/184	Female	81	1B	1164	6:40
Non demented control	09/039	Male	78	10	1145	17:40
Non demented control	04/57	Male	80	0A	1285	6:30
Alzheimer's disease	08/078	Male	78	5C	1300	6:35
Alzheimer's disease	10/016	Male	77	5C	1208	5:39
Alzheimer's disease	08/132	Male	77	6C	1340	6:35
Alzheimer's disease	05/54	Female	81	5C	1061	6:15

¹Clinical diagnosis with neuropathological conformation

²PMD, post mortem delay time (hours:minutes)

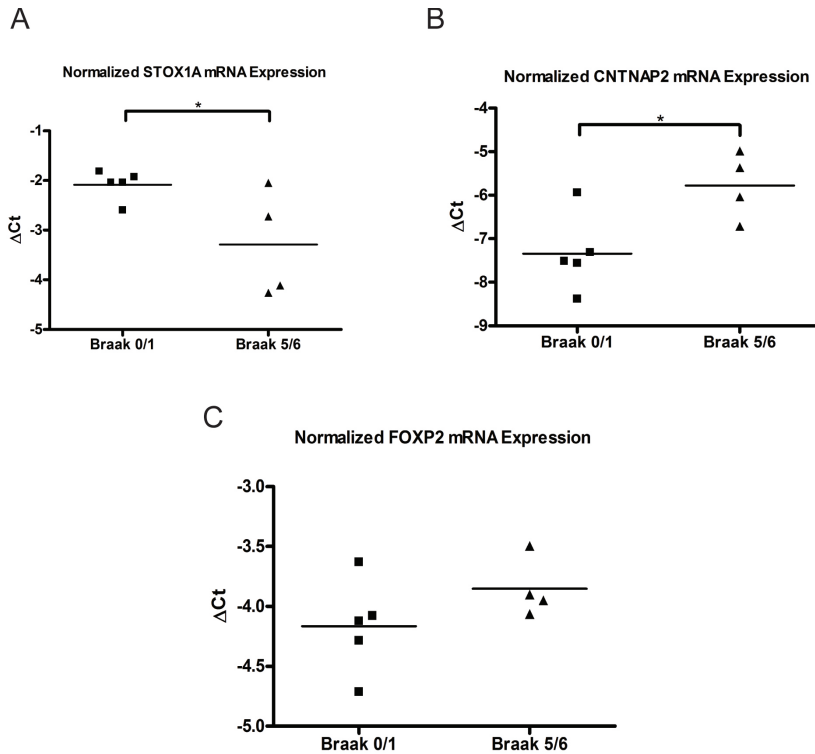


Figure 2. Expression analysis of STOX1A, CNTNAP2 and FOXP2 in patients with LOAD. (A) Quantitative RT-PCR showing a significant increased mRNA expression for STOX1A (lower Δ Ct) and (B) a significant decreased mRNA expression for CNTNAP2 (higher Δ Ct) in advanced stages of LOAD (Braak 5/6,) compared to non-demented controls (Braak 0/1). (C) No significant changes in FOXP2 mRNA expression levels were found in advanced stages of LOAD (Braak 5/6) compared to non-demented controls (Braak 0/1). *P*-values were calculated using a two-tailed unpaired *t*-test, * indicate *P*<0.05.

Discussion

In this study we searched for target genes of STOX1A, a transcription factor which has been shown to be functionally involved in LOAD [4]. With the use of chromatin immunoprecipitation followed by shotgun cloning we identified CNTNAP2 to be directly and negatively regulated by STOX1A in the neuroblastoma cell-line SK-N-SH. Knockdown of endogenous STOX1A by siRNA increases mRNA levels of CNTNAP2 in these cells. However, increased levels of CNTNAP2 mRNA did not result in increased CNTNAP2 protein levels indicating that other mechanisms counteract the effect of STOX1A siRNA knockdown on CNTNAP2 mRNA translation like miRNAs. Additional experiments are necessary to reveal the mechanisms that regulate CNTNAP2 mRNA translation under these conditions. Interestingly, we show that CNTNAP2 is downregulated in the hippocampus of LOAD patients, where STOX1A mRNA levels were upregulated. This suggests that the reduction of CNTNAP2 expression in LOAD patients is directly associated with

increased expression of *STOX1A*. Differential expression of *CNTNAP2* has, to our knowledge, not yet been associated with AD. We can therefore only speculate on the role of *CNTNAP2* in AD pathology.

CNTNAP2 is a gene involved in neural-glia interactions and clustering of ion channels in myelinated axons [19, 20]. A recessive nonsense mutation in the *CNTNAP2* gene has been found to be associated with autism, focal epilepsy, mental retardation, hyperactivity and cortical dysplasia [21-24]. Therefore, much effort has been made unravelling the function of *CNTNAP2*. Currently, several studies have shown that at the juxtaparanodal regions of myelinated axons of the CNS (central nervous system) and PNS (peripheral nervous system) *CNTNAP2* is important for the clustering of Shaker-like K⁺ channels and neural-glia interactions [19, 20, 25]. While the mechanisms and function of this clustering remain unclear there are several studies which elucidate the importance of ion channel clustering at the juxtaparanodal region in myelinated axons.

In one of the studies performed it was shown that disrupted juxtaparanodal regions in myelinated axons are linked to cognitive abnormalities in transient axonal glycoprotein-1 (*TAG-1*) deficient mice [26]. These mice show reduced *CNTNAP2* expression levels suggesting that disrupted *CNTNAP2* expression is associated with cognitive abnormalities as observed in these mice [26].

Another suggested function for molecular organization at the nodes of Ranvier in myelinated axons was recently proposed in a study where re-myelinated lesions of multiple sclerosis (MS) patients were analysed. In this study it has been suggested that during myelin repair the aggregation of nodal, paranodal and juxtaparanodal constituents, in particular ion channels, precede re-myelination [27]. This indicates that defects in domain organization surrounding the nodes of Ranvier in myelinated axons could aggravate re-myelination failure in de-myelinated MS lesions [27] and therefore may contribute to neurodegeneration. Re-myelination defects have previously also been associated with AD [28], suggesting that defects in domain organization at the nodes of Ranvier of myelinated axons could also be associated with proper re-myelination in AD. Another study elucidating the role of domain organisation at the nodes of Ranvier in myelinated axons showed that in the grey matter of triple-transgenic AD (3xTg-AD) mice the levels of myelin-associated proteins, including ion channels, are significantly lower than controls [29]. A recent study performed by Strauss and collaborators [21] shows that patients diagnosed with cortical dysplasia-focal epilepsy (CDFE) syndrome have a single-base deletion resulting in a premature stop codon in the *CNTNAP2* gene and is therefore predicted to yield a non-functional protein. Histopathological inspection of brain regions from these patients showed that several neurons have intense neurofilament tangle staining [21]. As neurofilament tangles are one of the constituents of neurofibrillary tangles (NFT) in AD [30], the findings of Straus and collaborators indicates that disruption of *CNTNAP2* could directly contribute to NFT formation also seen in AD.

In conclusion, several studies indicate that defects in proper domain organization at the nodes of Ranvier in myelinated axons is important for proper axonal functioning and when compromised is associated with neurodegeneration. While speculative, decreased levels of *CNTNAP2* by upregulated *STOX1A* expression in LOAD could

therefore contribute to neurodegeneration and cognitive decline.

Another member of the forkhead family of transcription factors, FOXP2, has also been shown to directly downregulate CNTNAP2 [18]. Although a possible outcome for FOXP2 overexpression in LOAD is unclear we speculated that decreased levels of CNTNAP2 expression in the hippocampus of LOAD, as found in this study, could in part also be the result of upregulated FOXP2 expression as also shown for STOX1A. However, we did not find upregulated expression of FOXP2 in the hippocampus of LOAD patients. Therefore it is unlikely that FOXP2 contributes to reduced CNTNAP2 expression levels in the hippocampus of LOAD patients.

Nevertheless, our results indicate a potential role for CNTNAP2 in AD pathology, a gene which we found to be directly regulated by STOX1A. As both CNTNAP2 and STOX1A are deregulated in LOAD, in the future, it would therefore be nice to see if genetic variants in STOX1 or CNTNAP2 are associated with AD pathology. This could indicate that these genes are capable of influencing AD disease progression by itself which elucidates their role in AD pathology. It does not seem, however, that the predominant pre-eclampsia STOX1 mutation Y153H [3] is involved in the pathology of LOAD.

In this study we primarily focussed on the link between STOX1A, CNTNAP2 and LOAD. However, other genes associated with the obtained STOX1A ChIP-regions could be of great significance as well. For example, the *EPB41L3* gene has been shown to be required for the proper domain clustering of Kv1 channels by CNTNAP2 at the juxtaparanodal axonal membrane [31]. Furthermore, as for *CNTNAP2*, other genes associated with ASD are also found in the list of obtained ChIP-cloning fragment, these include neurexin 3 (*NRXN3*), and *CNTNAP5* [32, 33]. As shown for *CNTNAP2* these potential STOX1A target genes could also have implications in LOAD. Their association with ASD also suggest a role for STOX1A as an upstream regulator in ASD. Additional experiments are therefore needed to validate these genes as direct targets for STOX1A.

Besides *CNTNAP2*, we also validated *ITGA9* as a direct target gene. *ITGA9* has been shown to be involved in axon regeneration [34]. Exploration of STOX1A as an upstream regulator of the *ITGA9* gene could possibly reveal a function for STOX1A in axon regeneration. Together, we show that our data can be very informative in the exploration of the biological role of STOX1A in neuronal signalling.

Materials and Methods

Human tissues

Human brain specimens of Alzheimer's disease cases (Braak stages 6, n = 4) and non-demented control cases (Braak stages 1, n = 5) were matched for age and were obtained at autopsy through the Netherlands Brain Bank (<http://www.brainbank.nl>). Clinical diagnosis was neuropathologically confirmed on formalin-fixed, paraffin-embedded tissue from different sites. Staging of AD was neuropathologically evaluated according to Braak and Braak [16]. Demographics of the cases included in this study are listed in Table 1.

Cell culture and transfection

SK-N-SH human neuroblastoma cells were obtained from the American Type Culture Collection (ATCC, Manassas, VA). All reagents for cell culture were purchased from Invitrogen Life Technologies, Inc. (Burlington, Canada). SK-N-SH cells were cultured at 37 °C in a humidified atmosphere of 5% CO₂ in Iscove's Modified Dulbecco's Medium (IMDM) supplemented with 10% fetal calf serum and 100 U/ml penicillin, and 100 g/ml streptomycin. Cells were subcultured in medium every 2–3 days following harvesting by trypsinization (HBSS containing 5% trypsin). The ORF (Open Reading Frame) of the *STOX1A* gene was subcloned into the pFN21A HaloTag® CMV Flexi® vector according to the manufacturers protocol (Promega) and transfected into SK-N-SH cells. For transfection the calcium phosphate method was used [17]. Briefly, at the time of transfection, cells were at 70% confluence. By vortexing 2X HEBS (HEPES-buffered saline) with a solution of 2.5 M CaCl₂ and 20 µg of plasmid DNA a co-precipitate of DNA and CaPO₄ was allowed to form. After incubation for 30 min at room temperature, the precipitate was added to the cells and the medium was changed after 24 hours. Cells were harvested 48 hours post-transfection for further analysis. RNA was isolated as described in the Quantitative PCR and RT-PCR section.

Knockdown of *STOX1A* was performed by transfecting 4 siRNA's against *STOX1A* and control siRNA (Qiagen) in SK-N-SH cells with Lipofectamine™ RNAiMAX (Invitrogen) according to the manufactures protocol. Cells were harvested 48 hours post-transfection and RNA was isolated as described in the Quantitative PCR and RT-PCR section.

Chromatin immunoprecipitation cloning (ChIP-cloning)

Transiently *STOX1A*-transfected SK-N-SH cells were treated with formaldehyde to create protein-DNA crosslinks. Cytoplasmic lysis was performed to reduce competition of cytoplasmic *STOX1A*-Halotag proteins against nuclear *STOX1A*-Halotag proteins with the Halotag resin. Nuclear lysate was subsequently fragmented by sonication (Ranging from 200 till 1000 bp). The nuclear lysates were split into two equal parts of which one was treated with Halotag blocking ligand to function as a negative control. Both the samples and controls were treated using Halotag resin according to the Halo-ChIP system protocol in the presence of proteinase inhibitors. After reversal of crosslinks the DNA was purified using the MinElute PCR Purification Kit (QIAGEN). DNA was then blunt ended according to the Zero Blunt® PCR Cloning Kit (Invitrogen). At least 4 experimental and 4 control samples were combined and concentrated using the MinElute PCR Purification Kit (QIAGEN). Both pooled experimental and control samples were then cloned into the pCR®-Blunt vector and subsequently transformed into One Shot® TOP10 Competent Cells according to the Zero Blunt® PCR Cloning Kit (Invitrogen). The amount of positive clones on the experimental plate were visually inspected and compared to the control plate. The amount of colonies present on the experimental plate compared to the amount of positive colonies on the control plate was used as an indication of ChIP DNA enrichment. Colonies of experimental and control plates were selected and inserts were PCR amplified using the M13 Forward and M13 reversed primers present in the

backbone of the pCR[®]-Blunt vector. PCR amplified inserts were then analysed by DNA sequencing using the M13 Forward primer and Big Dye Terminators followed by separation on an ABI3130xl Genetic Analyser (Applied biosystems). To determine the positions of the obtained DNA sequences we used the function BLAT on the University of California, Santa Cruz, Genome Server (<http://genome.ucsc.edu/>), which enabled identification of putative STOX1A binding regions. Sequences for both the experimental and controls that were positioned in repeat masked regions were rejected. This resulted in a list of 283 experimental (Supplementary Table 1) and 42 background (Supplementary Table 2) sequences.

Quantitative PCR and RT-PCR

Standard quantitative PCR was performed on an ABI7300 (Applied Biosystems) using a probe and primers specific for the region in intron 1 of the CNTNAP2 gene obtained in the ChIP-shotgun cloning procedure. Probe and primer characteristics were: CNTNAP2_forward 5' AGCAGAAGGAGTTGAAATGC 3', CNTNAP2_reversed 5' GCTGTCATTTGGCAGTAGC 3' and 5'-FAM 3'-TAMRA labeled probe: 5' GCAGATAGGGGGATCGCAGC 3'. Reactions were performed in the presence of 1M betaine and ROX reference dye, and corrected for input using the non-intron-spanning Glyceraldehyde 3-phosphate dehydrogenase (GAPDH) gene expression assay (Applied Biosystems). Input ChIP DNA was obtained from at least four independent ChIP experiments.

RNA isolation from transfected SK-N-SH cells was performed using the RNeasy kit (Qiagen) including on-column DNase treatment. For isolation of RNA from the hippocampal region of non-demented controls and brains with advanced LOAD we cut between 10-20 cryostat sections (30 µm each) from each patient sample (see human tissues section for details) and immediately mixed them with 1 ml RNABee. After addition with 100 µl of chloroform the samples were mixed and centrifuged for 15 min. The aqueous phase was collected and further treated using the RNeasy kit (Qiagen) including on-column DNase treatment. Quantitative RT-PCR using gene expression assays (Applied Biosystems) for FOXP2 and CNTNAP2 were performed on an ABI7300.

Probe and primer characteristics for STOX1A were: STOX1A_forward 5' TTCTCCACGGACACAGAGT 3', STOX1A_reversed 5' TATGCTTGCCTTTAGACAAT 3' and 5'-FAM 3'-TAMRA labelled probe: 5' AGAGCAGTCAACCACTCACATCTAAT 3'. Normalization was done with gene expression assays for PBGD (Applied Biosystems). Data of transfected cells was obtained from at least four transfections, each RNA sample was measured in triplicate.

Western blot

Protein lysates from transfected cells were obtained by directly scraping cells into Loading Buffer including β-mercaptoethanol. Lysates were separated by SDS-polyacrylamide gel electrophoresis, and electroblotted onto a PVDF-membrane. An antibody recognizing the Halotag (Promega) or CNTNAP2 (Sigma) protein, were used

in combination with goat anti-rabbit horseradish peroxidase-conjugated secondary antibody (DAKO). Protein bands were detected by an enhanced-chemiluminescence assay (GE Healthcare) on a LAS3000.

Data analysis

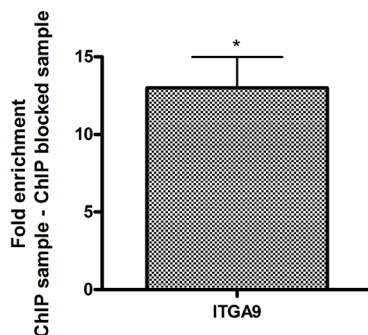
For Real-time PCR data, a threshold cycle number, Ct, was measured as the PCR cycle at which the amount of amplified target reaches the threshold value. Quantification was determined by the $2^{-\Delta\Delta C_t}$ method as described in Applied Biosystems “Guide to Performing Relative Quantitation of Gene Expression Using Real-Time Quantitative PCR”, Section VII, Relative Quantitation of Gene Expression Experimental Design and Analysis” http://www3.appliedbiosystems.com/cms/groups/mcb_support/documents/generaldocuments/cms_042380.pdf). Statistical analysis of the obtained data was carried out with the GraphPad Prism program. Significance in Figure 1 (and supplementary figures 1 and 2) was calculated with a one sample t-test with a theoretical mean of 0. Significance in Figure 2 was calculated using a two-tailed unpaired t-test. * indicate $P < 0.05$, ** indicate $P < 0.01$, *** indicate $P < 0.001$. Bars are mean \pm SEM.

Acknowledgements

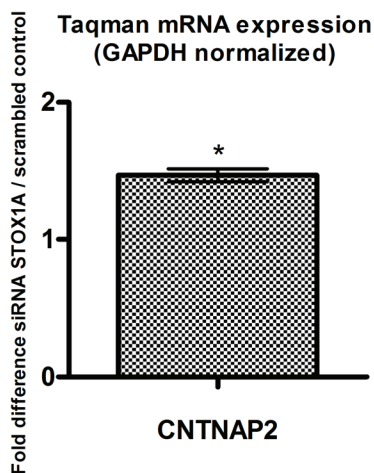
The human neuroblastoma cell line SK-N-SH was obtained from the American Type Culture Collection (ATCC; Rockville, MD, USA), and kindly provided by Dr. R. Veerhuis (Clinical Chemistry Dept., VUMC).

Supplementary Figures

2



Supplementary Figure 1. STOX1A binds to a region associated with the *ITGA9* gene. Results show a mean 13,01 fold (mean $\Delta\Delta Ct$ is $-3,68$) enrichment for *ITGA9* in STOX1A stimulated ChIP DNA compared with their negative controls (ChIP sample vs ChIP blocked sample). Bar is mean \pm SEM. * indicates $P < 0.05$ (one sample t-test with theoretical mean 0). N = 4, each sample was measured in triplicate.



Supplementary Figure 2. The effect of STOX1A knockdown in the SK-N-SH neuroblastoma cell line. CNTNAP2 mRNA expression was determined with quantitative RT-PCR showing a mean 1,47 fold (mean $\Delta\Delta Ct$ is $-0,55$) increased mRNA expression in STOX1A siRNA treated cells compared to their negative controls. Bars are mean \pm SEM. * indicate $P < 0.05$, (one sample t-test with theoretical mean 0). N = 3, each sample was measured in triplicate.

Supplementary Tables

Supplementary table 1. Potential STOX1A bound regions

Gene ID	Chromosomal Region	Gene ID	Chromosomal Region
MYSM1	chr1:58,902,181-58,902,644	TRIB2	chr2:12,790,297-12,790,516
xxxxx	chr1:162,133,367-162,133,546	MCM6	chr2:136,343,733-136,343,896
RGL1	chr1:182,073,027-182,073,110	xxxxx	chr2:206,557,679-206,557,796
xxxxx	chr1:182,870,028-182,870,153	PARD3B	chr2:206,084,100-206,084,223
FRAMEF1	chr1:12,777,496-12,777,702	xxxxx	chr2:184,682,478-184,682,659
ZNF643	chr1:40,700,479-40,700,705	CALPN14	chr2:31,304,515-31,304,578
xxxxx	chr1:48298098-48298375	xxxxx	chr2:10,931,500-10,931,734
xxxxx	chr1:212,005,122-212,005,281	ARHGAP15	chr2:143,885,565-143,885,783
xxxxx	chr1:2,739,405-2,739,863	PID1	chr2:229,789,533-229,789,714
TXNDC12	chr1:52,279,845-52,280,060	xxxxx	chr2:100,451,915-100,452,270
xxxxx	chr1:45,051,096-45,051,370	xxxxx	chr2:22,569,048-22,569,122
xxxxx	chr1:164,189,403-164,189,739	xxxxx	chr3:96,505,565-96,505,871
FAF1	chr1:50,684,369-50,684,727	ATP1B3	chr3:143,127,532-143,127,806
xxxxx	chr1:236,957,151-236,957,324	ITGA9	chr3:37,521,134-37,521,554
xxxxx	chr1:224,817,464-224,817,746	ITGA9	chr3:37,657,387-37,657,815
FHL3	chr1:38,235,576-38,235,860	SYNPR	chr3:63,449,413-63,449,652
xxxxx	chr1:17,085,952-17,086,077	CHCHD6	chr3:128,031,745-128,032,036
TPR	chr1:184,582,115-184,582,224	xxxxx	chr3:153,876,686-153,876,866
xxxxx	chr1:82,504,749-82,504,935	LRRC31	chr3:171,060,733-171,061,151
LRRC39	chr1:100,392,174-100,392,316	ATG7	chr3:11,404,044-11,404,281
xxxxx	chr1:101,982,873-101,983,032	xxxxx	chr3:48,231,365-48,231,500
DISC1	chr1:229,959,153-229,959,250	xxxxx	chr3:82,035,149-82,035,231
KIFAP3	chr1:168,302,270-168,302,439	PTPRG	chr3:61,948,314-61,948,398
LPHN2	chr1:81,971,383-81,971,440	xxxxx	chr3:121,884,506-121,884,712
SOAT1	chr1:177,550,174-177,550,289	STOX2	chr4:185,166,123-185,166,226
xxxxx	chr1:213,141,291-213,141,450	PDLIM5/ LIM	chr4:95,797,508-95,797,576
xxxxx	chr1:101,982,876-101,983,033	xxxxx	chr4:155,896,136-155,896,232
TNN3	chr1:74,455,977-74,456,278	KLHL2	chr4:166,374,387-166,374,694
AJAP1	chr1:4,618,989-4,619,194	xxxxx	chr4:128,025,611-128,025,921
CNTNAP5	chr2:125,010,676-125,010,957	xxxxx	chr4:125,450,510-125,450,651
xxxxx	chr2:117,292,001-117,292,194	xxxxx	chr4:83,096,158-83,096,266
SPAG16	chr2:213,882,301-213,882,408	AFAP1	chr4:7,932,035-7,932,327
SRBD1	chr2:45,681,047-45,681,207	xxxxx	chr4:130,494,411-130,494,649
PDE11A	chr2:178,248,305-178,248,538	xxxxx	chr4:15,274,370-15,274,506
LYPD6B	chr2:149,630,000-149,630,142	FAT4	chr4:126,585,285-126,585,425
LASS6	chr2:169,249,759-169,249,951	xxxxx	chr4:92,436,821-92,436,984
xxxxx	chr2:200,637,796-200,637,935	xxxxx	chr4:124,600,860-124,601,134
xxxxx	chr2:237,852,825-237,853,018	xxxxx	chr4:164,518,031-164,518,101
xxxxx	chr2:60,383,098-60,383,510	xxxxx	chr5:56,809,248-56,809,454
xxxxx	chr2:207,796,446-207,796,680	NPY6R	chr5:137,171,620-137,171,807
RBKS	chr2:27,949,403-27,949,575	xxxxx	chr5:169,690,749-169,690,805
MYT1L	chr2:1,983,497-1,983,860	ADAMTS2	chr5:178,516,263-178,516,283
xxxxx	chr2:200,637,798-200,637,941	SYNPO	chr5:149,995,911-149,996,156
xxxxx	chr2:16,235,887-16,235,993	SLIT3	chr5:168,246,847-168,247,249
xxxxx	chr2:237,701,531-237,701,651	FGF1	chr5:141,974,074-141,974,299
xxxxx	chr2:218,072,300-218,072,480	SIL1	chr5:138,439,577-138,439,972
xxxxx	chr2:46,945,733-46,945,881	xxxxx	chr5:32,230,619-32,230,983
		xxxxx	chr5:102,034,014-102,034,104

STOX1A Negatively Regulates CNTNAP2 · 2

2

Gene ID	Chromosomal Region	Gene ID	Chromosomal Region
PDGFRB	chr5:149,475,700-149,475,898	xxxxx	chr8:6,965,228-6,965,372
PCDHB8	chr5:140,538,103-140,538,183	xxxxx	chr8:103,758,969-103,759,081
EPB41L4A	chr5:111,529,800-111,529,855	xxxxx	chr8:117,280,844-117,280,979
xxxxx	chr5:129,690,195-129,690,308	RNF19A	chr8:101,381,201-101,381,264
SGCD	chr5:156,029,167-156,029,257	PXDNL	chr8:52,452,013-52,452,188
PPIL6	chr6:109,819,265-109,819,298	xxxxx	chr8:36,230,991-36,231,338
CDYL	chr6:4,883,236-4,883,476	FNTA	chr8:43,039,447-43,039,533
SYNE1	chr6:152,990,411-152,990,527	MCPH1	chr8:6,422,973-6,423,451
xxxxx	chr6:83,260,962-83,261,259	xxxxx	chr8:82,306,564-82,306,700
xxxxx	chr6:147,830,995-147,831,173	BMP1	chr8:22,104,029-22,104,330
STK38	chr6:36,620,136-36,620,226	xxxxx	chr8:69,838,325-69,838,582
xxxxx	chr6:8,242,299-8,242,471	xkr4	chr8:56,313,512-56,313,665
xxxxx	chr6:54,450,535-54,450,707	MELK	chr9:36,633,263-36,633,520
SIM1	chr6:100,992,438-100,992,669	Mob1 homolog	chr9:27,337,545-27,337,643
xxxxx	chr6:36,996,589-36,996,746	xxxxx	chr9:137,334,963-137,335,146
xxxxx	chr7:51,781,850-51,782,017	xxxxx	chr9:101,294,560-101,294,759
WBSCR17	chr7:70,420,433-70,420,562	xxxxx	chr9:137,157,069-137,157,416
TRIP6	chr7:100,308,057-100,308,083	xxxxx	chr9:35,027,329-35,027,531
SHFM1	chr7:96,174,558-96,174,681	xxxxx	chr9:101,294,562-101,294,759
PRKAR2B	chr7:106,571,369-106,571,786	NBIF	chr9:14,186,532-14,186,687
xxxxx	chr7:10,423,780-10,428,759	JAK2	chr9:4,988,437-4,988,721
RAPGEF5	chr7:22,183,342-22,183,419	KIF24	chr9:34,312,083-34,312,329
PRKAG2	chr7:151,097,816-151,097,986	xxxxx	chr10:60,832,406-60,832,533
RBM33	chr7:155,163,305-155,163,414	xxxxx	chr10:8,394,225-9,474,224
SFRP4	chr7:37,920,251-37,920,821	xxxxx	chr10:52,344,134-52,344,297
xxxxx	chr7:152,956,629-152,956,704	SGMS1	chr10:51,776,710-51,776,860
xxxxx	chr7:105,759,453-105,759,875	SLC16A9	chr10:61,127,290-61,127,889
HDAC9	chr7:18,622,899-18,623,151	KCNMA1	chr10:78,854,843-78,855,109
xxxxx	chr7:39,538,023-39,538,116	CDH23	chr10:72,915,506-72,915,595
xxxxx	chr7:49,130,485-49,130,817	DNMBP	chr10:101,728,540-101,728,850
xxxxx	chr7:12,665,243-12,665,439	xxxxx	chr10:9,964,445-9,964,576
xxxxx	chr7:66,627,376-66,627,724	LIPA	chr10:90,977,426-90,977,840
xxxxx	chr7:30,580,476-30,581,032	C10ORF59	chr10:90,219,610-90,220,000
xxxxx	chr7:6,499,724-6,499,973	DOCK1	chr10:129,098,906-129,098,938
PTPRZ1	chr7:121,472,887-121,472,970	xxxxx	chr10:133,460,102-133,460,527
CNTNAP2	chr7:145,644,227-145,644,441	xxxxx	chr11:27,290,596-27,290,678
CNTNAP2	chr7:145,592,668-145,593,046	xxxxx	chr11:33,768,551-33,768,833
CNTNAP2	chr7:146,726,641-146,726,934	xxxxx	chr11:85,458,174-85,458,289
PTN,pleiotro	chr7:136,628,461-136,628,641	xxxxx	chr11:85,458,171-85,458,288
xxxxx	chr7:113,201,150-113,201,427	xxxxx	chr11:14,628,192-14,628,280
xxxxx	chr7:41,192,107-41,192,453	xxxxx	chr11:3,505,213-3,505,432
PPP1R3A	chr7:113,321,925-113,322,033	PAAF1	chr11:73,299,129-73,299,320
METTL2B	chr7:127,915,177-127,915,379	INHBC	chr12:56,120,212-56,120,294
Clip2	chr7:73,430,008-73,430,095	YAF2	chr12:40,881,285-40,881,405
cd36, CD36	chr7:80,094,620-80,094,715	xxxxx	chr12:33,375,084-33,375,283
CREB5	chr7:28,587,758-28,587,874	xxxxx	chr12:56,455,254-56,455,401
TBRG4	chr7:45,114,664-45,114,929	TSPAN9	chr12:3,219,732-3,219,910
xxxxx	chr8:136,497,678-136,497,757	xxxxx	chr12:705,818-705,977

2 · STOX1A Negatively Regulates CNTNAP2

Gene ID	Chromosomal Region	Gene ID	Chromosomal Region
RILPL1	chr12:122,539,659-122,539,819	RAB11FIP4	chr17:26,743,776-26,743,890
CSAD	chr12:51,839,344-51,839,463	xxxxx	chr17:61,725,796-61,725,967
GRIP1	chr12:65,123,998-65,124,199	ACCN1	chr17:28,620,319-28,620,611
GRIP1	chr12:65,123,998-65,124,190	ACCN1	chr17:29,476,644-29,476,863
xxxxx	chr13:59,845,125-59,845,301	xxxxx	chr17:49,247,593-49,247,934
EDNRB	chr13:77,386,662-77,386,792	ITGB4	chr17:71,263,928-71,264,144
GPC6	chr13:92,972,084-92,972,541	xxxxx	chr17:59,751,311-59,751,797
xxxxx	chr13:58,880,578-58,880,666	AXIN2	chr17:60,975,238-60,975,884
xxxxx	chr13:94,155,143-94,155,253	ZNF232	chr17:4,954,122-4,954,251
SLC15A1	chr13:98,177,474-98,177,590	xxxxx	chr17:4,271,304-4,271,550
SPATA13	chr13:23,746,178-23,746,348	xxxxx	chr18:67,415,690-67,415,868
xxxxx	chr13:94,155,151-94,155,253	EPB41L3	chr18:5,477,803-5,478,046
RB1	chr13:47,875,341-47,875,455	EPB41L3	chr18:5,477,807-5,478,049
EML1	chr14:99,344,718-99,344,886	EPB41L3	chr18:5,464,774-5,465,031
xxxxx	chr14:63,884,162-63,884,305	xxxxx	chr19:38,495,417-38,495,637
xxxxx	chr14:70,226,446-70,226,738	xxxxx	chr19:38,546,354-38,546,674
NRXN3	chr14:77,859,932-77,860,231	ZC3H4	chr19:52,270,429-52,270,782
PLEK2	chr14:66,935,921-66,936,043	UNC13A	chr19:17,592,713-17,593,010
SFTA3	chr14:36,020,863-36,021,048	xxxxx	chr20:5,208,591-5,208,613
MAP3K9	chr14:70,272,501-70,272,563	HCK-1	chr20:30,124,075-30,124,306
xxxxx	chr14:73,925,445-73,925,725	HCK-2	chr20:30,124,083-30,124,306
FOXN3	chr14:89,139,656-89,139,788	xxxxx	chr20:20981453-20981697
xxxxx	chr15:19,542,031-19,542,234	xxxxx	chr20:38,819,120-38,819,254
xxxxx	chr15:40,818,789-40,818,892	xxxxx	chr20:6,409,295-6,409,467
AKAP13	chr15:84,010,618-84,010,896	DLGAP4	chr20:34,509,731-34,509,862
xxxxx	chr15:82,611,783-82,611,922	SLC24A	chr20:19,470,315-19,470,636
BNC1	chr15:81,732,821-81,733,055	xxxxx	chr20:56,954,592-56,954,633
LRRC49	chr15:69,093,804-69,094,064	xxxxx	chr20:22,425,650-22,425,844
xxxxx	chr15:99,878,885-99,879,341	TAF4	chr20:60,035,671-60,035,808
xxxxx	chr15:99,878,882-99,879,342	xxxxx	chr21:46,839,434-46,839,770
COX4NB	chr16:84,383,552-84,383,681	DSCAM	chr21:40,500,445-40,500,705
xxxxx	chr16:72,436,596-72,436,785	xxxxx	chr21:29,070,614-29,070,718
xxxxx	chr16:5,554,482-5,554,580	TEF	chr22:40,106,822-40,107,059
IMMA BOLA-ii	chr16:30,018,957-30,018,988	SPECC1L	chr22:23,136,287-23,136,502
GCSH	chr16:79,685,641-79,685,719	SPECC1L	chr22:23,131,454-23,131,641
ZCCHC14	chr16:86,022,913-86,023,162	xxxxx	chr22:48,533,162-48,533,485
xxxxx	chr16:83,956,243-83,956,474	Dach2	chrX:85,692,067-85,692,170
WVVOX	chr16:77,452,146-77,452,327	xxxxx	chrX:42,003,959-42,004,274
FBXO31	chr16:85,962,723-85,962,930	xxxxx	chrX:47,499,512-47,499,753
SIAH1	chr16:46,985,440-46,985,778	IL1RAPL2	chrX:104,156,125-104,156,405
NTAN1 / PD)	chr16:15,040,004-15,040	BRCC3	chrX:153,962,819-153,962,892
FBXO31	chr16:85,962,723-85,962,930	MAP7D3	chrX:135,155,247-135,155,406
CDYL2	chr16:79,224,798-79,225,011	xxxxx	chrX:23,430,034-23,430,351
ABCC11	chr16:46,818,452-46,818,695	MTND5	chrM:13,203-13,348
xxxxx	chr16:9,563,950-9,564,093		
xxxxx	chr16:72,859,536-72,859,639		
A2BP1	chr16:6,105,879-6,106,056		
NFAT	chr16:68,230,694-68,230,926		

Supplementary table 1. Background regions

Gene ID	Chromosomal Region
LOC388630	chr1:48,083,241-48,083,398
xxxxx	chr1:188,584,756-188,584,913
xxxxx	chr1:225,821,071-225,821,358
GOLPH3L	chr1:148,907,336-148,907,424
xxxxx	chr2:19,126,992-19,127,222
xxxxx	chr2:56,566,107-56,566,628
xxxxx	chr2:164,619,339-164,619,453
UBE2D2	chr5:138,933,187-138,933,417
xxxxx	chr5:36,727,352-36,727,431
BXDC1	chr6:111,443,336-111,443,433
xxxxx	chr7:128,052,033-128,052,507
MAD1L1	chr7:2,066,599-2,066,676
xxxxx	chr7:28,897,200-28,897,271
RELN	chr7:103,294,128-103,294,225
xxxxx	chr7:140,312,334-140,312,510
RPL8	chr8:145,987,229-145,987,271
xxxxx	chr8:72,095,204-72,095,338
xxxxx	chr9:86,325,049-86,325,258
xxxxx	chr9:112,325,280-112,325,579
xxxxx	chr9:7,390,649-7,390,727
GLIS3	chr9:3,997,177-3,997,447
RPL12	chr9:129,252,059-129,252,156
xxxxx	chr10:19,414,208-19,414,332
xxxxx	chr10:120,657,634-120,657,919
xxxxx	chr10:113,790,106-113,790,223
xxxxx	chr11:9,306,630-9,306,689
xxxxx	chr11:14,387,044-14,387,122
xxxxx	chr11:21,690,638-21,690,684
xxxxx	chr12:88,753,565-88,753,669
SPATS2	chr12:48,079,443-48,079,562
xxxxx	chr13:18,681,821-18,681,957
xxxxx	chr14:70,384,616-70,384,701
VRK1	chr14:96,381,405-96,381,808
xxxxx	chr16:59,534,555-59,534,644
ALOX12B	chr17:7,928,474-7,928,637
xxxxx	chr17:12,259,283-12,259,601
xxxxx	chr17:27,438,809-27,438,960
xxxxx	chr19:11,565,514-11,565,644
xxxxx	chr21:20,791,023-20,791,269
xxxxx	chr21:43,564,596-43,564,683
GNB1L	chr22:18,199,983-18,200,115
TSPAN7	chrX:38,361,789-38,362,093

Supplementary table 2

Associated gene	Forward Primer	Reversed Primer	Probe
<i>CNTNAP2</i>	5' AGCAGAAGGAGTTGAAATGC 3'	5' GCTGTCATTTGGCAGTAGC 3'	5' CAGATAGGGGGATCGCAGCC 3'
<i>ITGA9</i>	5' GAGGGTGATGACAAGTTTGG 3'	5' ATATGGATGCAAAAGGAACC 3'	5' CTGGCCAGAGGAGAGCTTTCAGC 3'
<i>ACCNA1</i>	5' CTAGCTTCCTTGGGCTTCTG 3'	5' CCAAGAGAGGGTCCTTGC 3'	5' TCAAGTGGTGTCCTCCATCGGGG 3'
<i>SPECC11</i>	5' ATTGCAGAGGTTTTTATGG 3'	5' GGCTGTAGCCTCAACTCTGC 3'	5' CAGCCCTGCCCACTCCTGT 3'

References

- 1 Brennan RG. (1993) The winged-helix DNA-binding motif: another helix-turn-helix takeoff. *Cell*, 74, 773-6.
- 2 Tuteja G and Kaestner KH. (2007) SnapShot: forkhead transcription factors I. *Cell*, 130, 1160.
- 3 van Dijk M, Mulders J, Poutsma A, Konst AA, Lachmeijer AM, Dekker GA, Blankenstein MA and Oudejans CB. (2005) Maternal segregation of the Dutch preeclampsia locus at 10q22 with a new member of the winged helix gene family. *Nat Genet*, 37, 514-9.
- 4 van Dijk M, van Bezu J, Poutsma A, Veerhuis R, Rozemuller AJ, Scheper W, Blankenstein MA and Oudejans CB. (2010) The Pre-Eclampsia Gene STOX1 Controls a Conserved Pathway in Placenta and Brain Upregulated in Late-Onset Alzheimer's Disease. *J Alzheimers Dis*, 19, 673-679
- 5 Newman M, Musgrave IF and Lardelli M. (2007) Alzheimer disease: amyloidogenesis, the presenilins and animal models. *Biochim Biophys Acta*, 1772, 285-97.
- 6 Majercak J, Ray WJ, Espeseth A, Simon A, Shi XP, Wolffe C, Getty K, Marine S, Stec E, Ferrer M, Strulovici B, Bartz S, Gates A, Xu M, Huang Q, Ma L, Shughrue P, Burchard J, Colussi D, Pietrak B, Kahana J, Beher D, Rosahl T, Shearman M, Hazuda D, Sachs AB, Koblans KS, Seabrook GR and Stone DJ. (2006) LRRTM3 promotes processing of amyloid-precursor protein by BACE1 and is a positional candidate gene for late-onset Alzheimer's disease. *Proc Natl Acad Sci U S A*, 103, 17967-72.
- 7 Arngrimsson R, Sigurard TS, Frigge ML, Bjarnadottir RI, Jonsson T, Stefansson H, Baldursd'ottir A, Einarsd'ottir AS, Palsson B, Snorrard'ottir S, Lachmeijer AM, Nicolae D, Kong A, Bragason BT, Gulcher JR, Geirsson RT, Stef'ansson K (1999) A genome-wide scan reveals a maternal susceptibility locus for pre-eclampsia on chromosome 2p13. *Hum Mol Genet* 8, 1799-1805.
- 8 Bacanu SA, Devlin B, Chowdari KV, DeKosky ST, Nimgaonkar VL, Sweet RA (2002) Linkage analysis of Alzheimer disease with psychosis. *Neurology* 59, 118-120.
- 9 Bassett SS, Avramopoulos D, Perry RT, Wiener H, Watson Jr. B, Go RC, Fallin MD (2006) Further evidence of a maternal parent-of-origin effect on chromosome 10 in late-onset Alzheimer's disease. *Am J Med Genet B Neuropsychiatr Genet* 141, 537-540.
- 10 Ertekin-Taner N, Ronald J, Asahara H, Younkin L, Hella M, Jain S, Gnida E, Younkin S, Fadale D, Ohyagi Y, Singleton A, Scanlin L, de Andrade M, Petersen R, Graff-Radford N, Hutton M, Younkin S (2003) Fine mapping of the alpha-T catenin gene to a quantitative trait locus on chromosome 10 in late-onset Alzheimer's disease pedigrees. *Hum Mol Genet* 12, 3133-3143.
- 11 Farrer LA, Bowirrat A, Friedland RP, Waraska K, Korczyn AD, Baldwin CT (2003) Identification of multiple loci for Alzheimer disease in a consanguineous Israeli-Arab community. *Hum Mol Genet* 12, 415-422.
- 12 Lachmeijer AM, Arngrimsson R, Bastiaans EJ, Frigge ML, Pals G, Sigurdardottir S, St'efansson H, P'alsson B, Nicolae D, Kong A, Aarnoudse JG, Gulcher JR, Dekker GA, ten Kate LP, St'efansson K (2001) A genome-wide scan for preeclampsia in the Netherlands. *Eur J Hum Genet* 9, 758-764.
- 13 Laivuori H, Lahermo P, Ollikainen V, Widen E, Haiva-Mallinen L, Sundstrom H, Laitinen T, Kaaja R, Ylikorkala O, Kere J (2003) Susceptibility loci for preeclampsia on chromosomes 2p25 and 9p13 in Finnish families. *Am J Hum Genet* 72, 168-177.
- 14 Myers A, Holmans P, Marshall H, Kwon J, Meyer D, Ramic D, Shears S, Booth J, DeVrieze FW, Crook R, Hamshere M, Abraham R, Tunstall N, Rice F, Carty S,

- Lillystone S, Kehoe P, Rudrasingham V, Jones L, Lovestone S, Perez-Tur J, Williams J, Owen MJ, Hardy J, Goate AM (2000) Susceptibility locus for Alzheimer's disease on chromosome 10. *Science* 290, 2304-2305.
- 15 Oudejans CB, Mulders J, Lachmeijer AM, van Dijk M, Konst AA, Westerman BA, van Wijk IJ, Leegwater PA, Kato HD, Matsuda T, Wake N, Dekker GA, Pals G, ten Kate LP, Blankenstein MA (2004) The parent-of-origin effect of 10q22 in preeclamptic females coincides with two regions clustered for genes with down-regulated expression in androgenetic placentas. *Mol Hum Reprod* 10, 589-598
- 16 Braak H and Braak E. (1991) Neuropathological staging of Alzheimer-related changes. *Acta Neuropathol*, 82, 239-59.
- 17 Song W and Lahiri DK. (1995) Efficient transfection of DNA by mixing cells in suspension with calcium phosphate. *Nucleic Acids Res*, 23, 3609-11.
- 18 Vernes SC, Newbury DF, Abrahams BS, Winchester L, Nicod J, Groszer M, Alarcon M, Oliver PL, Davies KE, Geschwind DH, Monaco AP and Fisher SE. (2008) A functional genetic link between distinct developmental language disorders. *N Engl J Med*, 359, 2337-45.
- 19 Poliak S, Gollan L, Martinez R, Custer A, Einheber S, Salzer JL, Trimmer JS, Shrager P and Peles E. (1999) Caspr2, a new member of the neurexin superfamily, is localized at the juxtaparanodes of myelinated axons and associates with K⁺ channels. *Neuron*, 24, 1037-47.
- 20 Poliak S, Salomon D, Elhanany H, Sabanay H, Kiernan B, Pevny L, Stewart CL, Xu X, Chiu SY, Shrager P, Furley AJ and Peles E. (2003) Juxtaparanodal clustering of Shaker-like K⁺ channels in myelinated axons depends on Caspr2 and TAG-1. *J Cell Biol*, 162, 1149-60.
- 21 Strauss KA, Puffenberger EG, Huentelman MJ, Gottlieb S, Dobrin SE, Parod JM, Stephan DA and Morton DH. (2006) Recessive symptomatic focal epilepsy and mutant contactin-associated protein-like 2. *N Engl J Med*, 354, 1370-7.
- 22 Alarcon M, Abrahams BS, Stone JL, Duvall JA, Perederiy JV, Bomar JM, Sebat J, Wigler M, Martin CL, Ledbetter DH, Nelson SF, Cantor RM and Geschwind DH. (2008) Linkage, association, and gene-expression analyses identify CNTNAP2 as an autism-susceptibility gene. *Am J Hum Genet*, 82, 150-9.
- 23 Arking DE, Cutler DJ, Brune CW, Teslovich TM, West K, Ikeda M, Rea A, Guy M, Lin S, Cook EH and Chakravarti A. (2008) A common genetic variant in the neurexin superfamily member CNTNAP2 increases familial risk of autism. *Am J Hum Genet*, 82, 160-4.
- 24 Bakkaloglu B, O'Roak BJ, Louvi A, Gupta AR, Abelson JF, Morgan TM, Chawarska K, Klin A, Ercan-Sencicek AG, Stillman AA, Tanrivero G, Abrahams BS, Duvall JA, Robbins EM, Geschwind DH, Biederer T, Gunel M, Lifton RP and State MW. (2008) Molecular cytogenetic analysis and resequencing of contactin associated protein-like 2 in autism spectrum disorders. *Am J Hum Genet*, 82, 165-73.
- 25 Horresh I, Poliak S, Grant S, Brecht D, Rasband MN and Peles E. (2008) Multiple molecular interactions determine the clustering of Caspr2 and Kv1 channels in myelinated axons. *J Neurosci*, 28, 14213-22.
- 26 Savvaki M, Panagiotaropoulos T, Stamatakis A, Sargiannidou I, Karatzioula P, Watanabe K, Stylianopoulou F, Karageorgos D and Kleopa KA. (2008) Impairment of learning and memory in TAG-1 deficient mice associated with shorter CNS internodes and disrupted juxtaparanodes. *Mol Cell Neurosci*, 39, 478-90.
- 27 Coman I, Aigrot MS, Seilhean D, Reynolds R, Girault JA, Zalc B and Lubetzki C.

- 2
- (2006) Nodal, paranodal and juxtaparanodal axonal proteins during demyelination and remyelination in multiple sclerosis. *Brain*, 129, 3186-95.
- 28 Mitew S, Kirkcaldie MT, Halliday GM, Shepherd CE, Vickers JC and Dickson TC. (2010) Focal demyelination in Alzheimer's disease and transgenic mouse models. *Acta Neuropathol*, 119, 567-77.
- 29 Desai MK, Sudol KL, Janelins MC, Mastrangelo MA, Frazer ME and Bowers WJ. (2009) Triple-transgenic Alzheimer's disease mice exhibit region-specific abnormalities in brain myelination patterns prior to appearance of amyloid and tau pathology. *Glia*, 57, 54-65.
- 30 Sternberger NH, Sternberger LA, Ulrich J. (1985) Aberrant neurofilament phosphorylation in Alzheimer disease. *Proc Natl Acad Sci*, 82, 4274-4276
- 31 Horresh I, Bar V, Kissil JL, Peles E. Organization of myelinated axons by Caspr and Caspr2 requires the cytoskeletal adapter protein 4.1B. *J Neurosci*, 30, 2480-2489
- 32 Vaags AK, Lionel AC, Sato D, Goodenberger M, Stein QP, Curran S, Ogilvie C, Ahn JW, Drmic I, Senman L, Chrysler C, Thompson A, Russell C, Prasad A, Walker S, Pinto D, Marshall CR, Stavropoulos DJ, Zwaigenbaum L, Fernandez BA, Fombonne E, Bolton PF, Collier DA, Hodge JC, Roberts W, Szatmari P, Scherer SW. Rare deletions at the neurexin 3 locus in autism spectrum disorder. *Am J Hum Genet*, 90, 133-141
- 33 Pagnamenta AT, Bacchelli E, de Jonge MV, Mirza G, Scerri TS, Minopoli F, Chiochetti A, Ludwig KU, Hoffmann P, Paracchini S, Lowy E, Harold DH, Chapman JA, Klauck SM, Poustka F, Houben RH, Staal WG, Ophoff RA, O'Donovan MC, Williams J, Nöthen MM, Schulte-Körne G, Deloukas P, Ragoussis J, Bailey AJ, Maestrini E, Monaco AP; International Molecular Genetic Study Of Autism Consortium. Characterization of a family with rare deletions in CNTNAP5 and DOCK4 suggests novel risk loci for autism and dyslexia. *Biol Psychiatry*, 68, 320-328
- 34 Eva R, Dassie E, Caswell PT, Dick G, French-Constant C, Norman JC, Fawcett JW. (2010) Rab11 and its effector Rab coupling protein contribute to the trafficking of beta 1 integrins during axon growth in adult dorsal root ganglion neurons and PC12 cells. *J Neurosci*, 30, 11654-11669.

3

Chapter 3

SFRS7-mediated splicing of tau exon 10 is directly regulated by STOX1A in glial cells

Daan van Abel¹, Dennis R Hölzel², Shushant Jain², Fiona MF Lun³, Yama WL Zheng³, Eric Z Chen³, Hao Sun³, Rossa WK Chiu³, Dennis YM Lo³, Marie van Dijk¹, Cees BM Oudejans¹.

¹Department of Clinical Chemistry, ²Department of Clinical Genetics, Section Medical Genomics, ^{1,2}VU University Medical Center, Amsterdam, The Netherlands, ³Department of Chemical Pathology, Prince of Wales Hospital, Shatin, New Territories, Hong Kong SAR, China.

PLoS ONE, July 2011 | Volume 6 | Issue 7 | e21994

Background

In this study, we performed a genome-wide search for effector genes bound by STOX1A, a winged helix transcription factor recently demonstrated to be involved in late onset Alzheimer's disease and affecting the amyloid processing pathway.

Methodology/Principal Findings

Our results show that out of 218 genes bound by STOX1A as identified by chromatin-immunoprecipitation followed by sequencing (ChIP-Seq), the serine/arginine-rich splicing factor 7 (SFRS7) was found to be induced, both at the mRNA and protein levels, by STOX1A after stable transfection in glial cells. The increase in SFRS7 was followed by an increase in the 4R/3R ratios of the microtubule-associated protein tau (MAPT) by differential exon 10 splicing. Secondly, STOX1A also induced expression of total tau both at the mRNA and protein levels. Upregulation of total tau expression (SFRS7-independent) and tau exon 10 splicing (SFRS7-dependent), as shown in this study to be both affected by STOX1A, is known to have implications in neurodegeneration.

Conclusions

Our data further supports the functional importance and central role of STOX1A in neurodegeneration.

Introduction

Storkhead box 1 (STOX1A), a transcription factor structurally and functionally related to the forkhead family of transcription factors, characterized by a 100 amino acid DNA-binding motif termed the winged helix domain, was recently found to be a susceptibility gene for pre-eclampsia [1, 2], a hypertensive disorder of pregnancy which remains a major cause of maternal and perinatal mortality and morbidity [3]. Paradoxically, STOX1A was also found to be functionally involved in Late-Onset Alzheimer's Disease (LOAD) [4], a progressive neurodegenerative disease of the brain which is characterized by memory loss and impaired visiospatial skills involving elderly patients (>65 years) of both sexes [6]. In the latter study, van Dijk and co-workers showed that STOX1A is expressed abundantly in the brain, correlates with the severity of late onset Alzheimer's disease (LOAD) and transactivates the leucine-rich repeat transmembrane 3 (*LRRTM3*) gene [4]. Upregulation of the *LRRTM3* gene by STOX1A leads to increased amyloid- β precursor protein (APP) processing resulting in higher levels of amyloid β peptide [4]. Amyloid β deposition is a key event in the etiology of Alzheimer's disease (AD) [5, 6]. However, STOX1A transactivation of *LRRTM3* could not explain the complete STOX1A expression profile identified in the Alzheimer brain. Given the importance of this finding in neurodegeneration, but the lack of insight in the number and nature of genes controlled by STOX1A in the brain, we started a systematic search for downstream effector genes in the brain. For this, we performed a genome-wide search for STOX1A binding sites in the neuroblastoma cell-line SK-N-SH by chromatin-immunoprecipitation followed by sequencing (ChIP-Seq) [7]. Subsequently, genes selected for their involvement in pathways leading to LOAD and other neurodegenerative diseases were explored in detail.

Gene symbol	Name
RAB10	ras-related GTP-binding protein
AHCY	S-adenosylhomocysteine hydrolase
FSIP	fibrous sheath interacting protein 1
RPL17	ribosomal protein L17
SFRS7	splicing factor, arginine/serine-rich 7
CALM2	calmodulin 2
CHST12	carbohydrate (chondroitin 4) sulfotransferase
WNT2B	wingless-type MMTV integration site family
CADD45B	Growth arrest and DNA-damage-inducible, beta
CLASP1	CLIP-associating protein 1
PSMF1	proteasome inhibitor subunit 1
ACTG1	actin, gamma 1 propeptide
FANK1	fibronectin type III and ankyrin repeat domains

Table 1. STOX1A regulated genes identified using ChIP sequencing. CEAS annotation software was used to filter for regions of known functional importance for which 13 genes were positioned directly in known promoter regions.

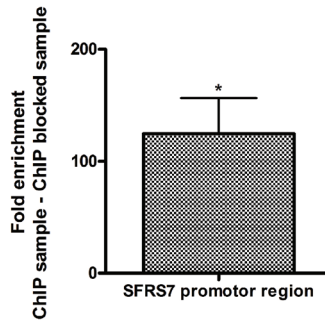


Figure 1. Validation by quantitative PCR of SFRS7 binding by STOX1A. Results show a mean 125 fold (mean $\Delta\Delta C_t$ is 6,96) enrichment for SFRS7 in STOX1A stimulated ChIP DNA compared with their negative controls (ChIP sample vs ChIP blocked sample). Bars are mean \pm SEM. Asterisks indicate $P < 0.05$ (one sample t-test with theoretical mean 0). Data were obtained from at least five independent ChIP samples from which each DNA sample was measured in triplicate.

Results

High throughput sequencing identifies a STOX1A DNA binding region in the promoter of SFRS7, a gene involved in the splicing of tau exon 10.

Using a genome-wide, antibody-independent approach, 218 genomic regions were found to be bound by STOX1A in SK-N-SH cells (Dataset S1). With the algorithm Cis-regulatory Element Annotation System (CEAS) we filtered for known functionally important genomic regions [8]. This resulted in a top list of 115 hits associated with their corresponding regulated genes (Dataset S2). Out of 13 genes directly positioned in known promoter elements (Table 1), we selected the serine/arginine splicing factor 7 (*SFRS7*) for in-depth functional analysis given its proven effect on tau exon 10 splicing [9, 17]. Misregulation of tau exon 10 splicing has a pathogenic role in neurodegenerative diseases [10, 11].

SFRS7 mRNA and protein expression levels are increased in SK-N-SH cells stably transfected with STOX1A.

Following independent confirmation by Q-PCR of the STOX1A binding site in the *SFRS7* promoter region (Fig. 1), the effect of STOX1A on *SFRS7* transcription and translation was tested in SK-N-SH cells stably transfected with STOX1A or MOCK (negative control) constructs (Fig. 2A). Both *SFRS7* mRNA (Fig. 2B) and protein levels (Fig. 2C) were found to be increased significantly and specifically upon STOX1A overexpression.

STOX1A effectuates changes in 4R/3R tau ratio in SK-N-SH cells.

Isoforms of the tau protein exhibit either three (3R) or four microtubule-binding repeats (4R) depending on alternative splicing of tau exon 10 [11]. As it has been shown that *SFRS7* effects tau 4R splicing [9, 17], we argued that the increased *SFRS7* transcript levels cause a change in tau 4R/3R ratios. Indeed, STOX1A leads to a significant increase in the tau 4R/3R ratio (Fig. 2D). Secondly, endogenous total tau levels were also elevated, both at the mRNA (Fig. 3A) and protein levels (Fig. 3B).

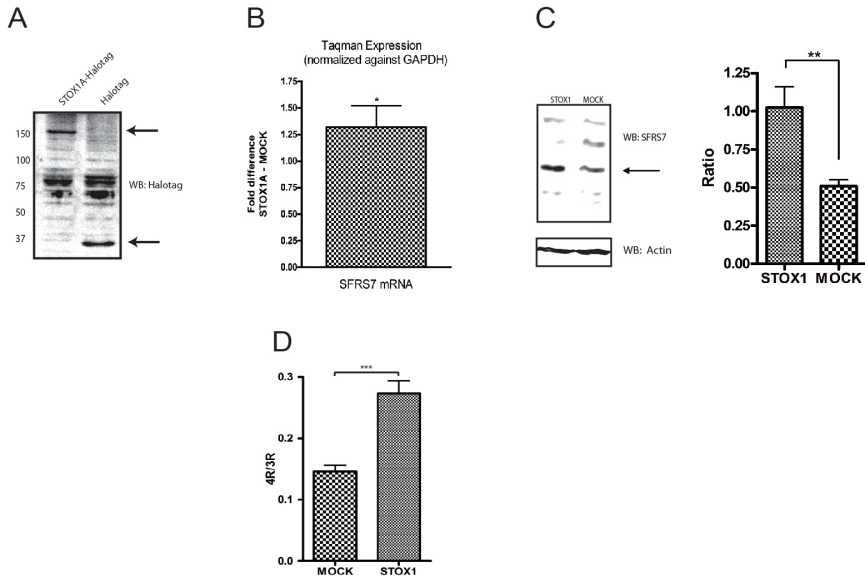


Figure 2. STOX1A-induced SFRS7 expression is followed by increased tau splicing in SK-N-SH cells. (A) Expression of STOX1A protein was determined with an anti-Halotag specific antibody by western blot using total cell protein extracts obtained from stable STOX1A (left lane) and MOCK (right lane) transfected SK-N-SH cells. A specific band representing STOX1A-halotag protein was observed at its expected size of 150 kd. Halotag protein (MOCK) was detected at its expected size of 34 kd. Western blot image is a representative of at least 3 independent experiments. (B) Quantitative RT-PCR data shows a mean 1.32 fold (mean $\Delta\Delta Ct$ is 0,4) increased mRNA expression for SFRS7. Bars are mean \pm SEM. * indicate $P < 0.05$ (one sample t-test with theoretical mean 0). N = 4, each sample was measured in triplicate. (C, left image) Expression of endogenous SFRS7 protein was determined with an SFRS7 specific antibody by western blot using total cell protein extracts obtained from stable STOX1A and MOCK transfected SK-N-SH cells. An antibody specific for actin was used as a loading control. (C, right graph) Quantification of SFRS7 protein was performed using densitometry. The ratio number of obtained band intensities for STOX1A divided by actin was compared to the ratio number of obtained band intensities for MOCK divided by actin for 3 independent experiments. A significant increase for the STOX1A ratio number was found compared to the MOCK ratio number. P -values were calculated using two-tailed unpaired t-test, error bars represent \pm SEM, ** indicate $P < 0.01$. (D) Ratio numbers were obtained by dividing endogenous 4R and 3R tau mRNA concentrations for SK-N-SH cells stably transfected with STOX1A or MOCK constructs. Endogenous 4R and 3R mRNA concentrations were obtained as described in the material and methods section. A highly significant increase of the 4R/3R tau ratio was seen for STOX1A compared to MOCK transfected cells. P -values were calculated using two-tailed unpaired t-test, error bars represent \pm SEM, *** indicate $P < 0.001$. N = 4, each sample was measured in triplicate.

SFRS7-dependent tau exon 10 splicing by STOX1A is specific for glial cells.

The cell line, SK-N-SH, we used for the above *in-vitro* experiments comprises a heterogeneous subpopulation of neuroblastic (N-type) and substrate-adherent (S-type) cells [12–15]. As we observed a change in morphology due to clonal selection following stable transfection (Fig. 4A vs 4B) we tested the possibility that the phenomenon we observed was cell-specific, i.e. either restricted to the neuroblastic (N-type) or glial (S-type) cell. Immunostaining for disialoganglioside (GD2) (Figs. 4C, -D) and calcyclin (Figs. 4E–F) showed the stably-transfected cells to consist of glial cells (S-type) only (calcyclin- positive, GD2-negative) [15]. Furthermore, no significant changes in SFRS7 expression and tau 4R/3R ratios were found upon stable transfection of STOX1A in the SK-N-SH N-type subclone cell-lineage SH-

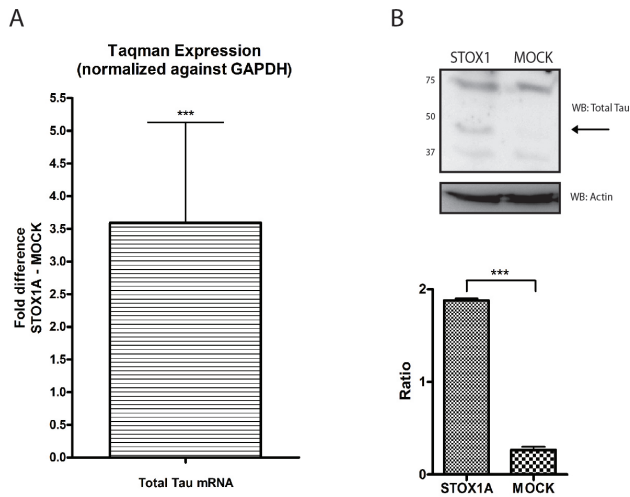


Figure 3. STOX1A upregulates total tau RNA and protein levels in stable transfected SK-N-SH cells. (A) Quantitative RT-PCR show a mean 3,59 fold (mean $\Delta\Delta C_t$ 1,84) increased mRNA expression for total tau. Bars are mean \pm SEM. $P < 0.05$ (one sample t-test with theoretical mean 0). $N = 4$, each sample was measured in triplicate. (B, upper image) Expression of endogenous total tau protein was determined with a total tau specific antibody by western blot using total cell protein extracts obtained from stable STOX1A and MOCK transfected SK-N-SH cells. An antibody specific for actin was used as a loading control. Western blot image is a representative of at least 3 independent experiments. (B, lower graph) Quantification of total tau protein was performed using densitometry. The ratio number of obtained band intensities for STOX1A divided by actin was compared to the ratio number of obtained band intensities for MOCK divided by actin for 3 independent experiments. A significant increase for the STOX1A ratio number was found compared to the MOCK ratio number. P -values were calculated using two-tailed unpaired t-test, error bars represent SEM, *** indicate $P < 0.001$.

SY5Y (data not shown). Given this, and to independently confirm that the effect of STOX1A on exon 10 tau splicing via SFRS7 is glial cell-specific, we tested U-373 MG cells as a cellular model for glial cells. To confirm that in the STOX1A-SFRS7-tau splicing pathway, the effect of SFRS7 on tau splicing is direct in U-373 MG cells we performed siRNA knockdown experiments against SFRS7 in the untransfected U-373 MG cell-line and measured 3R and 4R tau concentrations for SFRS7 siRNA treated and control samples to calculate 4R/3R tau ratios. Significant SFRS7 knockdown was confirmed by measuring endogenous SFRS7 mRNA levels (Fig. 5A) and protein levels on western blot (Fig. 5B). Furthermore, a significant decrease in the 4R/3R ratio for SFRS7 siRNA treated cells was seen compared to the scrambled control (Fig. 5C) which was confirmed on western blot (Fig. 5D). Next, we stably transfected U-373 MG cells with STOX1A to determine the effect of STOX1A on tau exon 10 splicing via SFRS7. First, we characterized the STOX1A expression pattern in U-373 MG cells using immunofluorescence which showed strong nuclear (Fig. 6A, -C) staining for STOX1A protein. Furthermore, expression of STOX1A was confirmed on western blot (Fig. 6G). Secondly, we determined the effect of stable STOX1A expression on SFRS7 expression and tau exon 10 splicing. Identical effects on SFRS7 mRNA (Fig. 7A) and protein (Fig. 7B) levels were seen as for the SK-N-SH (S-type) cells (Fig. 2). Furthermore, 4R/3R tau ratio's (Fig. 7C) were significantly increased which was confirmed on western blot (Fig. 7D) thereby showing the effect of STOX1A on tau processing via SFRS7 in glial cells. Finally, as for the SK-N-SH

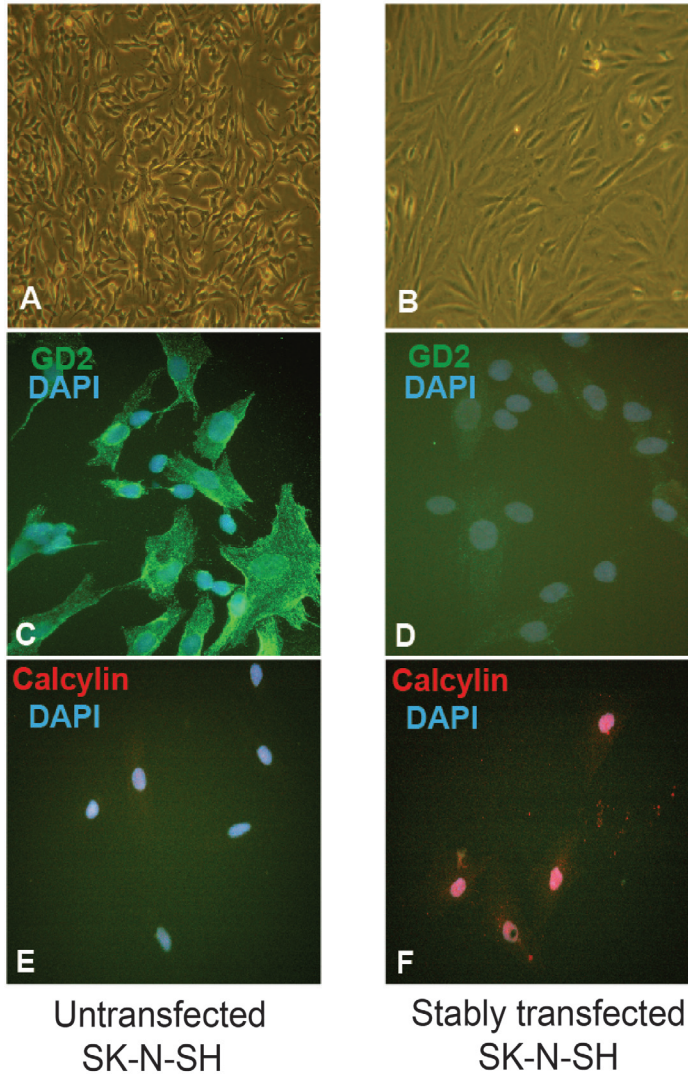


Figure 4. Stably transfected SK-N-SH cells consist of glial cells only. (A) Morphology of untransfected SK-N-SH cells or (B) stably transfected SK-N-SH cells. The G418 (Roche) antibiotic selection procedure for selection of positive STOX1A and MOCK stable transfected cells resulted by clonal selection in a homogeneous cell population that is composed of the glial (S-type) type. (C) Immunophenotype of untransfected SK-N-SH cells showing intense membrane staining for GD2 but lack nuclear calcylin staining (E). No GD2 membrane staining was observed in stably transfected SK-N-SH cells (D) while cells show high calcylin nuclear staining (F). Green: GD2, Red: Calcylin, Blue: DAPI.

(S-type) cells (Fig. 3), significantly increased endogenous total tau expression, both at the mRNA (Fig. 8A) and protein levels (Fig. 8B), was seen upon stable STOX1A overexpression in the U-373 MG cell-line.

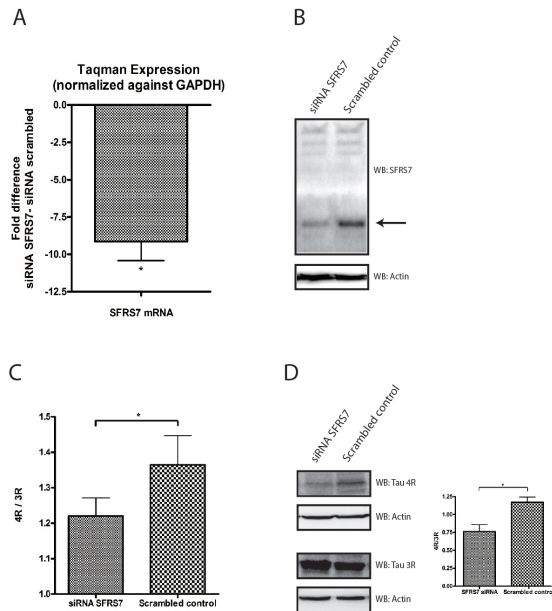


Figure 5. SFRS7 acts as a tau exon 10 splicing enhancer in the glial cell-line U-373 MG. (A) Knockdown of endogenous SFRS7 protein was determined with quantitative RT-PCR showing a mean 9,13 fold (mean $\Delta\Delta\text{Ct}$ 3.19) decreased endogenous mRNA expression for SFRS7. Bars are mean \pm SEM. * indicate $P < 0.05$ (one sample t-test with theoretical mean 0). N= 4, each sample was measured in triplicate. (B) Knockdown of endogenous SFRS7 protein was determined with a SFRS7 specific antibody by western blot using total cell protein extracts obtained from SFRS7 siRNA and scrambled transfected U-373 MG cells. An antibody specific for actin was used as a loading control. Westernblot image is a representative of at least 3 independent experiments. (C) Ratio numbers were obtained by dividing endogenous 4R and 3R tau mRNA concentrations from U373-MG cells transfected with siRNA SFRS7 or scrambled siRNA. Endogenous 4R and 3R mRNA concentrations were obtained as described in the material and methods section. A significant decrease of the 4R/3R tau ratio was seen for siRNA SFRS7 compare to scrambled siRNA transfected cells. P -values were calculated using two-tailed unpaired t-test, error bars represent \pm SEM, * indicate $P < 0.05$. N= 4, each sample was measured in triplicate. With the use of densitometry on obtained westernblot images (D) a similar significant decrease of the 4R/3R tau ratio was seen on a protein level (D, right graph). Significance was calculated by combining the densitometry data from 3 independent experiments. P -values were calculated using two-tailed unpaired t-test, error bars represent \pm SEM, * indicate $P < 0.05$

Discussion

Here we describe the genome-wide exploration of genomic regions bound by STOX1A in the neuroblastoma cell-line SK-N-SH. For this, an antibody-free chromatin immunoprecipitation procedure was used followed by massively parallel sequencing. Of the genes bound, the SFRS7 gene was selected for in-depth functional analysis. We found that SFRS7-mediated splicing of tau exon 10 is directly regulated by STOX1A in glial cells. Previously we showed the effect of STOX1A on the amyloid pathway in neuronal SK-N-SH cells [4]. Here we show the effect of STOX1A on both total tau expression as well as tau processing (exon 10 splicing) in glial cells. The effect of STOX1A on tau expression and processing additionally confirms the role of this transcription factor in central pathways underlying neurodegeneration including AD. The data on tau splicing appear initially in conflict with the observation made by Gao and co-workers who found that SFRS7 acts as a tau exon 10 splicing silencer in SK-

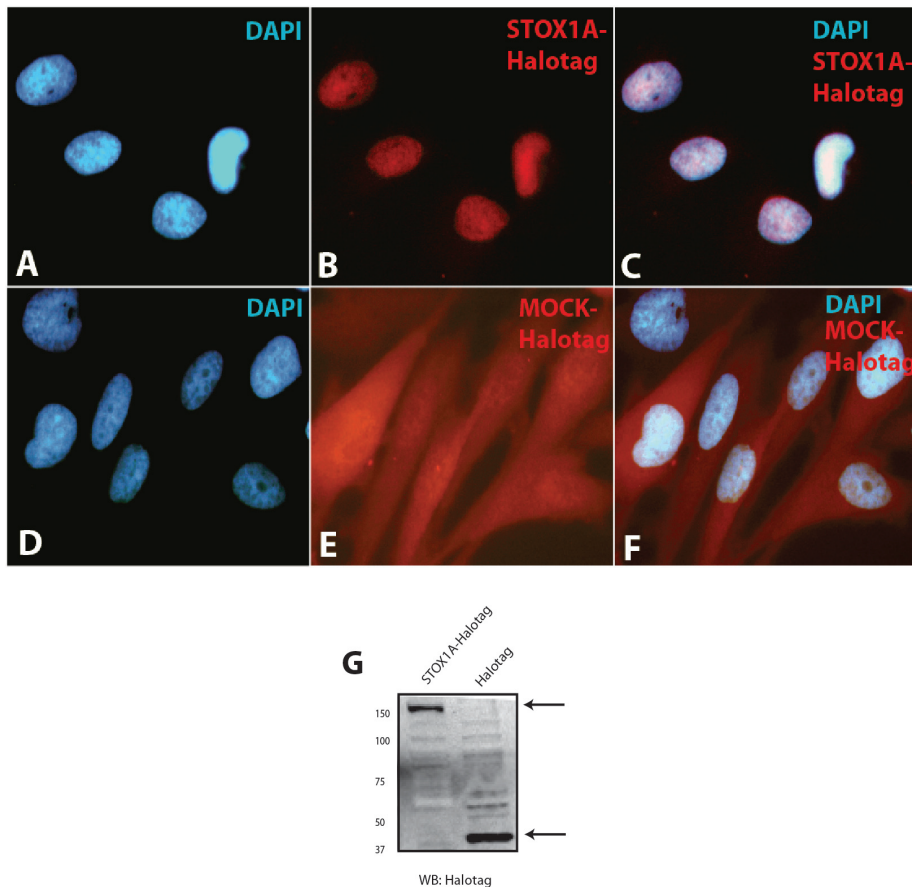


Figure 6. Expression analysis of STOX1A in stable transfected U-373 MG cells. (A, –C) Immunofluorescence shows primarily nuclear staining for STOX1A-Halotag protein in stable transfected U-373 MG cells while stable MOCK-Halotag transfected U-373 MG cells shows diffuse cytoplasmic staining (D, –F). (G) Expression of STOX1A protein was determined with an anti-Halotag specific antibody by western blot using total cell protein extracts obtained from stable STOX1A (left lane) and MOCK (right lane) transfected U373 cells. A specific band representing STOX1Ahalotag protein was observed at its expected size of 150 kd. Halotag (MOCK) protein was detected at its expected size of 34 kd. Westernblot image is a representative of at least 3 independent experiments.

N-SH cells thereby decreasing the ratio of 4R/3R tau [9]. Our results show the reverse. However, we cannot exclude that Gao and co-workers used a mixed SK-N-SH cell population consisting of primarily N-type and little S-type cells, while ours consisted of the S-type subpopulation only. Possibly, in our situation, the S-type cells transfected more easily. Therefore, transfected S-type cells were able to overgrow the N-type cells which died from the neomycin selection. This resulted in a cell population consisting of the S-type subpopulation only. Furthermore, while our results indicate that SFRS7 acts as a splicing enhancer in the S-type of cells, the effect of STOX1A on SFRS7 is also restricted to the S-type cells whereas we could not find any significant changes in SFRS7 expression upon stable STOX1A expression in the N-type subclone cell line SH-SY5Y (data not shown). This does not exclude the role of SFRS7 acting as a tau

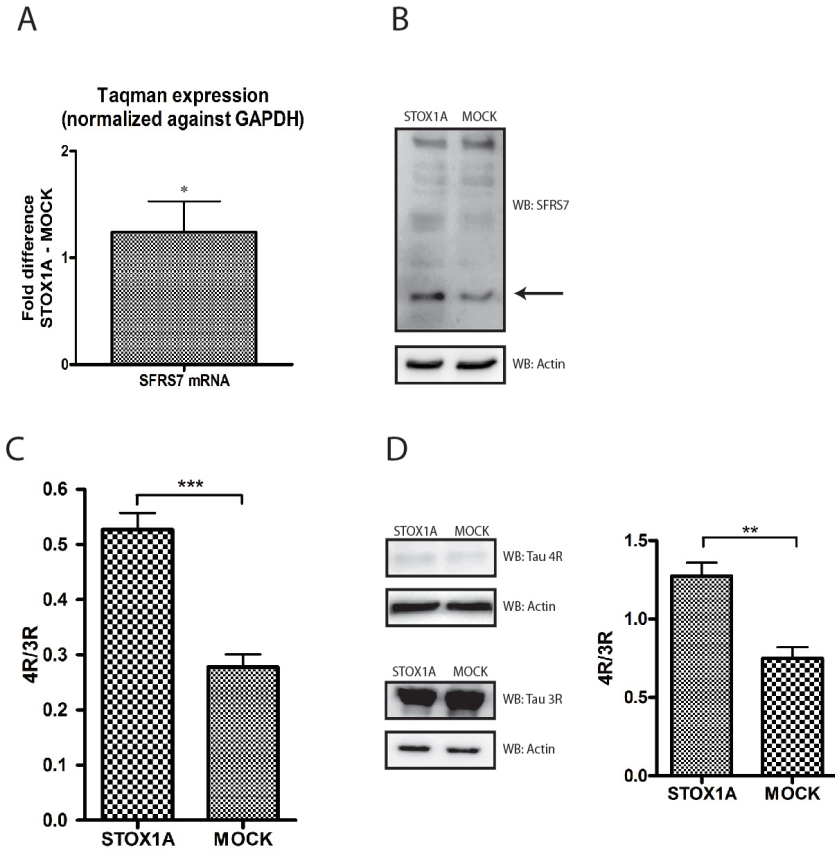


Figure 7. Tau exon 10 splicing is increased upon stable STOX1A overexpression via SFRS7 in U-373 MG cells. (A) Quantitative RT-PCR shows a mean 1,24 fold (mean $\Delta\Delta Ct$ is 0,306) increased mRNA expression for SFRS7. Bars are mean \pm SEM. * indicate $P < 0.05$ (one sample t-test with theoretical mean 0). N = 4, each sample was measured in triplicate. (B) Expression of endogenous SFRS7 protein was determined with a SFRS7 specific antibody by western blot using total cell protein extracts obtained from stable STOX1A and MOCK transfected U-373 MG cells. Western blot image is a representative of at least 3 independent experiments. (C) Ratio numbers were obtained by dividing endogenous 4R and 3R tau mRNA concentrations for U373-MG cells stably transfected with STOX1A or MOCK constructs. Endogenous 4R and 3R mRNA concentrations were obtained as described in the material and methods section. A highly significant increase of the 4R/3R tau ratio was seen for STOX1A compare to MOCK transfected cells. P -values were calculated using two-tailed unpaired t-test, error bars represent \pm SEM, *** indicate $P < 0.001$. N = 4, each sample was measured in triplicate. With the use of densitometry on obtained westernblot images (D) a similar significant decrease of the 4R/3R tau ratio was seen on a protein level. Significance was calculated by combining the densitometry data from 3 independent experiments. P -values were calculated using two-tailed unpaired t-test, error bars represent \pm SEM, * indicate $P < 0.05$

exon 10 splicing silencer in the neuronal S-type cells, in fact, SFRS7 has been shown to suppress tau exon 10 inclusions in the neuroblastoma cell-line SH-SY5Y by Ding et al. [17]. Given this, we hypothesize that both the function of SFRS7 acting as a splicing enhancer or silencer, and the effect of STOX1A on SFRS7 expression is cell-type dependent (neuronal versus glial). Therefore our aim was to further investigate the function of STOX1A on SFRS7 in glial cells where SFRS7 acts as an exon 10 splicing enhancer. This theory is supported by our finding that knockdown of SFRS7

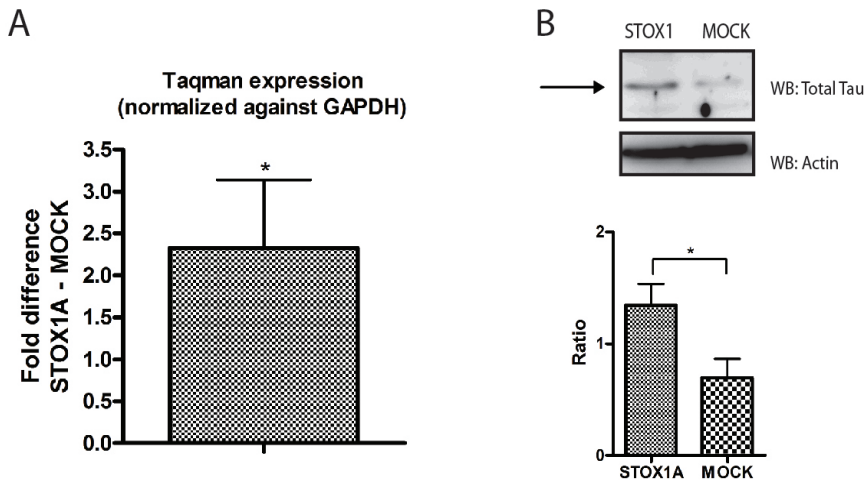


Figure 8. STOX1A effectuates endogenous total tau expression in U-373 MG cells. (A) Quantitative RT-PCR show a mean 2,33 fold (mean $\Delta\Delta C_t$ is 1,22) increased mRNA expression for total tau. Bars are mean \pm SEM. * indicate $P < 0.05$ (one sample t-test with theoretical mean 0). N= 4, each sample was measured in triplicate. (B) Expression of endogenous total tau protein was determined with a total tau specific antibody by westernblot using total cell protein extracts obtained from STOX1A and MOCK transfected U-373 MG cells. An antibody specific for actin was used as a loading control. Westernblot image is a representative of at least 3 independent experiments. (B, lower graph) Quantification of total tau protein was performed using densitometry. The ratio number of obtained band intensities for STOX1A divided by actin was compared to the ratio number of obtained band intensities for MOCK divided by actin for 3 independent experiments. A significant increase for the STOX1A ratio number was found compared to the MOCK ratio number. P -values were calculated using two-tailed unpaired t-test, error bars represent \pm SEM, *** indicate $P < 0.001$.

in the U-373 MG cell-line shows an decrease in the 4R/3R tau ratio while stable over-expression of STOX1A, which induces SFRS7 expression, increases the 4R/3R tau ratio.

The opposite effect on tau exon 10 splicing seen after SFRS7 downregulation, as shown for glial cells in this paper, supports the cell type dependent regulation of this splicing factor which was also observed by Ding and co-workers [17]. Possibly, SFRS7 acts as a tau exon 10 splicing enhancer in glial cells by binding to yet to be discovered exonic and intronic enhancers, which would not be surprising because it has been shown that SFRS7 mainly acts as a splicing enhancer, instead of silencer as shown by Gao and co-workers [17–20].

In LOAD, neurofibrillary tangles are one of the main hallmarks [21]. While we previously found that in advanced stages of LOAD (Braak 3–6), STOX1A primarily stains positive in hippocampal neurons with neurofibrillary tangles (but also microglia) [4], the implication in LOAD with our presented findings for STOX1A in glial cells would therefore be possibly limited. However, while STOX1A expression is found primarily in the brain and dysregulation of the balance between glial 4R/3R tau ratio by a selective increase in either 3R-tau or 4R-tau is commonly seen in a range of diverse neurodegenerative diseases other than LOAD, including frontotemporal dementia with Parkinsonism linked to chromosome 17 (FTDP-17), Pick's disease (PD), progressive supra nuclearpalsy (PSP), and corticobasal degeneration [22],

further exploration of where STOX1A and/or SFRS7 expression are found in these neurodegenerative diseases would yield great insight into their involvement.

Interestingly, independently of SFRS7 transactivation by STOX1A we also observed a significant increase in total tau mRNA and protein levels in both SK-N-SH (S-type) and U-373 MG cells. While this effect is not seen after knockdown of SFRS7, this effect is also STOX1A-dependent. As no binding site was identified for STOX1A in the tau promoter (Dataset S1), it would therefore be interesting to further investigate which gene, other than tau or SFRS7 but bound by STOX1A, controls total tau expression in glial cells.

Although we selected a single gene for functional analysis, combined or follow-up analysis of the other genes identified will likely generate novel results providing and permitting mechanistic insight in pathways important for e.g. neurodegeneration. The antibody-free ChIP procedure can be applied to other transcription factors and cellular systems as well and is highly informative when combined with massively parallel sequencing as done in the present paper.

In conclusion, while previous findings by van Dijk and co-workers have shown a functional link between STOX1A and LOAD, we here provide further evidence that STOX1A has important functions in the pathways leading to neurodegeneration.

Materials and Methods

Cell culture and transfection

SK-N-SH human neuroblastoma cells were obtained from the American Type Culture Collection (ATCC, Manassas, VA). All reagents for cell culture were purchased from Invitrogen Life Technologies, Inc. (Burlington, Canada). SK-N-SH and U-373 MG cells were cultured at 37°C in a humidified atmosphere of 5% CO₂ in Iscove's Modified Dulbecco's Medium (IMDM) supplemented with 10% fetal calf serum and 100 U/ml penicillin, and 100 g/ml streptomycin. Cells were subcultured in medium every 2–3 days following harvesting by trypsinization (HBSS containing 5% trypsin). The ORF (Open Reading Frame) of the STOX1A gene was subcloned into the Halotag pF5K neomycin CMV Flexi vector according to the manufacturers protocol (Promega). For transfection the calcium phosphate method was used [16]. Briefly, at the time of transfection, cells were at 70% confluence. By vortexing 2X HEBS (HEPES-buffered saline) with a solution of 2.5 M CaCl₂ and 20 µg of plasmid DNA a co-precipitate of DNA and CaPO₄ was allowed to form. After incubation for 30 min at room temperature, the precipitate was added to the cells and the medium was changed after 24 h. Cells were used 48 h post-transfection for further analysis.

For stable transfections SK-N-SH or U-373 MG cells were transfected either with the pF5K-STOX1A or empty pF5K constructs. Selection of positive clones was possible due to the presence of the neomycin resistant gene present in the constructs. Positive clones were maintained in complete IMDB medium supplemented with 800 µg/ml G418 (Roche) until reaching confluence and subcultured every 2–3 days for about 4 weeks. A population of positive clones was harvested for further analysis. As confirmed with qRT-PCR (See below) using TaqMan probes (Applied Biosystems) for STOX1A, two stable SK-N-SH cell-lines which over-expressed STOX1A 25 and

30 fold, and 6 stable U-373 MG cell-lines with a mean 64 fold over-expression of STOX1A were selected. Protein expression of the STOX1A-Halotag proteins was confirmed by western blot.

Additionally, plasmid DNA quantification using qPCR (see below) with primers and probe specific for the constructs backbone showed similar copy numbers in each cell-line.

Knockdown of endogenous SFRS7 was performed by transfecting siRNA's against SFRS7 and control siRNA (Santa Cruz) in untransfected U-373 MG cells with Lipofectamine™ RNAiMAX (Invitrogen) according to the manufactures protocol. Cells were harvested 48 hours post-transfection and RNA was isolated as described in the Quantitative PCR and RT-PCR section.

Chromatin immunoprecipitation

Transfected cells were treated with formaldehyde to create protein-DNA crosslinks. Cytoplasmatic lysis was performed to reduce competition of cytoplasmatic STOX1A-Halotag proteins against nuclear STOX1A-Halotag proteins with the Halotag resin. Nuclear lysate was subsequently fragmented by sonication. The nuclear lysates were split into two equal parts of which one was treated with Halotag blocking ligand to function as a negative control. Both the samples and controls were treated using Halotag resin according to the Halo-ChIP system protocol in the presence of proteinase inhibitors. After reversal of crosslinks the DNA was purified using the Qiaquick PCR purification kit (Qiagen). The ChIP-Seq method can be found in the additional material section (Text S1).

Quantitative PCR and RT-PCR

Standard quantitative PCR was performed on an ABI7300 (Applied Biosystems) using probes (5'-FAM 3'-TAMRA labeled SFRS7 probe 5'-CGCCCAGGGCTCGA GTGAC-3') and primers (SFRS7 forward: 5'-ACGCGACATGATGACAGAC- 3', SFRS7 reversed: 5'-CGCATATATAAACGCGAACC-3') specific for the SFRS7 region obtained in the ChIP-Seq experiments in the presence of 1M betaine and ROX reference dye, and corrected for input using the non-intron-spanning Glyceraldehyde 3-phosphate dehydrogenase (GAPDH) gene expression assay (Applied Biosystems). Input ChIP DNA was obtained from at least five independent ChIP experiments.

RNA isolation from transfected cells was performed using the RNeasy kit (Qiagen) including on-column DNase treatment. Quantitative RT-PCR using gene expression assays (Applied Biosystems) for SFRS7 and total tau was performed on an ABI7300. In addition, transfection efficiencies were corrected by plasmid DNA quantification using the pF5 CMV-neo Flexi® Vector backbone present in all plasmids (pF5 forward: 5'-GCTTCGAGCAGACATGATAAG-3', pF5 reversed: 5'-AGCAATAGCATCACAAA TTTCA-3', 5'-FAM 3'-TAMRA labeled pF5 probe: 5'-TGGACAAACCACAACT AGAATGCAGT-3'). Data were obtained from at least four transfections from which each RNA sample was measured in triplicate.

Western blot

Protein lysates from stable transfected cells were obtained by directly scraping cells into loading Buffer including β -mercaptoethanol. Lysates were separated by SDS-polyacrylamide gel electrophoresis, and electroblotted onto a PVDF-membrane. An antibody recognizing the Halotag protein (Promega) was used in combination with goat anti-rabbit horseradish peroxidase-conjugated secondary antibody (DAKO). To detect endogenous levels of SFRS7 and tau, SFRS7 antibody (9G8, Santa Cruz) or total tau antibody (Abcam) was used in combination with donkey anti-goat IgG horseradish peroxidase-conjugated secondary antibody (Santa Cruz) and goat anti-rabbit horseradish peroxidase-conjugated secondary antibody (DAKO), respectively. Mouse monoclonal antibodies specific for the tau 3R (RD3, clone 8E6/C11) or 4R (RD4, clone 1E1/A6) splice variants were obtained from Millipore and used in combination with goat anti-mouse horseradish peroxidase-conjugated secondary antibody (DAKO). Endogenous actin used for loading controls was detected with mouse monoclonal anti-actin antibody (Sigma Aldrich) used in combination with goat anti-mouse horseradish peroxidase-conjugated secondary antibody (DAKO). Protein bands were detected by an enhanced-chemiluminescence assay (GE Healthcare) on a LAS3000.

Immunofluorescence

For immunofluorescence, untransfected and stable transfected SK-N-SH cells were grown on glass coverslips. Coverslips were fixed in 4% (PFA) paraformaldehyde for 15 min at room temperature. After fixation, coverslips were rinsed in PBS, 0.1% Triton X-100 and incubated with 1% Triton X-100 in PBS for 15 min at room temperature for permeabilization. Coverslips were washed in wash buffer (PBS, 0.1% Triton X-100, 2% BSA (Bovine serum albumin)) blocked with PBS, 0.1% Triton X-100, 5% BSA for 1 h and incubated with Calcyclin (Santa Cruz biotechnology) or GD2 (BD Pharmingen) antibody at 4°C overnight.

After washing with wash buffer, cells were incubated for 1 hour with the appropriate secondary antibodies conjugated with Alexa Fluor 488 or Alexa Fluor 568 (Invitrogen), washed with washing buffer and mounted with vectashield mounting solution containing DAPI for DNA counterstaining (Vector Laboratories).

For STOX1A-Halotag immunofluorescence, stable transfected cells grown on coverslips were incubated with TMR-Halotag ligand according the manufactures instructions (Promega). Coverslips were fixed in 4% (PFA) paraformaldehyde for 15 min at room temperature. After fixation, coverslips were washed with washing buffer and mounted with vectashield mounting solution containing DAPI for DNA counterstaining (Vector Laboratories).

Tau splicing Assay and ratio calculation

qRT-PCR was performed with RNA isolated from the stable STOX1A transfected SK-N-SH and U-373 MG cell-lines and transiently transfected SFRS7 and scrambled siRNA U-373 MG cells on a Lightcycler 480 (Roche) using the SYBR Green master kit and primers specific for the 3R (3R-forward: 5'-GGAAGGTGCAAATAGTC-3', 3R-reversed: 5'-CGACTGGACTCTGTCCTTGA-3') or 4R tau

(4R-forward: 5'-CGGGAAGGTGCAGATAATTAA-3', 4R-reversed: 5'-GCCTAATGAGCCACACTTGGAG-3') isoforms. Due to the high degree of homology between 3R and 4R isoforms, the 3R 5'-3' primer has 4 Locked Nucleic Acid (LNA) modifications to ensure specificity. cDNA was synthesized with the SuperScript III Reverse Transcriptase kit (Invitrogen). Constructs containing the 3R or 4R tau isoforms with known DNA concentrations were used for the generation of a standard curve (concentrations for the constructs containing the 3R isoform were 10^{-2} , 10^{-3} , 10^{-4} , 10^{-5} and 10^{-6} ng/ μ l and for the constructs containing the 4R isoform 10^{-3} , 10^{-4} , 10^{-5} , 10^{-6} and 10^{-7} ng/ μ l). Experimental samples were measured and concentrations calculated by comparison to the standard curve. Tau ratios were calculated by dividing the mean 4R tau concentrations by the mean 3R tau concentrations of the treated samples. The same was done for the control treated samples. An unpaired t-test was used to calculate significance between the treated 4R/3R tau ratio and control treated 4R/3R tau ratio. Error bars represent \pm SEM.

Data analysis

For Real-time PCR data, a threshold cycle number, Ct, was measured as the PCR cycle at which the amount of amplified target reaches the threshold value. Quantification was determined by the $2^{-\Delta\Delta C_t}$ method as described in Applied Biosystems "Guide to Performing Relative Quantitation of Gene Expression Using Real-Time Quantitative PCR", Section VII, Relative Quantitation of Gene Expression Experimental Design and Analysis (http://www3.appliedbiosystems.com/cms/groups/mcb_support/documents/generaldocuments/cms_042380.pdf). Statistical analysis of the obtained data was carried out with the GraphPad Prism program.

For quantification of westernblots densitometry was used. Westernblot pictures were analysed with the software ImageJ according to the tutorial described on the website: <http://lukemiller.org/index.php/2010/11/analyzing-gels-and-western-blots-with-image-j/>. Statistical analysis on the obtained density values was carried out with Microsoft Excell and the GraphPad Prism program.

Acknowledgments

The human astrocytoma cell line U-373 MG was obtained from the American Type Culture Collection (ATCC; Rockville, MD, USA), and kindly provided by Dr. R. Veerhuis (Clinical Chemistry dept., VUMC).

Author Contributions

Conceived and designed the experiments: DvA MvD CBMO. Performed the experiments: DvA FMFL YWLZ EZC HS DRH. Analyzed the data: DvA RWKC YMDL SJ MvD CBMO. Contributed reagents/materials/analysis tools: SJ YMDL. Wrote the paper: DvA MvD CBMO.

Supporting Information

Dataset S1.

BED file as outputted by QuEST. The BED file provided can be directly uploaded into the UCSC browser (<http://genome.ucsc.edu/>) as a custom track. The human assembly (NCBI36/hg 18) was selected as reference genome. Custom tracks show genomic regions in blue and potential binding peaks in red as calculated by QuEST. (<http://www.plosone.org/article/fetchSingleRepresentation.action?uri=info:doi/10.1371/journal.pone.0021994.s001>)

Dataset S2.

Regions (BED file, Dataset S1) of functional importance generated by CEAS as RefSeq genes. Can be opened in Microsoft Excell.

(<http://www.plosone.org/article/fetchSingleRepresentation.action?uri=info:doi/10.1371/journal.pone.0021994.s002>)

Text S1. Supplementary ChIP sequencing methods.

Massively Parallel Genomic Sequencing

Multiple samples of precipitated HaloChIP DNA were validated with QPCR on enrichment with a confirmed STOX1 bound region found in a previously performed ChIP-shotgun cloning procedure (Data not shown). Enriched samples were pooled and used for high-throughput sequencing (ChIP-Seq) on a Genome Analyzer IIx (Illumina). 10–80 ng of pooled HaloChIP DNA was used for DNA library construction by the Genomic DNA Sample Preparation Kit (Illumina) following the manufacturer's protocol of sample preparation for ChIP-Sequencing of DNA. Enriched adapter-ligated DNA fragments in the range of 200–350 bp were size selected using 2% agarose electrophoresis. The selected DNA libraries were then additionally amplified using a 15-cycle PCR. The adapter ligated DNA was purified directly using spin columns provided in a QIAquick PCR purification kit (Qiagen).

Sequence Alignment

Single-read sequencing for 36 cycles was performed. All 36-bp sequence reads were aligned to the repeat-masked human genomic reference sequence (NCBI Build 36, version 48) downloaded from the Ensembl Genome Browser (<http://www.ensembl.org>), using the ELAND program in the GAPipeline-1.4.0 software package provided by Illumina. A result output file was generated after running ELAND.

ChIPseq peak calling

For peak calling we used the ELAND output files in the program QuEST 2.4. Firstly, ChIP default parameters were selected for a transcription factor with defined motif and narrow binding site (bandwidth = 30 bp and region size = 300 bp). Stringent peak calling parameters were then selected as recommended by QuEST (ChIP threshold = 0.164, Enrichment fold = 3 and Rescue fold = 3).

Each peak was ranked according to a Q-value produced from the p-values calculated by Benjamini correction in QuEST. This ranking indicated the certainty of enrichment between the experimental versus control data on a genome-wide level.

References

- 1 van Dijk M, Mulders J, Poutsma A, Konst AA, Lachmeijer AM, et al. (2005) Maternal segregation of the Dutch preeclampsia locus at 10q22 with a new member of the winged helix gene family. *Nat Genet* 37: 514–519.
- 2 Brennan RG (1993) The winged-helix DNA-binding motif: another helix-turnhelix takeoff. *Cell* 74: 773–776.
- 3 Duley L (2009) The global impact of pre-eclampsia and eclampsia. *Semin Perinatol* 33: 130–137.
- 4 van Dijk M, van Bezu J, Poutsma A, Veerhuis R, Rozemuller AJ, et al. (2010) The pre-eclampsia gene *STOX1* controls a conserved pathway in placenta and brain upregulated in late-onset Alzheimer's disease. *J Alzheimers Dis* 19: 673–679.
- 5 Newman M, Musgrave IF, Lardelli M (2007) Alzheimer disease: amyloidogenesis, the presenilins and animal models. *Biochim Biophys Acta* 1772: 285–297.
- 6 Hardy J, Allsop D (1991) Amyloid deposition as the central event in the aetiology of Alzheimer's disease. *Trends Pharmacol Sci* 12: 383–388.
- 7 Schuster SC (2008) Next-generation sequencing transforms today's biology. *Nature Methods* 5: 16–18.
- 8 Shin H, Liu T, Manrai AK, Liu XS (2009) CEAS: cis-regulatory element annotation system. *Bioinformatics* 25: 2605–2606.
- 9 Gao L, Wang J, Wang Y, Andreadis A (2007) SR protein 9G8 modulates splicing of tau exon 10 via its proximal downstream intron, a clustering region for frontotemporal dementia mutations. *Mol Cell Neurosci* 34: 48–58.
- 10 Ksiezak-Reding H, Shafit-Zagardo B, Yen SH (1995) Differential expression of exons 10 and 11 in normal tau and tau associated with paired helical filaments. *J Neurosci Res* 41: 583–593.
- 11 Goedert M, Spillantini MG, Potier MC, Ulrich J, Crowther RA (1989) Cloning and sequencing of the cDNA encoding an isoform of microtubule-associated protein tau containing four tandem repeats: differential expression of tau protein mRNAs in human brain. *EMBO J* 8: 393–399.
- 12 Biedler JL, Helson L, Spengler BA (1973) Morphology and growth, tumorigenicity, and cytogenetics of human neuroblastoma cells in continuous culture. *Cancer Res* 33: 2643–2652.
- 13 Barnes EN, Biedler JL, Spengler BA, Lyser KM (1981) The fine structure of continuous human neuroblastoma lines SK-N-SH, SK-N-BE(2), and SK-N-MC. *In Vitro* 17: 619–631.
- 14 Ross RA, Spengler BA, Biedler JL (1983) Coordinate morphological and biochemical interconversion of human neuroblastoma cells. *J Natl Cancer Inst* 71: 741–747.
- 15 Acosta S, Lavarino C, Paris R, Garcia I, de Torres C, et al. (2009) Comprehensive characterization of neuroblastoma cell line subtypes reveals bilineage potential similar to neural crest stem cells. *BMC Dev Biol* 9: 12.
- 16 Song W, Lahiri DK (1995) Efficient transfection of DNA by mixing cells in suspension with calcium phosphate. *Nucleic Acids Res* 23: 3609–3611.
- 17 Ding S, Shi J, Qian W, Iqbal K, Grundke-Iqbal I, et al. (2011) Regulation of alternative splicing of tau exon 10 by 9G8 and Dyrk1A. *Neurobiol Aging* [Epub ahead of print].
- 18 Cramer P, Caceres JF, Cazalla D, Kadener S, Muro AF, et al. (1999) Coupling of transcription with alternative splicing: RNA pol II promoters modulate SF2/ASF and 9G8 effects on an exonic splicing enhancer. *Molecular Cell* 4(2): 251–258.
- 19 Galiana-Arnoux D, Lejeune F, Gesnel MC, Stevenin J, Breathnach R, et al. (2003)

- The CD44 alternative v9 exon contains a splicing enhancer responsive to the SR proteins 9G8, ASF/SF2, and SRp20. *J Biol Chem* 278(35): 32943–32953.
- 20 Li X, Shambaugh ME, Rottman FM, Bokar JA (2000) SR proteins Asf/SF2 and 9G8 interact to activate enhancer-dependent intron D splicing of bovine growth hormone pre-mRNA in vitro. *RNA* (New York, NY 6(12): 1847–1858.
- 21 Armstrong RA (2009) The molecular biology of senile plaques and neurofibrillary tangles in Alzheimer's disease. *Folia Neuropathol* 47(4): 289–299.
- 22 Arai T, Ikeda K, Akiyama H, Shikamoto Y, Tsuchiya K, et al. (2001) Distinct isoforms of tau aggregated in neurons and glial cells in brains of patients with Pick's disease, corticobasal degeneration and progressive supranuclear palsy. *Acta neuropathol* 101(2): 167–173.

4

Chapter 4

Transcription factor STOX1A promotes mitotic entry by binding to the CCNB1 promotor

Daan van Abel¹, Omar Abdul-hamid¹, Marie van Dijk¹, Cees BM Oudejans¹

¹Department of Clinical Chemistry, VU University Medical Center, Amsterdam, The Netherlands.

PLoS ONE, 2012 | Volume 7 | Issue 1 | e29769

Background: In this study we investigated the involvement of the transcription factor STOX1A in the regulation of the cell cycle.

Methodology/Principal Findings:

We found that several major cell cycle regulatory genes were differentially expressed upon STOX1A stimulation and knockdown in the neuroblastoma cell line SH-SY5Y. This includes STOX1A dependent differential regulation of cyclin B1 expression, a cyclin which is known to regulate mitotic entry during the cell cycle. The differential regulation of cyclin B1 expression by STOX1A is direct as shown with chromatin immunoprecipitation. Results furthermore suggest that mitotic entry is enhanced through the direct upregulation of cyclin B1 expression effectuated by STOX1A.

Conclusions: In conclusion, we hereby show that STOX1A is directly involved in the regulation of the cell cycle.

Introduction

Mammalian cell division is controlled by the expression of cyclins and activation of their associated cyclin dependent kinases (CDKs). While the CDK components are generally expressed ubiquitously during the cell cycle, expression of cyclins accumulate periodically during distinct phases (G1, S, G2, and M phase) of the cell cycle [1]. In each phase, binding of cyclins with their corresponding CDK forms an active cyclin/CDK complex. In general, G1 to S phase progression is controlled by CDK2 bound to S-phase cyclins [2] (E- and A-type) whereas G2 to M phase is triggered by CDK1 associated with mitotic cyclins [3] (A- and B-type). Active cyclin/cdk complexes can phosphorylate several substrates, which subsequently trigger cell cycle progression [4-6]. Many of these cyclin/cdk complex substrates and regulators of the cell cycle machinery itself have been characterized in detail, and recently it was shown to include a group of proteins belonging to the forkhead transcription factors. These transcription factors are characterized by a 100 amino acid DNA-binding motif termed the winged helix domain [7-10]. Several studies have confirmed the role of forkhead transcription factors in regulating the transcription of cell cycle regulatory genes during the cell cycle [8-10]. Additionally, it has been shown that multiple members of the forkhead transcription factors are regulated by components of the cell cycle itself. These include FOXM1 [8], FOXO1 [9], and FOXK2 [10].

Recently, Forkhead box 1A (STOX1A), a transcription factor structurally and functionally related to the forkhead family of transcription factors [11, 12], has been shown to be expressed abundantly in the brain and found to be upregulated in advanced stages of Late Onset Alzheimer's Disease (LOAD, Braak 3-6). Secondly, STOX1A was found to be expressed at the centrosomes of dividing cells [13]. Centrosomes serve as reaction centres for several key regulators of the cell cycle machinery [14, 15], where in particular G2 to M-phase transition is triggered by cyclin B1-CDK1 [16, 17]. Together with the increasing evidence that neurons, generally in a non-dividing state called G0, re-express a multitude of cell-cycle regulators in Alzheimer's disease (AD) [18-20], led us to explore the involvement of STOX1A in cell cycle related events. Here we show that in the neuroblastoma SH-SY5Y cell line STOX1A directly regulates the expression of the mitotic cyclin B1. Hereby we show that STOX1A, in addition to other members of the forkhead transcription factors, is directly involved in regulating the cell cycle. Upregulated expression of STOX1A in LOAD therefore potentially influences neuronal cell cycle re-entry.

Results

Expression analysis of SH-SY5Y cells stably transfected with STOX1A during distinct phases of the cell cycle.

To identify the expression pattern of STOX1A in stably transfected SH-SY5Y cells we performed immunofluorescence using an antibody against the Halotag attached to the STOX1A recombinant protein. During interphase we observed primarily nuclear and to a lesser extent cytoplasmic STOX1A staining (Fig 1A) which confirms the

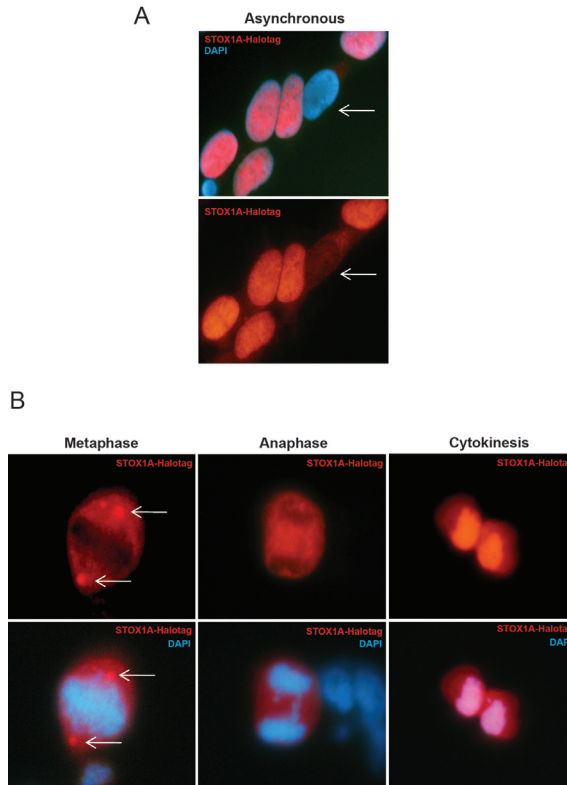


Figure 1. Expression analysis of STOX1A in stably transfected SH-SY5Y cells. (A) Immunofluorescence shows exclusively nuclear or cytoplasmic (white arrows) staining for STOX1A-Halotag protein in STOX1A stably transfected SH-SY5Y cells. (B) Cells undergoing mitosis showing a non-overlapping STOX1A / DAPI immunofluorescence pattern during metaphase and anaphase until cytokinesis when STOX1A immunofluorescence overlaps with DAPI (DNA) immunofluorescence.

model of STOX1A nucleo-cytoplasmic shuttling as previously described by our lab [12]. Nuclear localization represents the active form of STOX1A.

To investigate the expression pattern of STOX1A during mitosis, cells were arrested at the G2/M-phase boundary. As also observed for the forkhead transcription factor FOXK2 [10], STOX1A shows a non-overlapping immunofluorescence pattern with DNA (STOX1A-halotag / DAPI merge) shortly after nuclear envelope breakdown in prometaphase. The non-overlapping immunofluorescence pattern is best seen during metaphase and anaphase until cytokinesis occurs when STOX1A immunofluorescence overlaps with DNA (DAPI) (Fig 1B). As shown previously by us [15], STOX1A is concentrated at the centrosomes during metaphase (Fig 1B, white arrows).

STOX1A regulates cell proliferation in SH-SY5Y cells.

As the results above indicate that STOX1A is involved in mitosis, the effect of STOX1A on cell proliferation was tested by using STOX1A siRNA knockdown in comparison to scrambled siRNAs in the neuroblastoma SH-SY5Y cell line.

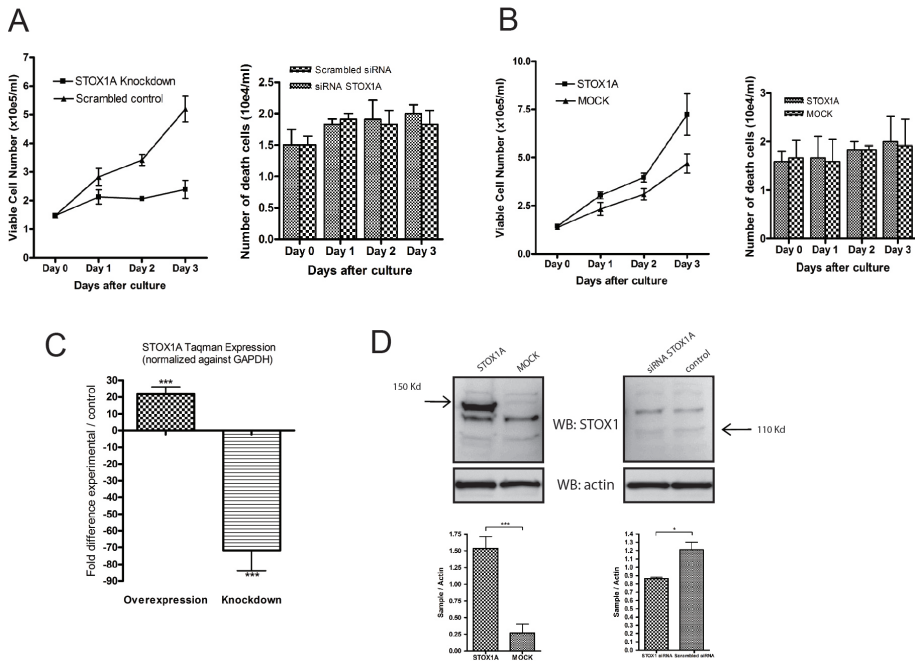


Figure 2. The effect of STOX1A on cell proliferation in the neuroblastoma cell-line SH-SY5Y. (A, left graph) The proliferation curve shows significantly decreased cell proliferation for STOX1A siRNA transfected SH-SY5Y cells compared to scrambled controls after 1, 2, and 3 days in culture. (A, right graph) In parallel we did not find significant differences in cell death between STOX1A siRNA and scrambled siRNA transfected cells at each of the indicated time points. (B, left graph) The proliferation curve shows significantly increased cell proliferation for STOX1A compared to MOCK stably transfected SH-SY5Y cells after 1, 2, and 3 days in culture. (B, right graph) In parallel we did not find significant differences in cell death between STOX1A and MOCK transfected cells at each of the indicated time points. Bars are mean \pm SEM. P-values for each timepoint were calculated using two-tailed unpaired t-test. (C) Overexpression and knockdown of STOX1A was determined with quantitative RT-PCR showing a mean 21 fold (mean $\Delta\Delta Ct$ 4.4) increase in mRNA expression for STOX1A in stably transfected SH-SY5Y cells compared to the controls (Left bar) and a mean 71 fold (mean $\Delta\Delta Ct$ 6.15) decreased mRNA expression for STOX1A siRNA transfected SH-SY5Y cells compared to the scrambled controls (right bar). Bars are mean \pm SEM. *** indicate $P < 0.001$ (one sample t-test with theoretical mean 0). N = 4, each sample was measured in triplicate. (D, Bottom left graph) Quantification of STOX1A-Halotag protein was performed using densitometry. The ratio number of obtained band intensities for STOX1A (at the expected band size of 150 Kd) divided by actin was compared to the ratio number of obtained band intensities for MOCK divided by actin for 3 independent experiments. A significant increase for the STOX1A ratio number was found compared to the MOCK ratio number. (D, Bottom right graph) Quantification of endogenous STOX1A protein was performed using densitometry. The ratio number of obtained band intensities for STOX1A siRNA (at the expected band size of 110 Kd) divided by actin was compared to the ratio number of obtained band intensities for scrambled siRNA divided by actin for 3 independent experiments. A significant increase for the STOX1A siRNA ratio number was found compared to the scrambled siRNA ratio number. P-values were calculated using two-tailed unpaired t-test, error bars represent \pm SEM, * indicate $P < 0.05$, *** indicate $P < 0.001$. Western blot images are a representative of at least 3 independent experiments.

Knockdown of STOX1A resulted in a significant reduction of cell proliferation compared to the scrambled siRNA control (Fig 2A, left graph). In parallel, at each time point, the amount of death cells were counted. However we did not find significant differences in cell dead between STOX1A siRNA or scrambled siRNA transfected cells (Fig 2A, right graph). In concordance with the reduction in cell proliferation upon STOX1A siRNA transfection, cells that were stably transfected with STOX1A showed a significant increase in cell proliferation compared to empty vector (MOCK)

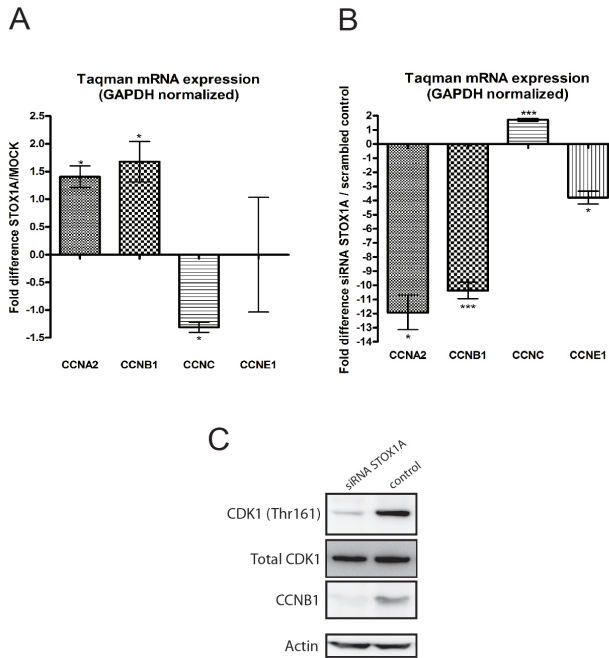


Figure 3. STOX1A induces changes in several major cell cycle regulatory genes. (A) The effect of stable STOX1A overexpression in the SH-SY5Y neuroblastoma cell line on four major mammalian cell cycle regulatory genes was determined with quantitative RT-PCR showing a mean 1,4 fold (mean $\Delta\Delta Ct$ is $-0,49$) and mean 1,72 fold (mean $\Delta\Delta Ct$ is $-0,78$) increased mRNA expression for CCNA2 and CCNB1, respectively, and a mean 1,22 fold (mean $\Delta\Delta Ct$ is $0,29$) decreased mRNA expression for CCNC in STOX1A stably transfected cell compared to their negative controls. (B) The effect of STOX1A knockdown in the SH-SY5Y neuroblastoma cell line on four major mammalian cell cycle regulatory genes was determined with quantitative RT-PCR showing a mean 11,8 fold (mean $\Delta\Delta Ct$ is $3,56$), mean 10.3 fold (mean $\Delta\Delta Ct$ is $3,37$) and mean 3,8 fold (mean $\Delta\Delta Ct$ is $1,92$) decreased mRNA expression for CCNA2, CCNB1 and CCNE1 respectively, and a mean 1,7 fold (mean $\Delta\Delta Ct$ is $-0,77$) increased mRNA expression for CCNC in STOX1A siRNA treated cells compared to their negative controls. (A,B) Bars are mean \pm SEM. * indicate $P < 0,05$, ** indicate $P < 0,01$, *** indicate $P < 0,001$ (one sample t-test with theoretical mean 0). N = 4, each sample was measured in triplicate. (C) Expression of endogenous CCNB1 protein and the active form of the CDK1 protein was determined by western blot using total cell protein extracts obtained from STOX1A siRNA and control treated SH-SY5Y cells. CCNB1 proteins were detected by a specific antibody recognizing total CCNB1 protein. CDK1 proteins were detected using an antibody detecting total CDK1 protein levels and a specific antibody recognizing the active form of CDK1 phosphorylated at threonine 161. An antibody specific for actin was used as a loading control. Westernblot image is a representative of at least 3 independent experiments.

transfected SH-SY5Y cells (Fig 2B, left graph). In parallel, at each time point, the amount of dead cells were counted. No significant differences in cell death between STOX1A and MOCK transfected cells were found (Fig 2B, right graph). Knockdown and stable overexpression of STOX1A in the SH-SY5Y cell-line was confirmed at the mRNA (Fig 2C) and protein level (Fig 2D).

Reduced cell proliferation by STOX1A siRNA knockdown and increased cell proliferation by STOX1A overexpression suggest STOX1A dependent cell cycle regulation. To test this we measured mRNA levels of four major mammalian cell cycle regulatory genes; cyclin A2 (CCNA2, involved in the S to G2 phase and G2 to M phase progression [21]), cyclin B1 (CCNB1, involved in G2 to M phase progression

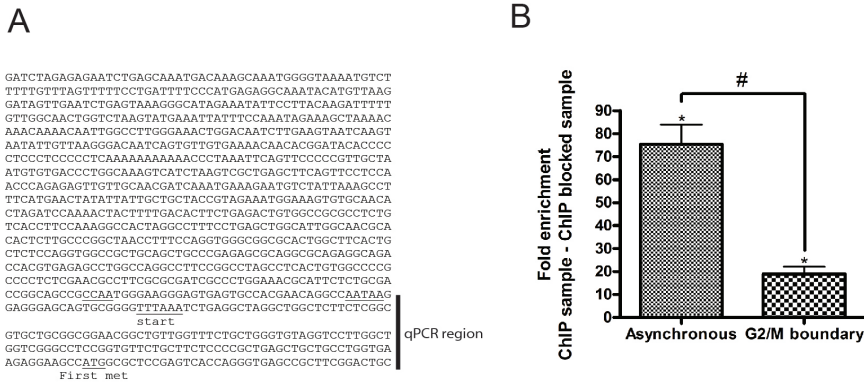


Figure 4. STOX1A binds to the 5' upstream regulatory region of the CCNB1 gene. (A) The DNA sequence previously characterized as the 5' upstream regulatory region of the CCNB1 gene [24, 25] indicating the fragment used for quantitative PCR. (B) Chromatin immunoprecipitation was performed with asynchronous STOX1A stably transfected cells in parallel with STOX1A stably transfected cells synchronized at the G2/M phase boundary. Significantly higher enrichment for the 5' upstream regulatory region of the CCNB1 gene was found in asynchronous cells compared to cells synchronized at the G2/M-phase boundary (left vs right bar). Bars are mean \pm SEM, P -values were calculated using two-tailed unpaired t-test. # indicates $P < 0.001$. (B, left bar). Quantitative PCR results show a mean 75 fold (mean $\Delta\Delta Ct$ is -6.23) enrichment for the 5' upstream regulatory region of the CCNB1 gene in STOX1A stimulated ChIP DNA, compared to their negative controls (ChIP sample vs ChIP negative sample) obtained from asynchronous STOX1A stably transfected SH-SY5Y cells. (B, right bar) Results show a mean fold 18 (mean $\Delta\Delta Ct$ is -4.18), enrichment for the 5' upstream regulatory region of the CCNB1 gene in STOX1A stimulated ChIP DNA, compared to their negative controls (ChIP sample vs ChIP negative sample) obtained from STOX1A stably transfected SH-SY5Y cells synchronized at the G2/M-phase boundary. Bars are mean \pm SEM. Asterisks indicate $P < 0.05$ (one sample t-test with theoretical mean 0).

[4]), cyclin C (CCNC, involved in G0 to G1 phase progression [22]), and cyclin E1 (CCNE1, involved in G1 to S phase progression [23]). In stably STOX1A transfected cells we found that CCNA2 and CCNB1 mRNA levels were significantly increased. CCNC mRNA levels were significantly downregulated but no significant differences in mRNA levels were seen for CCNE1 compared to stably MOCK transfected cells (Fig 3A). STOX1A siRNA knockdown resulted in significantly decreased mRNA levels of CCNA2, CCNB1 and CCNE1, and significantly upregulated CCNC mRNA levels compared to scrambled controls (Fig 3B). Since CCNB1 is the cyclin involved in mitosis, CCNB1 reduction upon STOX1A knockdown was also confirmed on westernblot. The CCNB1 associated kinase CDK1 showed reduced activity upon reduced CCNB1 protein levels as measured on westernblot using an antibody specifically recognizing the active form of CDK1 (Fig 3C). In contrast parallel, comparable protein levels of total CDK1 were found (Fig 3C).

STOX1A directly regulates expression of CCNB1 thereby enhancing progression into mitosis.

Given the importance of CCNB1 at the G2/M-phase boundary [6], and our results showing CCNB1 expression to be affected by both knockdown and overexpression of STOX1A we tested if STOX1A could also be directly involved in the regulation of CCNB1 through binding to its promoter region. Therefore we performed chromatin immunoprecipitation (ChIP). The 5' upstream regulatory region of the CCNB1 gene [24, 25] (Fig 4A) was tested for enrichment in STOX1A ChIP DNA compared

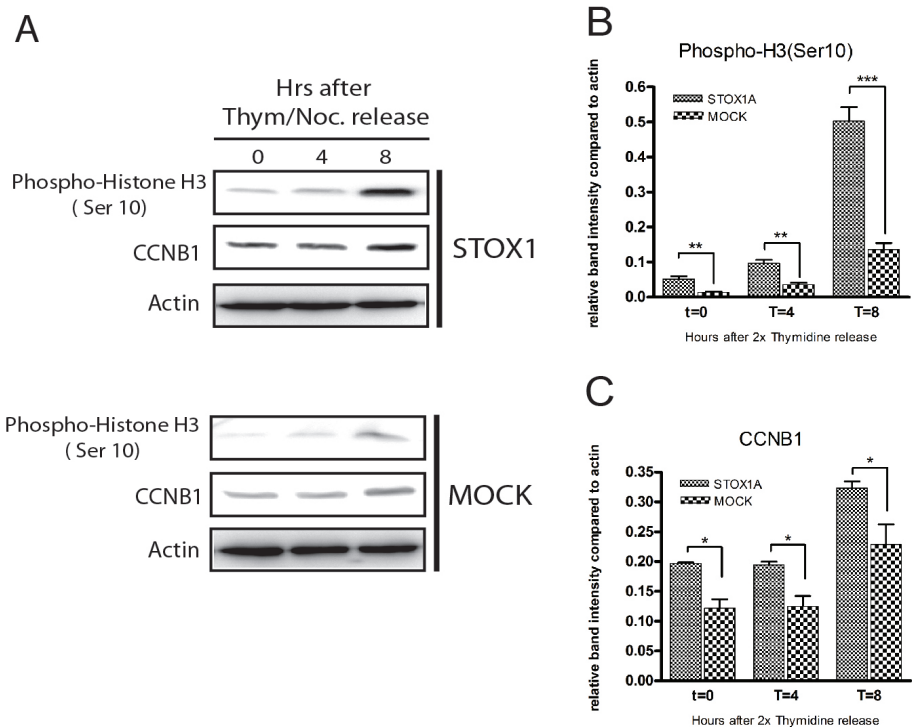


Figure 5. Direct upregulation of CCNB1 effectuates enhanced mitotic entry. (A) Stably transfected STOX1A and MOCK SH-SY5Y cells were synchronized in the S-phase and total cell extracts were prepared from 0, 4 and 8 h after release from the 2x thymidine block. Western blotting was performed using antibodies to Phospho-Histone H3 (Ser 10) and CCNB1. An antibody specific for actin was used as a loading control. Western blot image is a representative of at least 3 independent experiments. (B) Western blot (see 5A) quantification of Phospho-H3 (ser 10) was performed using densitometry. The ratio number of obtained band intensities for STOX1A divided by actin was compared to the ratio number of obtained band intensities for MOCK divided by actin for 3 independent experiments. A significant increase for the STOX1A ratio number was found at all time points compared to the MOCK ratio number. (C) Western blot (see 5A) quantification of CCNB1 was performed using densitometry. The ratio number of obtained band intensities for STOX1A divided by actin was compared to the ratio number of obtained band intensities for MOCK divided by actin for 3 independent experiments. A significant increase for the STOX1A ratio number was found at all time points compared to the MOCK ratio number. *P*-values were calculated using two-tailed unpaired *t*-test, error bars represent \pm SEM, * indicate $P < 0.05$, ** indicate $P < 0.01$, *** indicate $P < 0.001$.

to the negative control in unsynchronized stably STOX1A transfected SH-SY5Y cells. Because STOX1A expression analysis shows a non-overlapping STOX1A immunofluorescence-DNA (DAPI) pattern at specific phases during mitosis we speculated that a direct interaction of STOX1A with the 5' upstream regulatory region of the CCNB1 gene is like most transcription factors transiently lost during mitosis. Therefore, in parallel, we also tested enrichment of the 5' upstream regulatory region of the CCNB1 gene [24, 25] in stably STOX1A transfected SH-SY5Y cells arrested at the G2/M-phase boundary. We found significant enrichment for the 5' upstream regulatory region of the CCNB1 gene [24, 25] in STOX1A ChIP DNA compared to their negative controls in unsynchronized stably STOX1A transfected SH-SY5Y cells and cells synchronized at the G2/M-phase boundary (Fig 4B). Furthermore,

enrichment for the 5' upstream regulatory region of CCNB1 in the unsynchronized cells (Fig 4B, left bar) was compared with cells synchronized at the G2/M-phase boundary (Fig 4B, right bar). As expected, cells that were harvested directly after a G2/M-phase block showed a significantly lower enrichment for the 5' upstream regulatory region of the CCNB1 gene compared to cells that were growing asynchronously (Fig 4B).

To see if the direct regulation of STOX1A on CCNB1 expression would influence transition into the G2/M-phase boundary we synchronized STOX1A and MOCK stably transfected cells in the early S phase with thymidine. 0, 4, and 8 hours after thymidine release CCNB1 protein expression levels were significantly higher in STOX1A compared to MOCK transfected cells (Fig 5). Furthermore, western blot analysis also showed significantly higher protein expression of the mitosis marker phospho-histone H3 (ser 10) in STOX1A compared to the MOCK transfected cells at these timepoints (Fig 5).

Discussion

Here we show, in addition to other members of the forkhead transcription factors, that STOX1A is directly involved in controlling the cell cycle via CCNB1. CCNB1 expression is directly regulated via STOX1A by binding to a region previously characterized as the 5' upstream regulatory region of the CCNB1 gene [24, 25]. While CCNB1 is known to be a key regulator for mitotic entry [26], the direct up-regulation of CCNB1 by STOX1A led us to speculate if this would have an effect on this phase of the cell cycle. Indeed, in stably STOX1A transfected SH-SY5Y cells that were released from an S-phase block an earlier appearance of the specific mitosis marker PhosH3 (ser10) in parallel with higher CCNB1 protein levels was found. These results show that STOX1A transfected cells progress more rapidly into mitosis compared to control transfected cells. The finding that knockdown of STOX1A causes a decrease in CCNB1 protein levels and that the activity of CDK1 is also dramatically reduced elucidates a role for STOX1A in mitotic entry.

Enrichment of the 5' upstream regulatory region of the CCNB1 gene in STOX1A transfected SH-SY5Y cells growing asynchronously was significantly higher than in cells synchronized at the G2/M-phase boundary. This implies that during the G2/M phase of the cell cycle the transcriptional potential of STOX1A is temporarily lost. We therefore speculate that STOX1A is necessary for the entry of mitosis but transcriptional activity is transiently lost during mitosis. This is likely happening in metaphase and anaphase. During these phases STOX1A is not bound to DNA. This has also been shown for the forkhead transcription factor FOXK2 [10] and is in general also found for most other transcription factors which temporarily lose their transcriptional potential during mitosis. This is in contrast to Fox11 which continually remains associated with DNA during mitosis [27]. The translocation of STOX1A away from DNA in these specific phases during mitosis, thereby losing the potential to activate or repress target gene transcription, is possibly necessary for proper mitotic progression or exit.

CCNB1 concentrates at the centrosomes in metaphase during mitosis [17]. While

centrosomes serve as reaction centres for several key regulators of the cell cycle machinery [14, 15], and several forkhead transcription factors have been shown to physically interact with the cyclin B1 protein [8-10], we hypothesize that STOX1A also interacts with the cyclin B1 protein. Indeed, preliminary data using co-immunoprecipitation suggest this interaction (data not shown). This interaction further suggests that CDK1, the active binding partner of CCNB1, is potentially capable of regulating the transcriptional activity of STOX1A by phosphorylation. Previously, CDK1 has been shown to phosphorylate FOXM1 [8], FOXO1 [9], and FOXK2 [10] thereby influencing their activity.

While we studied the effect of STOX1A on CCNB1 in detail, it is likely that other cell cycle associated proteins are also directly or indirectly differentially affected by STOX1A. Significant changes of CCNA2 and CCNC1 mRNA levels upon STOX1A overexpression and knockdown, and significant downregulation of CCNE1 upon STOX1A knockdown suggest that STOX1A is also involved in regulating other checkpoints of the cell cycle.

As STOX1A is highly expressed in the brain and upregulated in LOAD makes exploration of STOX1A expression in neuronal cells in combination with cell cycle events very interesting; STOX1A might have a role in cell cycle re-entry as observed in AD.

In conclusion, we show for the first time that STOX1A is involved in regulating cell cycle events by binding to CCNB1 thereby regulating mitotic entry.

Materials and Methods

Cell culture and transfection

SH-SY5Y human neuroblastoma cells were obtained from the American Type Culture Collection (ATCC, Manassas, VA). All reagents for cell culture were purchased from Invitrogen Life Technologies, Inc. (Burlington, Canada). SH-SY5Y cells were cultured at 37 °C in a humidified atmosphere of 5% CO₂ in Iscove's Modified Dulbecco's Medium (IMDM) supplemented with 10% fetal calf serum and 100 U/ml penicillin, and 100 g/ml streptomycin. Cells were subcultured in medium every 2–3 days following harvesting by trypsinization (HBSS containing 5% trypsin). The ORF (Open Reading Frame) of the STOX1A gene was subcloned into the pF5K-neomycin CMV Flexi vectors according to the manufacturers protocol (Promega) and transfected into SH-SY5Y cells. For transfection the calcium phosphate method was used [28]. Briefly, at the time of transfection, cells were at 70% confluence. By vortexing 2X HEBS (HEPES-buffered saline) with a solution of 2.5 M CaCl₂ and 20 µg of plasmid DNA a co-precipitate of DNA and CaPO₄ was allowed to form. After incubation for 30 min at room temperature, the precipitate was added to the cells and the medium was changed after 24 h. For stable transfections SH-SY5Y cells were transfected either with the pF5K-STOX1A or empty pF5K constructs. Selection of positive clones was possible due to the presence of the neomycin resistant gene present in the constructs. Positive clones were maintained in complete IMDB medium supplemented with 800 µg/ml G418 (Roche) until reaching confluence and subcultured every 2-3 days for about 4 weeks. A population of positive clones was harvested for further analysis. As

confirmed with qRT-PCR (See below) using TaqMan probes (Applied Biosystems) for STOX1A, 3 stable SH-SY5Y cell-lines with an at least 10 fold STOX1A over-expression compared to mock transfected cells were selected. Additionally, plasmid DNA quantification using qPCR (see below) with primers and probe specific for the constructs backbone showed similar copy numbers between STOX1A and MOCK transfected cells.

Knockdown of STOX1A was performed by transfecting 4 siRNA's against STOX1A and control siRNA (Qiagen) in SH-SY5Y cells with Lipofectamine™ RNAiMAX (Invitrogen) according to the manufactures protocol. Cells were harvested 48 hours post-transfection and RNA was isolated as described in the Quantitative PCR and RT-PCR section.

Cell proliferation assay in vitro

In each well of a 6-well culture plate 1.5×10^5 untransfected, STOX1A or MOCK stably transfected SH-SY5Y cells were seeded. The untransfected cells were transfected with STOX1A siRNAs (see above). The cell numbers from three wells were counted every day with a time interval of 24 hours for a total of 72 hours. Viable cells were counted on a Countess® Automated Cell Counter (Invitrogen) according to the manufactures instructions. Three independent experiments were performed, and the means were used to depict the growth curve.

Cell synchronization

Cells were synchronized in an early S-phase by double thymidine treatment. Briefly, $\pm 20\%$ confluent cells were treated with 2 mM thymidine for 16 h. After being released to normal growing medium for 8 h, the cells were treated with 2 mM thymidine for an additional 16 h. Again, after being released to normal growing medium, cells were harvested or analysed in time intervals of 2 hours for a total of 8 hours.

For cells to be synchronized at the G2/M-phase boundary, cells were treated with a thymidine/nocodazole block. Briefly, $\pm 40\%$ confluent cells were treated with 2 mM thymidine for 24 h. After being released to normal growing medium for 3 h, the cells were treated with 100 ng/ml nocodazole for 12 h and the cells were arrested at the G2/M-phase boundary.

Chromatin immunoprecipitation

Stably transfected STOX1A cells (asynchronous or G2/M-phase boundary arrested) were treated with formaldehyde to create protein-DNA crosslinks. Cytoplasmic lysis was performed to reduce competition of cytoplasmic STOX1A-Halotag proteins against nuclear STOX1A-Halotag proteins with the Halotag resin. Nuclear lysate was subsequently fragmented by sonication. The nuclear lysates were split into two equal parts of which one was treated with Halotag blocking ligand to function as a negative control. Both the samples and controls were treated using Halotag resin according to the Halo-ChIP system protocol in the presence of proteinase inhibitors. After reversal of crosslinks the DNA was purified using the Qiaquick PCR purification kit (Qiagen).

Quantitative PCR and RT-PCR

Standard quantitative PCR was performed on an ABI7300 (Applied Biosystems) using a probe and primers specific for a fragment in the 949-bp region previously characterized as the 5' upstream regulatory region of the CCNB1 gene 24. Probe and primer characteristics were: CCNB1_foward 5' GTGCGGGGTTTAAATCTGAG 3', CCNB1_reversed 5' CATGGCTTCCTCTTCACCAG 3' and 5'-FAM 3'-TAMRA labeled probe: 5' TGTTCTGCTTCTCCCCGCTG 3'. Reactions were performed in the presence of 1M betaine and ROX reference dye, and corrected for input using the non-intron-spanning Glyceraldehyde 3-phosphate dehydrogenase (GAPDH) gene expression assay (Applied Biosystems). Input ChIP DNA was obtained from at least four independent ChIP experiments.

RNA isolation from transfected cells was performed using the RNeasy kit (Qiagen) including on-column DNase treatment. Quantitative RT-PCR using gene expression assays (Applied Biosystems) for CCNA2, CCNB1, CCNC, CCNE1 and STOX1A were performed on an ABI7300. In addition, transfection efficiencies were corrected by plasmid DNA quantification using the pF5 CMV-neo Flexi[®] Vector backbone present in all plasmids (pF5 forward: 5'-GCTTCGAGCAGACATGATAAG-3', pF5 reversed: 5'-AGCAATAGCATCACAAATTTCA-3', 5'-FAM 3'-TAMRA labeled pF5 probe: 5'-TGGACAAACCACAACCT AGAATGCAGT-3'). Data were obtained from at least four transfections from which each RNA sample was measured in triplicate.

Western blot

Protein lysates from transfected cells were obtained by directly scraping cells into Loading Buffer including β -mercaptoethanol. Lysates were separated by SDS-polyacrylamide gel electrophoresis, and electroblotted onto a PVDF-membrane. An antibody recognizing endogenous STOX1 (Sigma), Phospho-cdc2 Thr161 (cell signalling) or Phospho-Histone H3 (cell signalling) was used in combination with goat anti-rabbit horseradish peroxidase-conjugated secondary antibody (DAKO). An antibody recognizing CCNB1 (Millipore) and total cdc2 (clone POH1, cell signalling) were used in combination with goat anti-mouse IgG horseradish peroxidase-conjugated secondary antibody (DAKO). Protein bands were detected by an enhanced-chemiluminescence assay (GE Healthcare) on a LAS3000.

Immunofluorescence

For immunofluorescence, stably transfected SH-SY5Y cells were grown on glass coverslips. Coverslips were fixed in 4% (PFA) paraformaldehyde for 15 min at room temperature. After fixation, coverslips were rinsed in PBS, 0.1% Triton X-100 and incubated with 1% Triton X-100 in PBS for 15 min at room temperature for permeabilization. Coverslips were washed in wash buffer (PBS, 0.1% Triton X-100, 2% BSA (Bovine serum albumin)) blocked with PBS, 0.1% Triton X-100, 5% BSA for 1 h and incubated with anti-HaloTag (Promega) antibody at 4°C overnight. After washing with wash buffer, cells were incubated for 1 hour with anti-rabbit secondary antibodies conjugated with Alexa Fluor 568 (Invitrogen), washed with washing buffer and mounted with vectashield mounting solution containing DAPI for DNA

counterstaining (Vector Laboratories).

Data analysis

For Real-time PCR data, a threshold cycle number, Ct, was measured as the PCR cycle at which the amount of amplified target reaches the threshold value. Quantification was determined by the $2^{-\Delta\Delta Ct}$ method as described in Applied Biosystems “Guide to Performing Relative Quantitation of Gene Expression Using Real-Time Quantitative PCR”, Section VII, Relative Quantitation of Gene Expression Experimental Design and Analysis (http://www3.appliedbiosystems.com/cms/groups/mcb_support/documents/generaldocuments/cms_042380.pdf). Statistical analysis of the obtained data was carried out with the GraphPad Prism program.

Acknowledgements

The human neuroblastoma cell line SH-SY5Y was obtained from the American Type Culture Collection (ATCC; Rockville, MD, USA), and kindly provided by Dr. R. Veerhuis (Clinical Chemistry dept., VUMC).

Author contributions

DvA and OAH were responsible for performing the experiments and analyzing the data. Writing of the manuscript was done in close collaboration with MvD and CBMO. All authors read and approved the final manuscript.

Competing interests

None of the authors are aware of any actual or potential conflicts of interest

References

- 1 Bloom J, Cross FR .2007 Multiple levels of cyclin specificity in cell-cycle control. *Nat Rev Mol Cell Biol* 2007;; 8:149-60.
- 2 Woo RA, Poon RY 2003. Cyclin-dependent kinases and S phase control in mammalian cells. *Cell cycle* 2003;; 2:316-24.
- 3 Porter LA, Donoghue DJ 2003. Cyclin B1 and CDK1: nuclear localization and upstream regulators. *Prog Cell Cycle Res* 2003; ; 5:335-47.
- 4 Murray AW 2004. Recycling the cell cycle: cyclins revisited. *Cell* 2004; ; 116:221-34.
- 5 Pines J 2006. Mitosis: a matter of getting rid of the right protein at the right time. *Trends Cell Biol* 2006; ; 16:55-63.
- 6 Gong D, Ferrell JE, Jr 2010. The roles of cyclin A2, B1, and B2 in early and late mitotic events. *Mol Biol Cell* 2010; ; 21:3149-61.
- 7 Brennan RG 1993. The winged-helix DNA-binding motif: another helix-turn-helix takeoff. *Cell* 1993; ; 74:773-6.
- 8 Major ML, Lepe R, Costa RH 2004. Forkhead box M1B transcriptional activity requires binding of Cdk-cyclin complexes for phosphorylation-dependent recruitment of p300/CBP coactivators. *Mol Cell Biol* 2004; ; 24:2649-61.
- 9 Yuan Z, Becker EB, Merlo P, Yamada T, DiBacco S, Konishi Y, Schaefer EM, Bonni A et al. 2008. Activation of FOXO1 by Cdk1 in cycling cells and postmitotic neurons. *Science* 2008; ; 319:1665-8.
- 10 Marais A, Ji Z, Child ES, Krause E, Mann DJ, et al. Sharrocks AD 2010. Cell cycle-dependent regulation of the forkhead transcription factor FOXK2 by CDK.cyclin complexes. *J Biol Chem* 2010; ; 285:35728-39.
- 11 van Dijk M, Mulders J, Poutsma A, Konst AA, Lachmeijer AM, et al. Dekker GA, Blankenstein MA, Oudejans CB 2005. Maternal segregation of the Dutch pre-eclampsia locus at 10q22 with a new member of the winged helix gene family. *Nat Genet* 2005; ; 37:514-9.
- 12 van Dijk M, van Bezu J, van Abel D, Dunk C, Blankenstein MA, et al. Oudejans CB, Lye SJ 2010 . The STOX1 genotype associated with pre-eclampsia leads to a reduction of trophoblast invasion by alpha-T-catenin upregulation. *Hum Mol Gen* 2010; ; 19:2658-67.
- 13 Loffler H, Lukas J, Bartek J, Kramer A 2006. Structure meets function--centrosomes, genome maintenance and the DNA damage response. *Exp Cell Res* 2006; ; 312:2633-40.
- 14 Doxsey S, Zimmerman W, Mikule K 2006. Centrosome control of the cell cycle. *Trends Cell Biol* 2006 2005; ; 15:303-11.
- 15 van Dijk M, van Bezu J, Poutsma A, Veerhuis R, Rozemuller AJ, et al. Scheper W, Blankenstein MA, Oudejans CB 2010. The pre-eclampsia gene STOX1 controls a conserved pathway in placenta and brain upregulated in late-onset Alzheimer's disease. *J Alzheimers Dis* 2010; ; 19:673-9.
- 16 De Souza CP, Ellem KA, Gabrielli BG 2000. Centrosomal and cytoplasmic Cdc2/cyclin B1 activation precedes nuclear mitotic events. *Exp Cell Res* 2000; ; 257:11-21.
- 17 Jackman M, Lindon C, Nigg EA, Pines J 2003. Active cyclin B1-Cdk1 first appears on centrosomes in prophase. *Nature Cell Biol* 2003; ; 5:143-8.
- 18 Liu WK, Williams RT, Hall FL, Dickson DW, Yen SH 1995. Detection of a Cdc2-related kinase associated with Alzheimer paired helical filaments. *Am J Pathol*: 1995; 146:228-38.
- 19 Vincent I, Jicha G, Rosado M, Dickson DW 1997. Aberrant expression of mitotic cdc2/cyclin B1 kinase in degenerating neurons of Alzheimer's disease brain. *J*

- Neurosci 1997; ; 17:3588-98.
- 20 Moh C, Kubiak JZ, Bajic VP, Zhu X, Smith MA, et al.-Lee HG 2011. Cell cycle deregulation in the neurons of Alzheimer's disease. *Results Probl Cell Differ* 2011; ; 53:565-76.
- 21 Pagano M, Pepperkok R, Verde F, Ansorge W, Draetta G 1992. Cyclin A is required at two points in the human cell cycle. *EMBO J* 1992; ; 11:961-71.
- 22 Sage J 2004. Cyclin C makes an entry into the cell cycle. *Dev Cell* 2004; ; 6:607-8.
- 23 Ohtsubo M, Theodoras AM, Schumacher J, Roberts JM, Pagano M 1995. Human cyclin E, a nuclear protein essential for the G1-to-S phase transition. *Mol Cell Biol* 1995; ; 15:2612-24.
- 24 Pines J, Hunter T 1989. Isolation of a human cyclin cDNA: evidence for cyclin mRNA and protein regulation in the cell cycle and for interaction with p34cdc2. *Cell* 1989; ; 58:833-46.
- 25 Hwang A, Maity A, McKenna WG, Muschel RJ 1995. Cell cycle-dependent regulation of the cyclin B1 promoter. *J Biol Chem* 1995; ; 270:28419-24.
- 26 Bassermann F, Peschel C, Duyster J 2005. Mitotic entry: a matter of oscillating destruction. *Cell cycle (Georgetown, Tex)* 2005; ; 4:1515-7.
- 27 Yan J, Xu L, Crawford G, Wang Z, Burgess SM 2006. The forkhead transcription factor FoxI1 remains bound to condensed mitotic chromosomes and stably remodels chromatin structure. *Mol Cell Biol* 2006; ; 26:155-68.
- 28 Song W, Lahiri DK 1995. Efficient transfection of DNA by mixing cells in suspension with calcium phosphate. *Nucleic Acids Res* 1995; ; 23:3609-11.

5

Chapter 5

STOX1A induces phosphorylation of tau proteins at epitopes hyperphosphorylated in Alzheimer's disease

Daan van Abel¹, Omar Abdul-hamid¹, Wiep Scheper², Marie van Dijk¹, Cees BM Oudejans¹

¹Department of Clinical Chemistry, VU University Medical Center, Amsterdam,

²Department of Genome Analysis, Academic Medical Center, University of Amsterdam, Amsterdam, The Netherlands.

Submitted, 2012

Abstract

Intraneuronal fibrillary tangles are a major hallmark of several neurodegenerative diseases including Alzheimer's disease. The major constituents of these hallmarks are hyper-phosphorylated tau. In this study we used a neuronal cellular model which over-expresses transcription factor STOX1A in combination with the longest human tau isoform to test the effect of STOX1A overexpression on tau phosphorylation. Our results show that STOX1A induces phosphorylation of the longest human tau isoform at phospho-epitopes typically found in neurofibrillary tangles in Alzheimer's disease. In conclusion, our results show a STOX1A-dependent effect on tau phosphorylation found in neurodegenerative diseases such as Alzheimer's disease.

Introduction

Alzheimer's disease (AD) is a chronic neurodegenerative disease with severe neurodegeneration and cognitive impairment. Classically, AD pathology is characterized by amyloid beta ($A\beta$) containing senile plaques and intra-neuronal neurofibrillary tangles (NFT). While $A\beta$ is formed by the sequential cleavage of the amyloid precursor protein (APP), intra-neuronal aggregates of NFT are densely packed networks of the hyper-phosphorylated insoluble microtubule associated protein tau (MAPT) [7], [12], and [20]. Normal tau function, which has been shown to be important in stabilizing microtubules, neurite outgrowth and axonal transport, is tightly regulated by a balance between phosphorylation and dephosphorylation [26]. However, hyper-phosphorylation of tau as found in AD and other related neurodegenerative diseases causes failure of tau to bind and stabilize microtubules resulting in neuronal dysfunction [2], [5], [9], [27], and [35]. Therefore, much effort has been made to identify phosphorylated tau residues to understand the mechanisms that lead to NFT formation as found in AD and other similar neurodegenerative diseases. As a result, currently more than 30 serine/threonine residues have been identified in NFT-tau with the use of immunologic studies and mass spectroscopy [3], [22], [23], and [30]. Furthermore, several tau protein kinases and the major tau protein phosphatase have been characterized which are capable of regulating the phosphorylation status at many of these tau residues [17] and [38].

Recently, Storkhead box 1A (STOX1A), a transcription factor structurally and functionally related to the forkhead family of transcription factors has been shown to be expressed abundantly in the brain and the expression level to correlate with the severity of Late Onset Alzheimer Disease (LOAD, Braak 3–6) [14]. Transcription factors like STOX1A regulate the expression of hundreds of downstream target genes and we therefore speculated that STOX1A potentially influences transcriptional networks which are associated with phosphorylation and/or de-phosphorylation of tau residues. Furthermore, phosphorylation of tau is known to be driven by kinases which are activated in a cell cycle dependent manner [8] and [13]. STOX1A has recently been shown to be directly involved in the cell cycle [1] which further indicates/suggests a role for STOX1A in tau phosphorylation. Together, in this study we tested if there is a potential relationship between the phosphorylation status of tau proteins and STOX1A overexpression. To test this we used a neuronal cellular model in which stably transfected STOX1A cells were stably co-transfected with the longest human tau isoform (hTau40) in the neuroblastoma cell-line SH-SY5Y. With the use of western blot and antibodies recognizing phospho-specific tau epitopes we found that STOX1A hyperphosphorylates epitopes which are abundantly found in NFT in AD. In conclusion, these results suggest that elevated STOX1A expression in advanced stages of LOAD patients is linked to hyper-phosphorylation of tau as found in NFT.

Results

STOX1A induces tau phosphorylation

Several monoclonal antibodies have been created which specifically recognize phosphorylated tau residues as found in NFT of AD patients. In this study we used immunoblotting analysis with the previously characterized monoclonal phospho-specific tau antibodies AT8 [19] and [32], and E178 [25] and [33] to determine if STOX1A overexpression can effectuate the phospho-specific tau epitopes recognized by these antibodies (S202/T205 for AT8 [19] and [32] and S396 for E178 [25] and [33]). Therefore we stably co-transfected the previously characterized STOX1A stably transfected SH-SY5Y cells [1] with the htau40 or htau40control constructs (For clarity termed: STOX1A-htau40 and STOX1A-htau40control, respectively). Furthermore, to monitor the effect without STOX1A overexpression we also stably transfected wild type SH-SY5Y cells either with the htau40 or htau40control construct (For clarity termed: WT-htau40 and WT-htau40control, respectively). Protein expression of STOX1A in the stably transfected cell-lines STOX1A-htau40 and STOX1A-htau40control was validated with western blotting (Fig 1A). As expected no immunoreactivity of STOX1A overexpression was observed in the WT-htau40 or WT-htau40control cells (Fig 1A).

Overexpression of htau40 in the WT-htau40 and STOX1A-htau40 cells was confirmed with an antibody which detects both the phosphorylated and unphosphorylated tau protein. Results show that the WT-htau40 and STOX1A-htau40 cell-lines equally overexpressed the recombinant htau40 protein (Fig 1B, lower figure). When using the tau phospho-epitope specific antibodies AT8 and E178, we could primarily detect high immunoreactivity in the lanes corresponding to the STOX1A-htau40 cells (Fig 1B, middle and upper figure). Immunofluorescent expression analyses showed similar results (Fig 2). Furthermore, high immunofluorescence for AT8 was observed in mitotically active cells (Fig 2G and H, white arrows). The immunofluorescent detection pattern for the E178 antibody was identical as for AT8 antibody (data not shown).

Stably transfected STOX1A SH-SY5Y cells have enhanced CDK1 activity levels.

Above results show a STOX1A dependent effect on htau40 phosphorylation. It has been shown that in vitro tau phosphorylation is catalysed by several well described protein kinases. These include P44/42 (MAPK) [15], [17], [18], and [34]) and cyclin dependent kinases 1 and 5 (CDK1 and CDK5) [6], [24], [28] and [31]. While STOX1A has been found to be involved in cell cycle regulation [1], and secondly the above kinases are known for their implications in the cell cycle [10], [11] and [16] and the phosphorylation of tau protein [6], [28], and [29], we speculated there might be a correlation between STOX1A overexpression, tau phosphorylation, and activation of these kinases. Therefore, we tested if STOX1A overexpression could effectuate changes in expression and/or activation of these kinases.

As a model we used the previously characterized stably transfected STOX1A SH-SY5Y cells and compared those with their corresponding MOCK cells (for clarity: WT-STOX1A and WT-MOCK, [1]). Quantification of Westernblot results (Fig

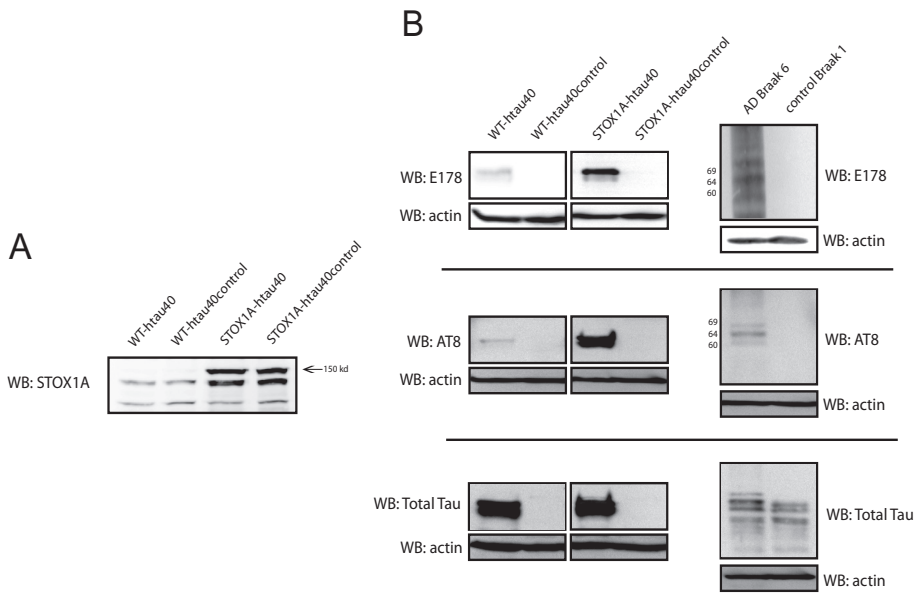


Figure 1 The effect of STOX1A on htau40 phosphorylation. Total cell extracts were prepared from WT-htau40, WT-htau40control, STOX1A-htau40 and STOX1A-htau40control. Western blotting was performed using an antibody against STOX1A (A). Western blot image is a representative of at least 3 independent experiments. (B) Western blotting was performed using the phospho-epitope specific antibody's E178 (upper figure) and AT8 (middle figure) or a phospho-epitope independent antibody against total tau (Lower figure). In parallel, as a positive control for specificity of tau phosphorylation, we used total brain homogenates from an Alzheimer's disease patient and compared it to a non-demented control. Western blot image is a representative of at least 3 independent experiments. An antibody specific for actin was used as a loading control.

3A) show that immunoreactivity levels of active CDK1 (Thr161) were significantly increased in WT-STOX1A compared to WT-MOCK cells (Fig 3B). However, no significant differences in immunoreactivity (Fig 3A) levels were found for total CDK1, CDK5, the CDK5 neuronal-specific activator p35 [37], MAPK or phospho-MAPK (Data not shown).

Discussion

In this study we used a neuronal cell model where htau40 was stably co-expressed in STOX1A overexpressing cell-lines previously created by us [1]. Our results show that the stably overexpressing STOX1A cells effectuate a robust increased phosphorylation of the co-expressed htau40 protein at specific epitopes recognized by the antibodies AT8 and E178. This effect was not seen in cells stably overexpressing htau40 without STOX1A overexpression. Therefore, this effect was STOX1A dependent. The phospho-epitopes recognized by AT8 and E178 antibodies are S202/T205 [19] and [32] and S396 [25] and [33], respectively. These residues have also been shown to be hyper-phosphorylated in NFT in Alzheimer's disease [4].

While we found abundant immunoreactivity for the AT8 and E178 antibodies in

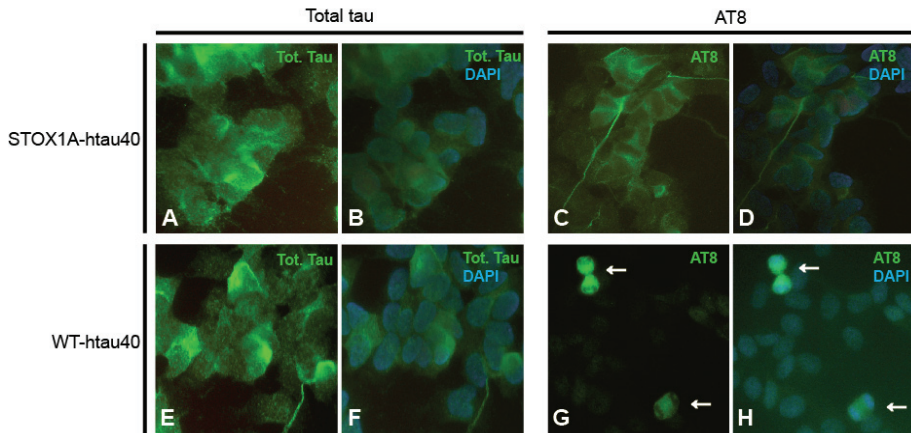


Figure 2. Immunofluorescent detection of tau in stably transfected SH-SY5Y cells. Immunostaining of overexpressed htau40 was detected with total tau (A, B, E and F) or AT8 (C, D, G and H) antibody in the STOX1A-htau40 (A, B, C and D) or WT-htau40 (E, F, G and H) cell lines. Arrows (G and H) indicate mitotically active cells. Green (A, B, E and F: Total tau), Green (A, B, E and F: AT8), Blue: DAPI.

5

STOX1A-htau40 cells compared to the STOX1A-htau40control cells, there was also a minor degree of immunoreactivity found in the WT-htau40 compared to the WT-htau40control cells (Fig 1B). The finding of this small amount of immunoreactivity can be explained by the specific staining of mitotically active cells by the AT8 and E178 antibodies, including in the WT-htau40 cells (Fig. 2G and H). This is consistent with previous findings where it has been shown that abnormal tau phosphorylation occurs specifically during mitosis [13].

The correlation between hyper-phosphorylated tau in NFT and AD pathology has led to a focus towards research on protein kinases and phosphatases that have been shown to phosphorylate and/or de-phosphorylate residues on tau proteins. In general, two types of tau kinases have been described which are the proline directed serine-threonine protein kinases and non-proline directed serine-threonine protein kinases [30]. The major focus lies on the proline directed serine-threonine protein kinases as Ser/Thr-Pro sites are the major abnormally phosphorylated tau sites found in AD [21] and [30]. In an attempt to provide a possible mechanism for STOX1A induced tau phosphorylation, we tested the expression and activity of the well described proline directed serine-threonine tau protein kinases CDK1, CDK5, and P44/42 (MAPK) which are associated with tau phosphorylation [6], [28] and [29] and cell cycle events [10], [11], and [16]. STOX1A has previously been shown to be involved in the regulation of the cell cycle as well [1] and therefore we speculated that there might be a correlation between STOX1A, the cell cycle and tau phosphorylation. Our results show that the active form of CDK1 (CDK1 phosphorylated at thr161) was induced in stably transfected STOX1A SH-SY5Y cells. Our data therefore indicate that STOX1A dependent tau phosphorylation is, at least in part, mediated through

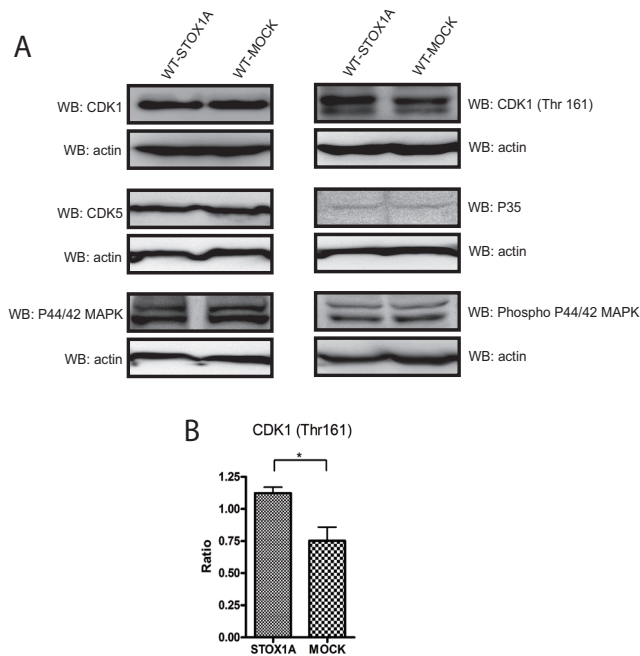


Figure 3. Stably STOX1A transfected SH-SY5Y cells have enhanced activity levels of CDK1. (A) Total cell extracts were prepared from WT-STOX1A and WT-MOCK SH-SY5Y cells and western blotting was performed using antibodies to P44/42 (ERK1/2), Phospho-P44/42 (Phospho-ERK1/2), CDK1, CDK1 (Thr161), CDK5 and P35. An antibody specific for actin was used as a loading control. Western blot image is a representative of at least 3 independent experiments. (B) Western blot quantification was performed using densitometry. The ratio number of obtained band intensities for WT-STOX1A divided by actin was compared to the ratio number of obtained band intensities for WT-MOCK divided by actin for 3 independent experiments. A significant increase for the WT-STOX1A ratio numbers was found for CDK1 (Thr161) compared to their WT-MOCK ratio numbers. P-values were calculated using two-tailed unpaired t-test, error bars represent \pm SEM, * indicate $P < 0.05$.

induced activity levels of CDK1. This is consistent with previous findings in our lab where cyclin B1 (CCNB1) expression, the activating binding partner of CDK1, was found to be directly upregulated by STOX1A [1]. This could explain the higher CDK1 kinase activity levels in these cells. Further insight in the exact mechanisms that result in the enhanced activity of CDK1 by STOX1A is therefore needed to clarify this. Furthermore, we do not exclude the effect of STOX1A overexpression on other known or currently undiscovered tau kinases or phosphatases. As STOX1A target genes are largely unknown, it is very likely that STOX1A transactivates expression of genes which could indirectly modulate the activity or expression of one or more tau kinases or phosphatases as well. Whole genome expression analysis using STOX1A induced experimental models could reveal these STOX1A target genes and their associated transcriptional networks. This would greatly expand our knowledge of how STOX1A operates and therefore functions in these networks.

In conclusion, our results suggest a correlation between STOX1A expression and tau phosphorylation. Overexpression of STOX1A in the disease progression of Alzheimer's disease could therefore be associated with the formation NFT.

Material and methods

Human tissues

Human brain specimens of an Alzheimer's disease case (Braak stage 6) and a non-demented control case (Braak stage 1) were obtained as previously described [14] and used as a positive and a negative control for tau phosphorylation in western blot.

Cell culture and transfection

SH-SY5Y human neuroblastoma cells were obtained from the American Type Culture Collection (ATCC, Manassas, VA). All reagents for cell culture were purchased from Invitrogen Life Technologies, Inc. (Burlington, Canada). SH-SY5Y cells were cultured at 37 °C in a humidified atmosphere of 5% CO₂ in Iscove's Modified Dulbecco's Medium (IMDM) supplemented with 10% fetal calf serum and 100 U/ml penicillin, and 100 g/ml streptomycin. Cells were subcultured in medium every 2–3 days following harvesting by trypsinization (HBSS containing 5% trypsin). The ORF (Open Reading Frame) of the STOX1A gene was sub-cloned into the pF5K-neomycin CMV Flexi vector according to the manufacturers protocol (Promega). The ORF of the longest human tau (hTau40) isoform was obtained from the pNG2 donor vector (Dr. E.M. Mandelkow) by digestion with the restriction enzymes NdeI and BamHI. Both sites were rendered blunt ended using Klenow. The htau40 insert was ligated into the HindIII and BamHI sites of the pcDNA4 vector (Invitrogen) that were blunted with Klenow, to obtain the pcDNA4-htau40 construct.

For transfection the calcium phosphate method was used [36]. Briefly, at the time of transfection, cells were at 70% confluence. By vortexing 2X HEBS (HEPES-buffered saline) with a solution of 2.5 M CaCl₂ and 20 µg of plasmid DNA a coprecipitate of DNA and CaPO₄ was allowed to form. After incubation for 30 min at room temperature, the precipitate was added to the cells and the medium was changed after 24 h. Three previously created stably transfected STOX1A SH-SY5Y cell-lines (WT-STOX1A) with STOX1A over-expression of at least 10 fold compared to mock transfected cells (WT-MOCK) [1] were stably co-transfected either with the htau40-pcDNA4 or empty pcDNA4 constructs (STOX1A-htau40 and STOX1A-htau40control). Furthermore, wild type SH-SY5Y cells were stably transfected either with the htau40-pcDNA4 or empty pcDNA4 constructs (WT-htau40 and WT-htau40control). Selection of WT-STOX1A and WT-MOCK cells was possible due to the presence of a Neomycin resistant gene as previously described [1]. Selection of positive clones with either the htau40-pcDNA4 or empty pcDNA4 constructs was possible due to the presence of a Zeocin[™] (Invitrogen) resistant gene present in these constructs. Positive clones were maintained in complete IMDM medium supplemented with 300 µg/ml Zeocin[™] (Invitrogen) until reaching confluence and sub-cultured every 2-3 days for about 4 weeks. Three stably transfected STOX1A-htau40, STOX1A-htau40control, WT-htau40 and WT-htau40control cell-lines were selected for further analysis. As confirmed with qRT-PCR using TaqMan probes (Applied Biosystems) for Total tau, the STOX1A-htau40 and WT-htau40 had an at least 60 fold htau40 mRNA over-expression compared to STOX1A-htau40control and WT-htau40control respectively (data not shown).

Western blot

Protein lysates from stably transfected cells were obtained by directly scraping cells into loading Buffer including β -mercaptoethanol. Lysates were separated by SDS-polyacrylamide gel electrophoresis, and electroblotted onto a PVDF-membrane. Rabbit polyclonal antibodies recognizing the STOX1A protein (Sigma), Total tau protein (clone Tau-5, Abcam), Phospho-P44/42, (MAPK, Cell signaling), Phospho-CDK1 (Thr161, Cell signaling) and P35 (Cell signalling) were used in combination with goat anti-rabbit horseradish peroxidase-conjugated secondary antibody (DAKO). Mouse monoclonal antibodies specific for Phospho-Tau S202/T205 (Clone AT8, Pierce Biotechnology), Phospho-Tau S396 (Clone E178, Abcam), P44/42, (Phospho-MAPK, Cell signaling), CDK1 (Clone POH1, Cell signaling) and CDK5 (Clone DC17, Millipore) were used in combination with goat anti-mouse horseradish peroxidase-conjugated secondary antibody (DAKO). Endogenous actin used for loading controls was detected with mouse monoclonal anti-actin antibody (Sigma Aldrich) and used in combination with goat anti-mouse horseradish peroxidase-conjugated secondary antibody (DAKO). Protein bands were detected by an enhanced-chemiluminescence assay (GE Healthcare) on a LAS3000.

Immunofluorescence

For immunofluorescence, WT-htau40, WT-htau40control, STOX1A-htau40 or STOX1A-htau40control cells were grown on glass coverslips. Coverslips were fixed in 4% (PFA) paraformaldehyde for 15 min at room temperature. After fixation, coverslips were rinsed in PBS, 0.1% Triton X-100 and incubated with 1% Triton X-100 in PBS for 15 min at room temperature for permeabilization. Coverslips were washed in wash buffer (PBS, 0.1% Triton X-100, 2% BSA [Bovine serum albumin]) blocked with PBS, 0.1% Triton X-100, 5% BSA for 1 h and incubated with AT8, E178 or Tau-5 antibody (See above) or without a first antibody (serving as a negative control) at 4°C overnight. After washing with wash buffer coverslips were incubated for 1 hour with anti-mouse secondary antibodies conjugated with Alexa Fluor 488 (Invitrogen), washed with washing buffer and mounted with vectashield mounting solution containing DAPI for DNA counterstaining (Vector Laboratories).

Data analysis

For quantification of westernblots densitometry was used. Westernblot pictures were analysed with the software ImageJ according to the tutorial described on the website: <http://lukemiller.org/index.php/2010/11/analyzing-gels-and-western-blots-with-image-j/>. Statistical analysis on the obtained density values was carried out with Microsoft Excell and the GraphPad Prism program.

References

- 1 D. van Abel, O. Abdul-Hamid, M. van Dijk, C.B. Oudejans, Transcription Factor STOX1A Promotes Mitotic Entry by Binding to the CCNB1 Promotor, *PloS one* 7 (2012) e29769.
- 2 A.C. Alonso, I. Grundke-Iqbal, K. Iqbal, Alzheimer's disease hyperphosphorylated tau sequesters normal tau into tangles of filaments and disassembles microtubules, *Nature Med.* 2 (1996) 783-787.
- 3 B.H. Anderton, J. Betts, W.P. Blackstock, J.P. Brion, S. Chapman, J. Connell, R. Dayanandan, J.M. Gallo, G. Gibb, D.P. Hanger, M. Hutton, E. Kardalinos, K. Leroy, S. Lovestone, T. Mack, C.H. Reynolds, M. Van Slegtenhorst, Sites of phosphorylation in tau and factors affecting their regulation, *Biochem. Soc. Symp.* (2001) 73-80.
- 4 J.C. Augustinack, A. Schneider, E.M. Mandelkow, B.T. Hyman, Specific tau phosphorylation sites correlate with severity of neuronal cytopathology in Alzheimer's disease, *Acta Neuropathol.* 103 (2002) 26-35.
- 5 C. Ballatore, V.M. Lee, J.Q. Trojanowski, Tau-mediated neurodegeneration in Alzheimer's disease and related disorders, *Nature Rev. Neurosci.* 8 (2007) 663-672.
- 6 K. Baumann, E.M. Mandelkow, J. Biernat, H. Piwnica-Worms, E. Mandelkow, Abnormal Alzheimer-like phosphorylation of tau-protein by cyclin-dependent kinases cdk2 and cdk5, *FEBS Lett.* 336 (1993) 417-424.
- 7 K. Blennow, M.J. de Leon, H. Zetterberg, Alzheimer's disease, *Lancet* 368 (2006) 387-403.
- 8 D.J. Bonda, V.P. Bajic, B. Spremo-Potparevic, G. Casadesus, X. Zhu, M.A. Smith, H.G. Lee, Review: cell cycle aberrations and neurodegeneration, *Neuropath. Appl. Neuro.* 36 (2010) 157-163.
- 9 G.T. Bramblett, M. Goedert, R. Jakes, S.E. Merrick, J.Q. Trojanowski, V.M. Lee, Abnormal tau phosphorylation at Ser396 in Alzheimer's disease recapitulates development and contributes to reduced microtubule binding, *Neuron* 10 (1993) 1089-1099.
- 10 J.C. Chambard, R. Lefloch, J. Pouyssegur, P. Lenormand, ERK implication in cell cycle regulation, *Biochim. Biophys. Acta* 1773 (2007) 1299-1310.
- 11 S. Cicero, K. Herrup, Cyclin-dependent kinase 5 is essential for neuronal cell cycle arrest and differentiation, *J. Neurosci.* 25 (2005) 9658-9668.
- 12 A. Delacourte, L. Buee, Normal and pathological Tau proteins as factors for microtubule assembly, *Int. Rev. Cytol.* 171 (1997) 167-224.
- 13 P. Delobel, S. Flament, M. Hamdane, C. Mailliot, A.V. Sambo, S. Begard, N. Sergeant, A. Delacourte, J.P. Vilain, L. Buee, Abnormal Tau phosphorylation of the Alzheimer-type also occurs during mitosis, *J. Neurochem.* 83 (2002) 412-420.
- 14 M. van Dijk, J. van Bezu, A. Poutsma, R. Veerhuis, A.J. Rozemuller, W. Scheper, M.A. Blankenstein, C.B. Oudejans, The pre-eclampsia gene STOX1 controls a conserved pathway in placenta and brain upregulated in late-onset Alzheimer's disease, *J. Alzheimers Dis.* 19 (2010) 673-679.
- 15 G. Drewes, B. Lichtenberg-Kraag, F. Doring, E.M. Mandelkow, J. Biernat, J. Goris, M. Doree, E. Mandelkow, Mitogen activated protein (MAP) kinase transforms tau protein into an Alzheimer-like state, *EMBO J.* 11 (1992) 2131-2138.
- 16 J.M. Enserink, R.D. Kolodner, An overview of Cdk1-controlled targets and processes, *Cell Div.* 5 (2010) 11.
- 17 I. Ferrer, T. Gomez-Isla, B. Puig, M. Freixes, E. Ribe, E. Dalfo, J. Avila, Current advances on different kinases involved in tau phosphorylation, and implications in Alzheimer's disease and tauopathies, *Curr. Alzheimer Res.* 2 (2005) 3-18.

- 18 M. Goedert, M. Hasegawa, R. Jakes, S. Lawler, A. Cuenda, P. Cohen, Phosphorylation of microtubule-associated protein tau by stress-activated protein kinases, *FEBS Lett.* 409 (1997) 57-62.
- 19 M. Goedert, R. Jakes, E. Vanmechelen, Monoclonal antibody AT8 recognises tau protein phosphorylated at both serine 202 and threonine 205, *Neurosci. Lett.* 189 (1995) 167-169.
- 20 M. Goedert, M.G. Spillantini, R. Jakes, D. Rutherford, R.A. Crowther, Multiple isoforms of human microtubule-associated protein tau: sequences and localization in neurofibrillary tangles of Alzheimer's disease, *Neuron* 3 (1989) 519-526.
- 21 A. Gomez-Ramos, M.A. Smith, G. Perry, J. Avila, Tau phosphorylation and assembly, *Acta Neurobiol. Exp.* 64 (2004) 33-39.
- 22 D.P. Hanger, J.C. Betts, T.L. Loviny, W.P. Blackstock, B.H. Anderton, New phosphorylation sites identified in hyperphosphorylated tau (paired helical filament-tau) from Alzheimer's disease brain using nano-electrospray mass spectrometry, *J. Neurochem.* 71 (1998) 2465-2476.
- 23 D.P. Hanger, H.L. Byers, S. Wray, K.Y. Leung, M.J. Saxton, A. Seereeram, C.H. Reynolds, M.A. Ward, B.H. Anderton, Novel phosphorylation sites in tau from Alzheimer brain support a role for casein kinase 1 in disease pathogenesis, *J. Biol. Chem.* 282 (2007) 23645-23654.
- 24 K. Imahori, T. Uchida, Physiology and pathology of tau protein kinases in relation to Alzheimer's disease, *J. Biochem.* 121 (1997) 179-188.
- 25 R. Jakes, M. Novak, M. Davison, C.M. Wischik, Identification of 3- and 4-repeat tau isoforms within the PHF in Alzheimer's disease, *EMBO J.* 10 (1991) 2725-2729.
- 26 G.V. Johnson, W.H. Stoothoff, Tau phosphorylation in neuronal cell function and dysfunction, *J. Cell. Sci.* 117 (2004) 5721-5729.
- 27 G. Lindwall, R.D. Cole, Phosphorylation affects the ability of tau protein to promote microtubule assembly, *J. Biol. Chem.* 259 (1984) 5301-5305.
- 28 W.K. Liu, R.T. Williams, F.L. Hall, D.W. Dickson, S.H. Yen, Detection of a Cdc2-related kinase associated with Alzheimer paired helical filaments, *Am. J. Pathol.* 146 (1995) 228-238.
- 29 J.P. Lopes, P. Agostinho, Cdk5: multitasking between physiological and pathological conditions, *Prog. Neurobiol.* 94 (2011) 49-63.
- 30 M. Morishima-Kawashima, M. Hasegawa, K. Takio, M. Suzuki, H. Yoshida, K. Titani, Y. Ihara, Proline-directed and non-proline-directed phosphorylation of PHF-tau, *J. Biol. Chem.* 270 (1995) 823-829.
- 31 J.J. Pei, H. Braak, C.X. Gong, I. Grundke-Iqbal, K. Iqbal, B. Winblad, R.F. Cowburn, Up-regulation of cell division cycle (cdc) 2 kinase in neurons with early stage Alzheimer's disease neurofibrillary degeneration, *Acta Neuropathol.* 104 (2002) 369-376.
- 32 R. Porzig, D. Singer, R. Hoffmann, Epitope mapping of mAbs AT8 and Tau5 directed against hyperphosphorylated regions of the human tau protein, *Biochem. Biophys. Res. Commun.* 358 (2007) 644-649.
- 33 R. Puri, T. Suzuki, K. Yamakawa, S. Ganesh, Hyperphosphorylation and aggregation of Tau in laforin-deficient mice, an animal model for Lafora disease, *J. Biol. Chem.* 284 (2009) 22657-22663.
- 34 C.H. Reynolds, M.A. Utton, G.M. Gibb, A. Yates, B.H. Anderton, Stress-activated protein kinase/c-jun N-terminal kinase phosphorylates tau protein, *J. Neurochem.* 68 (1997) 1736-1744.

- 35 N. Shahani, R. Brandt, Functions and malfunctions of the tau proteins, *Cell. Mol. Life. Sci.* 59 (2002) 1668-1680.
- 36 W. Song, D.K. Lahiri, Efficient transfection of DNA by mixing cells in suspension with calcium phosphate, *Nucleic Acids Res.* 23 (1995) 3609-3611.
- 37 L.H. Tsai, I. Delalle, V.S. Caviness, Jr., T. Chae, E. Harlow, p35 is a neural-specific regulatory subunit of cyclin-dependent kinase 5, *Nature* 371 (1994) 419-423.
- 38 M. Voronkov, S.P. Braithwaite, J.B. Stock, Phosphoprotein phosphatase 2A: a novel druggable target for Alzheimer's disease, *Future Med. Chem.* 3 (2011) 821-833.

6

Chapter 6

RNA-seq transcriptome analysis of STOX1A induced differential expression in neuronal cells

Daan van Abel, Hari K Thulluru, Omar Abdul-hamid, Marie van Dijk, Cees BM Oudejans
Department of Clinical Chemistry, VU University Medical Center, Amsterdam, The Netherlands.

In Preparation, 2012

Abstract

Previous studies in our lab have shown that transcription factor STOX1A has a potential role in the etiology of Alzheimer's disease and possibly other neurodegenerative diseases. Unfortunately, neuronal STOX1A transcriptional regulation is not yet fully understood but is of great importance to shed light on the underlying pathogenetic mechanisms operating in these diseases. In this study we used RNA-sequencing (RNA-seq) to determine changes in the transcriptomes between STOX1A compared to MOCK transfected neuronal SH-SY5Y cells. Data were analysed using TopHat and Cufflinks software and resulted in a significant amount of differential expression. Our data indicate that STOX1A has an important function in axonal guidance signalling, an important process during nervous system development.

Overall, the data presented in this study can be used as a valuable source of information for in-depth follow-up analysis and could reveal additional information on how STOX1A operates in neuronal transcriptional regulation.

Introduction

Storkhead box 1A (*STOX1A*), a transcription factor which contains a winged helix DNA-binding motif, is structurally and functionally similar to the family of forkhead box transcription factors [1-3]. Forkhead box transcription factors have been shown to be important regulators of the cell-cycle, cell proliferation, signal transduction, cell differentiation, - patterning and -metabolism, and therefore have been linked to several developmental mechanisms including embryonic development and neuro-developmental processes [4, 5]. Not surprisingly, many of them have been found to be associated with the pathology of a wide variety of diseases [6].

STOX1 is a susceptibility gene for pre-eclampsia in the Dutch population [2], a pregnancy associated disease [7]. Interestingly, *STOX1A* has also been found to be expressed abundantly in the brain, where increased expression of *STOX1A* in the hippocampus has been shown to correlate with the severity of Late-onset Alzheimer's disease (LOAD). Additionally, it was found that *STOX1A* dependent upregulation of one of its target genes, *LRRTM3*, leads to increased amyloid- β precursor protein (APP) processing resulting in higher levels of A β peptides [8]. Deposition of A β peptides is one of the key pathological hallmarks in LOAD [9].

Besides the role for *LRRTM3* in APP processing, the *LRRTM* family members are proposed to function as synaptic organizers during synapse development [10]. Two other genes, Integrin alpha-9 (*ITGA9*) and Contactin-associated protein-like 2 (*CNTNAP2*), recently found by ChIP-cloning as direct targets for *STOX1A* (unpublished results), have similar roles in synapse development. *ITGA9* in neurite outgrowth [11] and *CNTNAP2* as a cell type-specific promotor or inhibitor of neurite outgrowth [12]. Furthermore, expression of the microtubule associated protein tau (MAPT), also found to be differentially expressed by *STOX1A* [13], has a function in neurite outgrowth [14]. Defects in regulation of neurite outgrowth and similar processes like axon guidance signaling, have been linked to autism spectrum disorders (ASD) [15-17]. While speculatively, besides the association of *STOX1A* with LOAD, discovery of its target genes and their biological roles could also reveal novel potential roles for *STOX1A* in diseases like ASD.

Together, the results from previous studies have gained some interesting insights in the increasingly expanding functions in which *STOX1A* is potentially involved. These mechanisms are far from fully understood and therefore additional functional exploration and detailed studies are necessary to completely understand these emerging roles for *STOX1A* functioning in neuronal signalling. The expanding range of *STOX1A* target genes, their functions, and associated pathways can furthermore give novel insight on how *STOX1A* operates in disease like LOAD and neuronal developmental diseases like ASD. Therefore, in the present study we explored the downstream effects of *STOX1A* on neuronal transcriptional networks to expand and try to understand the biological processes that are controlled by *STOX1A* in neuronal cells on a genome-wide scale. For this, the transcriptome of neuronal SH-SY5Y cells stimulated with *STOX1A* was assessed using RNA sequencing (RNA-Seq) coupled to the TopHat and the Cufflinks software package [18].

Our results successfully demonstrate the use of RNA-seq transcriptome analysis to



Figure 1. The transcriptional profile for SH-SY5Y cells for chromosome 1. The RNAseq read density was plotted for STOX1A and MOCK samples along chromosome 1. Each bar represents the Log_2 frequency of reads plotted against chromosome coordinates along with a refseq track (top figure) representing all coding genes.

explore STOX1A induced differential expression. Furthermore, our data can be of great importance in yielding new insights into neuronal STOX1A signalling.

Results

RNA-seq data collection and Tophat alignment

As a model to study neuronal differential expression induced by STOX1A we used the neuroblastoma cell-line SH-SY5Y stably transfected with STOX1A or MOCK constructs. Total RNA was isolated from 3 stably transfected STOX1A and 3 stably transfected MOCK cell-lines and subsequently pooled (3x STOX1A and 3x MOCK). Each pool (STOX1A and MOCK) was further processed as described in the material and method section and sequencing on an Illumina machine was performed.

Fastq output files generated by the RNA-seq procedure were used as input for TopHat [19]. A paired-end RNA-seq run outputs fastq files consisting of a forward (R1) and a reverse (R2) sequence file per sample. The total number of TopHat input reads for the STOX1A DNA library were 208,266,806 R1 reads and 208,466,165 R2 reads. Input for the MOCK DNA library reads were 227,389,087 R1 reads and 227,564,492 R2 reads. The TopHat post-run key metrics are summarized in Table 1 which includes the quality of the mapped reads to the reference genome. As results show, a small percentage of reads (0.02% for STOX1A and 0.05% for MOCK) were removed from the analysis prior to mapping to the reference, due to low quality. The mean percentage of reads from all samples that were uniquely mapped by TopHat to the reference genome lies around 45 %. This percentage of mapped read coverage greatly exceeds the 30 Million reads that are recommended to achieve reliable measurement of mRNA expression across all genes in the genome [20].

To ensure uniformity of the read coverage of both STOX1A and MOCK reads, the TopHat BAM output files were imported into the SeqMonk program as described in the material and methods section and visually inspected. As an example, the read coverage of chromosome 1 is shown in Figure 1 for both the STOX1A and MOCK DNA library. As expected, no reads mapped to the centromere or areas of the chromosome without genes.

The final output of TopHat resulted in the detection of 386,360 splice junctions in the STOX1A DNA library and 349,161 splice junctions in the MOCK DNA library. Splice junction data was outputted as UCSC BED tracks for STOX1A (Supplementary

Table 1. Several metrics from the TopHat run were extracted from the log files.

	STOXIA-R1	STOXIA-R2	MOCK-R1	MOCK-R2
Reads processed	208,266,806	208,466,165	227,389,087	227,564,492
Reads with at least one reported alignment	98,374,552 (47.23%)	115,988,379 (55.64%)	715,449,93 (31.46%)	109,129,540 (47.96%)
Reads that failed to align	109,774,869 (52.71%)	92,312,338 (44.28%)	155,782,016 (68.51%)	118,319,269 (51.99%)
Reads suppressed due to low quality	117,385 (0.06%)	165,448 (0.08%)	62,078 (0.03%)	115,683 (0.05%)
Total Reported reads	126,225,239	154,378,283	93,360,477	148,890,531

Shown are the total amounts of reads, the percentages of those reads removed due to low quality and the percentage of total reads that were uniquely mapped to the UCSC Human genome build 18 (Hg18) reference genome by TopHat.

data 1) and MOCK (Supplementary data 2). TopHat read alignments were outputted in SAM format and further processed by Cuffdiff.

Differentially expressed genes

TopHat output was used as input for Cuffdiff to calculate the differential expression on both a gene level and a transcript level [18]. Furthermore, Cuffdiff also calculated alternative promoter usage (Table S1) and alternative splicing (Table S2) between STOX1A and MOCK samples. Here, we focus primarily on the gene and transcript level differential expression results.

Gene and transcript level differential expression results calculated by Cuffdiff were called at a q -value threshold of ≤ 0.05 and are presented as supplementary tables; differential gene expression (N = 1032, Table S3), differential isoform expression (N = 2618, Table S4), differential transcription start site groups (TSS groups, N = 1575, Table S5) and differential coding DNA sequences (CDS, N = 1635, Table S6). The expression level distribution of all genes between STOX1A and MOCK samples obtained by these four tests were plotted with the program CummeRbund [18]. Results show that normalized Fragments Per Kilobase of exon per Million fragments mapped (FPKM) densities for all genes are similar between both conditions (STOX1A vs MOCK) in all four Cuffdiff tests (Figure S1).

Visualisation of differential expression between STOX1A and MOCK for genes, isoforms, TSS groups and CDS at a q -value threshold of ≤ 0.05 was plotted with CummeRbund as volcano plots (Figure S2).

The top 10 most significantly up- and down- regulated genes, isoforms, TSS, and CDS between STOX1A and MOCK expression are given in Tables 2, 3, 4, and 6, respectively. As expected, STOX1A differential expression was found in all tests.

Among the top 10 upregulated genes we found the LOAD associated gene, nitric oxide synthase 1 (*NOS1*). *NOS1* was found to be significantly upregulated (Fold change 18.65, (Log_2 Fold change 4.22), p -value ≤ 0 , q -value ≤ 0), Table 3). *NOS1* is an important inter- and intracellular messenger molecule in several types of cells [21] and has been suggested to play a role in the etiology of LOAD [22, 23] but has also been associated with ASD [24]. The ASD associated gene, synapsin III (*SYN3*) [17], was significantly upregulated (Fold change 15.83, (Log_2 Fold change 3.98), p -value ≤ 0 , q -value ≤ 0), Table 3). *SYN3* and other synapsins are involved in neurite outgrowth

Table 2. Top 10 up- and down-regulated genes in STOX1A compared to MOCK treated cells as calculated by Cuffdiff at the 5% false-discovery rate (FDR, q -value = 0.05).

Gene Symbol	Description	Chromosome	FPKM MOCK	FPKM STOX1A	Fold change (Log ₂)	Fold change	p -value	q -value
IGF2BP1	insulin-like growth factor 2 mRNA binding protein 1	chr17	0,044	1,921	43,229	5,434	0	0
STOX1	storkhead box 1	chr10	0,272	4,714	17,313	4,114	0	0
SYN3	synapsin III	chr22	0,068	1,070	15,827	3,984	0	0
FAM5B	family with sequence similarity 5, member B	chr1	0,328	4,754	14,480	3,856	0	0
SOX14	SRY (sex determining region Y)-box 14	chr3	0,173	2,474	14,299	3,838	0	0
FGFR2	fibroblast growth factor receptor 2	chr10	0,260	3,194	12,261	3,616	0	0
NOS1	nitric oxide synthase 1 (neuronal)	chr12	0,040	0,448	11,218	3,488	0	0
TBC1D30	TBC1 domain family, member 30	chr12	0,203	2,245	11,062	3,468	0	0
TRIM67	tripartite motif-containing 67	chr1	0,535	5,723	10,696	3,419	0	0
SVT13	synaptotagmin XIII	chr11	0,196	1,987	10,112	3,338	0	0
C6orf192	chromosome 6 open reading frame 192	chr6	1,538	0,014	-107,011	-6,742	0	0
TRIM29	tripartite motif-containing 29	chr11	2,186	0,531	-4,115	-2,041	0	0
NELL1	NEL-like 1	chr11	7,601	2,208	-3,443	-1,783	0	0
COL3A1	collagen, type III, alpha 1	chr2	3,554	1,093	-3,252	-1,701	0	0
GPR64	Gprotein-coupled receptor 64	chrX	5,012	1,825	-2,746	-1,457	0	0
HGF	hepatocyte growth factor (hepatopoietin A; scatter factor)	chr7	2,857	1,311	-2,180	-1,124	0	0
LRRN3	leucine rich repeat neuronal 3	chr7	3,161	1,557	-2,030	-1,021	0	0
ABCC9	ATP-binding cassette, sub-family C (CFTR/MRP), member 9	chr12	2,949	0,803	-3,673	-1,877	2,22E-16	4,45E-14
ROBO2	roundabout, axon guidance receptor, homolog 2	chr3	1,426	0,510	-2,797	-1,484	1,14E-13	1,66E-11
GYC2	glycogenin 2	chrX	3,440	1,066	-3,228	-1,691	2,08E-12	2,57E-11

The fold change is the ratio of FPKM between STOX1A and MOCK and converted to Log₂. The differentially expressed genes were first ranked on their q -value and then fold change. The 10 with the highest or lowest fold change are shown here.

and synapse formation as well as in synaptic transmission [25].

Among the top 10 down regulated genes we found additional ASD associated genes. Results show that the ASD associated leucine rich repeat neuronal 3 (*LRRN3*) and roundabout homolog 2 (*ROBO2*) genes [26, 27] were significantly downregulated; *LRRN3* (Fold change -2.03, (Log₂ Fold change -1.02), p -value ≤ 0 , q -value ≤ 0) Table 3) and *ROBO2* (Fold change -2.80, (Log₂ Fold change -1.48), p -value = 1.14×10^{-13} , q -value 1.66×10^{-11}), Table 3). While little is known about the biological activities of *LRRN3*, the *ROBO2* gene functions in axonal guidance [28].

Among the top 10 upregulated isoforms we found Dynamin 2 (*DNM2*) which has been shown to be associated with LOAD [29, 30] and was found to be primarily differentially expressed on a transcript level (Refseq isoform specific ID: NM_001005361, Fold change 84.58 (Log₂ Fold change 6.402), p -value ≤ 0 , q -value ≤ 0 , Table 4). Dynamins play essential roles in endocytosis, but other functions associated with the actin cytoskeleton, mitogen-activated protein kinase (MAPK) signaling and apoptosis are also suggested [31].

Engulfment and cell motility protein 1 (*ELMO1*), has recently been found as an ASD candidate gene [17], was significantly upregulated on a transcript level (Refseq isoform specific ID: NR_038121, Fold change 20.99 (Log₂ Fold change 4.40), p -value ≤ 0 , q -value ≤ 0 , Table 3). *ELMO1* is suggested to play roles in the promotion of phagocytosis [32], dendritic spines morphogenesis [33], and cell migration (interneuron migration) [34].

Two specific downregulated isoforms were found to be associated with LOAD. Reticulon 4 (*RTN4*, or Nogo) [35], an inhibitor of neurite outgrowth [36] and insulin-like growth factor 2 (*IGF2*), a growth promoting hormone abundantly expressed in

Table 3. Top 10 up- and down-regulated isoforms in *STOX1A* compared to MOCK treated cells as calculated by Cuffdiff at the 5% false-discovery rate (FDR, q -value = 0.05).

Gene Symbol	Refseq Isoform ID	Description	Chromosome	FPKM MOCK	FPKM <i>STOX1A</i>	Fold change (Log ₂)	Fold change	p -value	q -value
DNM2	NM_001005361	dynamin 2	chr19	0,084	7,122	84,584	6,402	0	0
STOX1	NM_001130159	storkhead box 1	chr10	0,235	13,846	58,891	5,880	0	0
STOX1	NM_001130161	storkhead box 1	chr10	0,193	10,548	54,711	5,774	0	0
IGFBP1	NM_006546	insulin-like growth factor 2 mRNA binding protein 1	chr17	0,044	1,921	43,229	5,434	0	0
FGFR2	NM_000141	fibroblast growth factor receptor 2	chr10	0,089	2,189	24,730	4,628	0	0
FERMT2	NM_001135000	fermitin family homolog 2 (<i>Drosophila</i>)	chr14	0,294	6,730	22,921	4,519	0	0
ELMO1	NR_038121	engulfment and cell motility 1	chr7	0,533	11,172	20,978	4,391	0	0
FAM131B	NM_001031690	family with sequence similarity 131, member B	chr7	0,079	1,497	18,973	4,246	0	0
NOS1	NM_000620	nitric oxide synthase 1 (neuronal)	chr12	0,024	0,448	18,654	4,221	0	0
HOOK2	NM_013312	hook homolog 2 (<i>Drosophila</i>)	chr19	0,258	4,639	18,010	4,171	0	0
C6orf192	NM_052831	chromosome 6 open reading frame 192 (SLC18B1)	chr6	1,538	0,014	-107,011	-6,742	0	0
WASF2	NM_001201404	WAS protein family, member 2	chr1	8,623	0,279	-30,888	-4,949	0	0
RTN4	NM_007008	reticulin 4	chr2	18,671	0,643	-29,017	-4,859	0	0
IGF2	NM_001127598	insulin-like growth factor 2 (somatomedin A)	chr11	235,237	8,681	-27,099	-4,760	0	0
STX16	NM_001204868	syntaxin 16	chr20	1,702	0,087	-19,606	-4,293	0	0
PTPN12	NM_001131008	protein tyrosine phosphatase, non-receptor type 12	chr7	9,800	0,558	-17,578	-4,136	0	0
TARBP2	NM_004178	TAR (HIV-1) RNA binding protein 2	chr12	8,834	0,611	-14,452	-3,853	0	0
GPR64	NM_005756	G protein-coupled receptor 64	chrX	1,966	0,148	-13,292	-3,733	0	0
8-sep	NM_001098813	septin 8	chr5	7,407	0,682	-10,862	-3,441	0	0
ARL6IP6	NR_024526	ADP-ribosylation-like factor 6 interacting protein 6	chr2	8,259	0,878	-9,402	-3,233	0	0

The fold change is the ratio of FPKM between *STOX1A* and MOCK and converted to Log₂. The differentially expressed isoforms were first ranked on their q -value and then fold change. The 10 with the highest or lowest fold change are shown here.

the placenta and important in placental growth [37]; *RTN4* (Refseq isoform specific ID: NM_007008, Fold change -29.017 (Log₂ Fold change -4.95), p -value ≤ 0 , q -value ≤ 0 , Table 3) and *IGF2* (Refseq isoform specific ID: NM_001127598, Fold change -27.09 (Log₂ Fold change 4.76), p -value ≤ 0 , q -value ≤ 0 , Table 3)

While not within the top 10 of most significant *STOX1A* differentially expressed genes, we found additional genes with relevance in ASD with high significance and within the q -value threshold of ≤ 0.05 (Table S1). These include Contactin-associated protein-like 4 (*CNTNAP4*, Fold change -3.59, Log₂ Fold change -1.84, P -value = 4.59 x 10⁻⁰⁷, q -value = 2.27 x 10⁻⁰⁵) [38], Contactin-associated protein-like 5 (*CNTNAP5*, Fold change 6.14 Log₂ Fold change 2.62, P -value = 8.22 x 10⁻¹⁴, q -value = 1.22 x 10⁻¹¹) [39], neurexin 2 (*NRXN2*, Fold change 4.45, Log₂ Fold change 2.15, P -value = 0, q -value = 0) [40], Contactin-2 (*CNTN2*, Fold change 6.45, Log₂ Fold change 2.70, P -value = 2.13 x 10⁻¹¹, q -value = 2.22 x 10⁻⁰⁹) and SH3 and multiple ankyrin repeat domains 2 (*SHANK2*, Fold change 3.93, Log₂ Fold change 1.97, P -value = 1.66 x 10⁻⁰⁸, q -value = 1.08 x 10⁻⁰⁶) [41, 42].

Validation of *STOX1A* target genes

Previous studies in our lab resulted in the identification of several differentially expressed genes in *STOX1A* manipulated neuronal cell-lines. These consist of the *STOX1A* downstream target genes *LRRTM3* [8], microtubule-associated protein tau (*MAPT*) [13], Contactin-associated protein-like 2 (*CNTNAP2*, unpublished results) and Integrin alpha-9 (*ITGA9*, unpublished results). Additionally, *STOX1A* has also been shown to have a role in cell cycle regulation, specifically at the G2/M phase [43]. In the latter study we found several cyclin genes to be differentially expressed by

Table 4. Top 10 up- and down-regulated TSS groups in STOX1A compared to MOCK treated cells as calculated by Cuffdiff at the 5% false-discovery rate (FDR, q -value = 0.05).

Gene Symbol	TSS ID	Description	Chromosome	FPKM MOCK	FPKM STOX1A	Fold change	(Log ₂) Fold change	p -value	q -value
STOX1	TSS19336	storkhead box 1	chr10	0,428	24,395	57,007	5,833	0	0
IGF2BP1	TSS23967	insulin-like growth factor 2 mRNA binding protein 1	chr17	0,044	1,921	43,229	5,434	0	0
FAM131B	TSS26131	family with sequence similarity 131, member B	chr7	0,079	1,497	18,973	4,246	0	0
NOS1	TSS25258	nitric oxide synthase 1 (neuronal)	chr12	0,024	0,448	18,654	4,221	0	0
ELMO1	TSS965	engulfment and cell motility 1	chr7	0,722	11,802	16,336	4,030	0	0
FGFR2	TSS10118	fibroblast growth factor receptor 2	chr10	0,211	3,183	15,073	3,914	0	0
FAM5B	TSS21127	family with sequence similarity 5, member B	chr1	0,328	4,754	14,480	3,856	0	0
SOX14	TSS2041	SRX (sex determining region Y)-box 14	chr3	0,173	2,474	14,299	3,838	0	0
RAP1GAP	TSS15125	RAP1 GTPase activating protein	chr1	0,217	2,535	11,707	3,549	0	0
TBC1D30	TSS1456	TBC1 domain family, member 30	chr12	0,203	2,245	11,062	3,468	0	0
C6orf192	TSS19968	chromosome 6 open reading frame 192 (SLC18B1)	chr6	1,538	0,014	-107,011	-6,742	0	0
RTN4	TSS2786	reticulon 4	chr2	18,671	0,643	-29,017	-4,859	0	0
IGF2	TSS23255	insulin-like growth factor 2 (somatomedin A)	chr11	235,237	8,681	-27,099	-4,760	0	0
8-sep	TSS1410	septin 8	chr5	7,407	0,682	-10,862	-3,441	0	0
PTPN12	TSS25345	protein tyrosine phosphatase, non-receptor type 12	chr7	10,841	1,321	-8,205	-3,036	0	0
GUK1	TSS9380	ganylate kinase 1	chr1	62,525	12,049	-5,189	-2,376	0	0
UBE2H	TSS222	ubiquitin-conjugating enzyme E2H (UBC8 homolog, yeast)	chr7	9,585	1,868	-5,132	-2,359	0	0
C1orf93	TSS27960	chromosome 1 open reading frame 93	chr1	16,892	3,445	-4,904	-2,294	0	0
KLHL13	TSS9776	kelch-like 13 (Drosophila)	chrX	21,545	4,654	-4,629	-2,211	0	0
TRIM29	TSS2204	tripartite motif-containing 29	chr11	21,861	5,313	-4,115	-2,041	0	0

The fold change is the ratio of FPKM between STOX1A and MOCK and converted to Log₂. The differentially expressed TSS groups were first ranked on their q -value and then fold change. The 10 with the highest or lowest fold change are shown here.

STOX1A; Cyclin A2 (*CCNA2*), Cyclin B1 (*CCNB1*), Cyclin C (*CCNC*) [43]. Of the above validated STOX1A target genes we found *MAPT*, *ITGA9*, and *CCNC* to be significantly differentially expressed within the q -value threshold of ≤ 0.05 . Expression details for the latter genes are given in Table 5. *CCNC* was found to be specifically differentially expressed on a transcript level as no significant gene expression was detected (Table 5). A group of isoforms of another interesting cyclin, *CCNA1*, was found to be significantly upregulated at TSS id: TSS20256 (Fold change 2.25, Log₂ Fold change 1.17, P -value = 6.85×10^{-07} , q -value = 3.02×10^{-05}). The lowest fold change of a STOX1A validated gene was found for the *MAPT* isoform NM_016841 (log₂ fold change 1.09, table 5). This value (log₂ fold change 1.09) was therefore chosen as a reliable log₂ fold change threshold in further data exploration.

Table 5. Previously validated STOX1A target genes significantly differential expressed in this study as calculated by Cuffdiff at the 5% false-discovery rate (FDR, q -value = 0.05).

	Isoform	FPKM MOCK	FPKM STOX1A	Fold change	Log ₂ (Fold change)	p -value	q -value
ITGA9	NM_002207	8,271	22,250	2,69	1,428	2,12E-11	2,65E-09
MAPT	NM_016841	8,913	19,004	2,13	1,092	4,87E-08	2,91E-06
	NM_016834	0,744	1,928	2,59	1,374	1,33E-04	2,34E-03
CCNC	NM_001013399	9,011	2,437	-3,70	-1,886	2,29E-08	1,49E-06

The fold change is the ratio of FPKM between STOX1A and MOCK and converted to Log₂.

Table 6. Top 10 up- and down-regulated CDS in STOX1A compared to MOCK treated cells as calculated by Cuffdiff at the 5% false-discovery rate (FDR, q-value = 0.05).

Gene Symbol	CDS ID	Description	Chromosome	FPKM MOCK	FPKM STOX1A	Fold change (Log ₂)	Fold change	p-value	q-value
STOX1	P11035	storkhead box 1	chr10	0.235	13,846	58,891	5,880	0	0
STOX1	P5413	storkhead box 1	chr10	0.193	10,548	54,711	5,774	0	0
IGF2BP1	P3995	insulin-like growth factor 2 mRNA binding protein 1	chr17	0.044	1,921	43,229	5,434	0	0
FGFR2	P4526	fibroblast growth factor receptor 2	chr10	0.089	2,189	24,730	4,628	0	0
FERMT2	P23224	fermitin family homolog 2 (Drosophila)	chr14	0.294	6,730	22,921	4,519	0	0
FAM131B	P27220	family with sequence similarity 131, member B	chr7	0.079	1,497	18,973	4,246	0	0
NOS1	P23638	nitric oxide synthase 1 (neuronal)	chr12	0.024	0,448	18,654	4,221	0	0
HOOK2	P28828	hook homolog 2 (Drosophila)	chr19	0.258	4,639	18,010	4,171	0	0
FAM5B	P14757	family with sequence similarity 5, member B	chr1	0.328	4,754	14,480	3,856	0	0
SOX14	P5732	SRX (sex determining region Y)-box 14	chr3	0.173	2,474	14,299	3,838	0	0
AHCYL1	P1478	adenosylhomocysteinase-like 1	chr1	8,799	0.060	-145,611	-7,186	0	0
C6orf192	P20413	chromosome 6 open reading frame 192 (SLC18B1)	chr6	1,538	0.014	-107,011	-6,742	0	0
WASF2	P15809	WAS protein family, member 2	chr1	8,623	0.279	-30,888	-4,949	0	0
RTN4	P22238	reticulon 4	chr2	18,671	0.643	-29,017	-4,859	0	0
PTPN12	P28628	protein tyrosine phosphatase, non-receptor type 12	chr7	9,800	0.558	-17,578	-4,136	0	0
GPCR64	P6183	G protein-coupled receptor 64	chrX	1,966	0.148	-13,292	-3,733	0	0
8-sep	P19502	septin 8	chr5	7,407	0.682	-10,862	-3,441	0	0
ARL5A	P20649	ADP-ribosylation factor-like 5A	chr2	4,132	0.404	-10,237	-3,356	0	0
PTPRU	P23809	protein tyrosine phosphatase, receptor type, U	chr1	11,926	1,514	-7,875	-2,977	0	0
UBE2H	P18673	ubiquitin-conjugating enzyme E2H (UBC8 homolog, yeast)	chr7	9,585	1,868	-5,132	-2,359	0	0

The fold change is the ratio of FPKM between STOX1A and MOCK and converted to Log₂. The differentially expressed CDS were first ranked on their q-value and then fold change. The 10 with the highest or lowest fold change are shown here.

Canonical pathway analysis of differentially expressed genes and isoforms

Differentially expressed genes, isoforms, TSS groups, and CDS lists (Table S3, S4, S5 and S6) were submitted to Ingenuity Pathway Analysis (IPA), build 140500 (Ingenuity Systems, Inc., Redwood City, CA). Parameters were set at the q-value threshold of ≤ 0.05 and a log₂ fold change threshold of 1.09.

Canonical pathways analysis identified the pathways from the IPA library of canonical pathways that were most significantly enriched in the data sets. Consistently, our results show that the top Canonical pathway which was most significantly enriched in all Cuffdiff expression tests was Axonal guidance Signalling (Table 7).

Discussion

In our approach using RNA-seq to determine changes in the transcriptome between STOX1A compared to MOCK transfected neuronal SH-SY5Y cells we used a pipeline which includes the alignment of reads to a reference genome by TopHat [19] coupled to the Cufflinks software package for transcriptome assembly [18, 44, 45]. This resulted in a significant number of specific STOX1A induced differentially expressed genes. Additional LOAD associated genes and/or isoform specific transcripts were found to be differentially expressed by STOX1A in our Top 10 lists (*NOS1*, *DNM2*, and *RTN4*). Therefore, validation and functional exploration of these STOX1A differentially expressed genes and/or isoform specific transcripts could reveal new functional relationships between STOX1A and LOAD. It would also be very interesting to investigate if other STOX1A differentially expressed genes and/or isoform specific transcripts found in this study (but not previously associated with

Table 7. Top 5 significant canonical pathways affected by differential expression induced by STOX1A as determined by IPA.

Differential expression test	Top 5 Canonical Pathways	p-value
Gene	1. Axonal Guidance Signaling	1,29E-04
	2. Neuropathic Pain Signaling In Dorsal Horn Neurons	1,14E-03
	3. Synaptic Long Term Depression	1,30E-03
	4. Glutamate Receptor Signaling	6,83E-03
	5. nNOS Signaling in Neurons	1,24E-02
Isoforms	1. Axonal Guidance Signaling	7,88E-07
	2. Huntington's Disease Signaling	2,22E-04
	3. Neuropathic Pain Signaling In Dorsal Horn Neurons	2,24E-04
	4. Cardiac β -adrenergic Signaling	2,53E-04
	5. Synaptic Long Term Potentiation	1,50E-03
TSS group	1. Axonal Guidance Signaling	1,57E-05
	2. Neuropathic Pain Signaling In Dorsal Horn Neurons	4,03E-04
	3. Synaptic Long Term Potentiation	5,02E-03
	4. Synaptic Long Term Depression	1,02E-03
	5. Glutamate Receptor Signaling	1,51E-03
CDS	1. Axonal Guidance Signaling	4,75E-05
	2. Neuropathic Pain Signaling In Dorsal Horn Neurons	7,54E-04
	3. Dopamine-DARPP32 Feedback in cAMP Signaling	2,19E-03
	4. PTEN Signaling	3,14E-03
	5. Calcium Signaling	3,31E-03

Pathways with a *P*-value less than 0.05 were defined as significant.

LOAD) are in vivo differentially expressed in LOAD compared to control brains. These may represent novel candidates for involvement in LOAD, and speculatively, in the future could potentially serve as novel biomarkers.

As cell cycle events are recently suggested to be associated with LOAD and STOX1A has been shown to be involved in cell cycle regulation we expected differential expression of cell cycle proteins previous found to be validated. In concordance, we found the STOX1A validated cell cycle associated gene *CCNC* to be significantly downregulated. Interestingly, with the use of Cuffdiff we discovered that this gene was specifically regulated on a transcript level. Furthermore, we found significant upregulated differential expression of *CCNA1* isoforms expressed from the same TSS. *CCNA1* is a cyclin that has been suggested to function during the S- and the G2/M phase of the cell cycle [46]. The reactivation potential of STOX1A on *CCNA1* could therefore be potentially interesting as previous results have show that STOX1A has an important role during the G2/M phase of the cell cycle [43]. Therefore validation and exploration of the (in)direct functional relationship between STOX1A and *CCNA1* could further reveal the mechanisms in which STOX1A is involved during mitosis. Strangely, we could not detect the previously validated genes Cyclin

A2 (*CCNA2*) and Cyclin B1 (*CCNB1*) to be significantly differentially expressed by STOX1A. As expression of these cyclins is greatly dependent on cell cycle phase, we suggest that this may be the reason that these previous validated genes have skipped detection in this study. To correctly investigate the functional relationship between STOX1A and the cell cycle on a genome wide level it would therefore be necessary to synchronize the cells at specific phases of the cell cycle and then determine differential expression effectuated by STOX1A.

Furthermore, we found several potential STOX1A differentially expressed genes and/or isoform specific transcripts (*SYN3*, *NOS1*, *LRRN3*, *ROBO2*, and *ELMO1*) in our top 10 lists which have previously been shown to be associated with autism spectrum disorders (ASD), a neurodevelopmental disorder. In addition, within our cutoff value (q -value ≤ 0.05 , \log_2 fold change 1.09), we also indentified other potential STOX1A differentially expressed genes and/or isoform specific transcripts which have previously been linked to ASD; *CNTNAP4*, *CNTNAP5*, *NRXN2*, *CNTN2*, and *SHANK2*. Most of these ASD associated genes have a known or suggested function in pathways regulating neurite outgrowth and/or axon guidance signaling [17]. Axon guidance signalling is an important process in the development of the central nervous system CNS [47] and interestingly, defective axonal guidance signalling has been suggested as one of the underlying mechanisms in the pathophysiology of autism spectrum disorders (ASD) [17, 27]. Our results show significant enrichment of axonal guidance signaling in IPA pathway analyses of differential expression induced by STOX1A which further suggests a potential link with ASD. Additionally, recent studies in our lab identified *LRRTM3* [8], *CNTNAP2* (unpublished results), and *ITGA9* (unpublished results) as target genes for STOX1A in the neuroblastoma cell-line SK-N-SH. These genes have also been found to be linked to ASD [15-17]. We could however not confirm significant differential expression for *CNTNAP2* or *LRRTM3* in this study. The reason for this is possibly due to the difference in cell-lines used between the studies, SK-N-SH compared to SH-SY5Y in this study. Also different STOX1A transfection methods, transient in SK-N-SH versus stable in SH-SY5Y were used. We however did find *ITGA9* to be significantly upregulated. Together, the great overlap of STOX1A induced differential expression with genes associated with ASD, and significant overrepresentation of a pathway associated with this disease, makes it very interesting to explore the functional relationship between STOX1A and ASD. However, this potential relationship would first have to be clarified by validation and functional experimentation of relevant genes and transcripts that are differentially expressed by STOX1A.

In conclusion, we have shown that the amount of data generated in this study can be used as a valuable source of information for further experimentation and could give great insight in the biological role of STOX1A in neuronal transcriptional networks. This information is crucial in the understanding of the underlying functional mechanisms of STOX1A in diseases like LOAD, where STOX1A has been shown to be deregulated. Furthermore, our data can also serve to reveal novel roles for STOX1A in other diseases like ASD, as suggested by this study.

Materials and methods

Cell culture and transfection

SH-SY5Y human neuroblastoma cells were obtained from the American Type Culture Collection (ATCC, Manassas, VA). All reagents for cell culture were purchased from Invitrogen Life Technologies, Inc. (Burlington, Canada). SH-SY5Y cells were cultured at 37 °C in a humidified atmosphere of 5% CO₂ in Iscove's Modified Dulbecco's Medium (IMDM) supplemented with 10% fetal calf serum and 100 U/ml penicillin, and 100 g/ml streptomycin. Cells were subcultured in medium every 2–3 days following harvesting by trypsinization (HBSS containing 5% trypsin). The ORF (Open Reading Frame) of the STOX1A gene was sub-cloned into the pF5K-neomycin CMV Flexi vector according to the manufacturers protocol (Promega). For transfection the calcium phosphate method was used [48]. Briefly, at the time of transfection, cells were at 70% confluence. By vortexing 2X HEBS (HEPES-buffered saline) with a solution of 2.5 M CaCl₂ and 20 µg of plasmid DNA a coprecipitate of DNA and CaPO₄ was allowed to form. After incubation for 30 min at room temperature, the precipitate was added to the cells and the medium was changed after 24 h. For stable transfections, SH-SY5Y cells were transfected either with the pF5K-STOX1A or empty pF5K constructs. Selection of positive clones was possible due to the presence of the neomycin resistant gene present in the constructs. Positive clones were maintained in complete IMDB medium supplemented with 800 µg/ml G418 (Roche) until reaching confluence and subcultured every 2–3 days for about 4 weeks. 3 stable SH-SY5Y cell-lines with an at least 10 fold STOX1A over-expression compared to mock transfected cells were selected as described previously [43].

Transcript assembly and quantification by RNA-sequencing

Total RNA (1 µg / sample, DNase-treated, RIN ≥9.8) was subjected to a double round of poly-A mRNA purification, fragmented and primed for cDNA library synthesis using the TruSeq RNA sample preparation kit (FC-122-1001). All procedures were done according to the manufacturers instructions (Illumina). Following validation (Agilent 2100 Bioanalyzer, DNA High Sensitivity) and normalization (area under curve 200-1000 bp fragments), samples were clustered (TruSeq paired-end cluster kit v3-cBot-HS) (PE-401-3001) followed by paired-end sequencing (100 bp) (TruSeq SBS kit v3-HS (200 cycles) (FC-401-3001) on a HiSeq2000. To maximize coverage with inclusion of low abundance transcripts [44, 49], each lane contained a single DNA library. Cluster densities were between 623-970 K/mm², Q-scores (≥Q30) between 43.2-80.5 %, and FastQ output between 44.44-69.17 GB for both forward (R1) and reverse reads (R2). RNA-seq reads (unzipped, concatenated R1 and R2 fastQ files) were aligned to the pre-assembled reference genome (Illumina iGenome, data source UCSC, version hg18, June 20, 2011) using TopHat (1.4.0) in combination with Bowtie (0.12.5) and SAMtools (0.1.18) with default settings (adjusted for maximal threading) [19]. Transcript assembly, abundance estimation (defined as Fragments Per Kilobase of exon per Million fragments mapped, FPKM) and differential expression was performed by sequential analysis of TopHat output files (accepted_hits.bam). For this, transcripts were assembled using cufflinks (1.3.0)

which has implemented correction for fragment bias to account for biases in library preparation [50]. Differential analysis of significant changes on a gene and transcript level between experimental (STOX1A) and control (MOCK) conditions, was tested with Cuffdiff.

Results of differential gene, isoform, transcription start site group (TSS group) and coding sequence expression (CDS), as outputted by cuffdiff, were sorted in Excell (Microsoft) by q -value (False discovery rate (FDR) adjusted p -value of the test statistic).

TopHat and Cufflinks were installed and run on a 64-bit Linux desktop computer, Intel core I5 3.3 GHz quad-core and 16GB of internal memory. Running time for TopHat was approximately 1 week per DNA library (corresponding to one lane). Running time for cufflinks/cuffdiff was approximately 1 day per analysed TopHat output.

Visualization of mapped reads

Aligned TopHat reads were visualized with the program SeqMonk (<http://www.bioinformatics.babraham.ac.uk/projects/seqmonk/>). The BAM files generated by TopHat were directly uploaded into SeqMonk and then converted into probes to create average alignment tracks viewable as a bar chart as described in the online tutorial. The \log_2 of the frequency of the probes was plotted to better visualize the extensive range of the read coverage.

Ingenuity canonical pathway analysis

Canonical pathways analysis identified the pathways from the IPA library of canonical pathways that were most significant to the data set. Molecules from the data set that met the q -value cutoff of 0.05 (and \log_2 fold change 1.09) and were associated with a canonical pathway in the Ingenuity Knowledge Base were considered for the analysis. The significance of the association between the data set and the canonical pathway was measured in 2 ways: 1) A ratio of the number of molecules from the data set that map to the pathway divided by the total number of molecules that map to the canonical pathway is displayed. 2) Fisher's exact test was used to calculate a P -value determining the probability that the association between the genes in the dataset and the canonical pathway is explained by chance alone.

Supplementary Figure 1

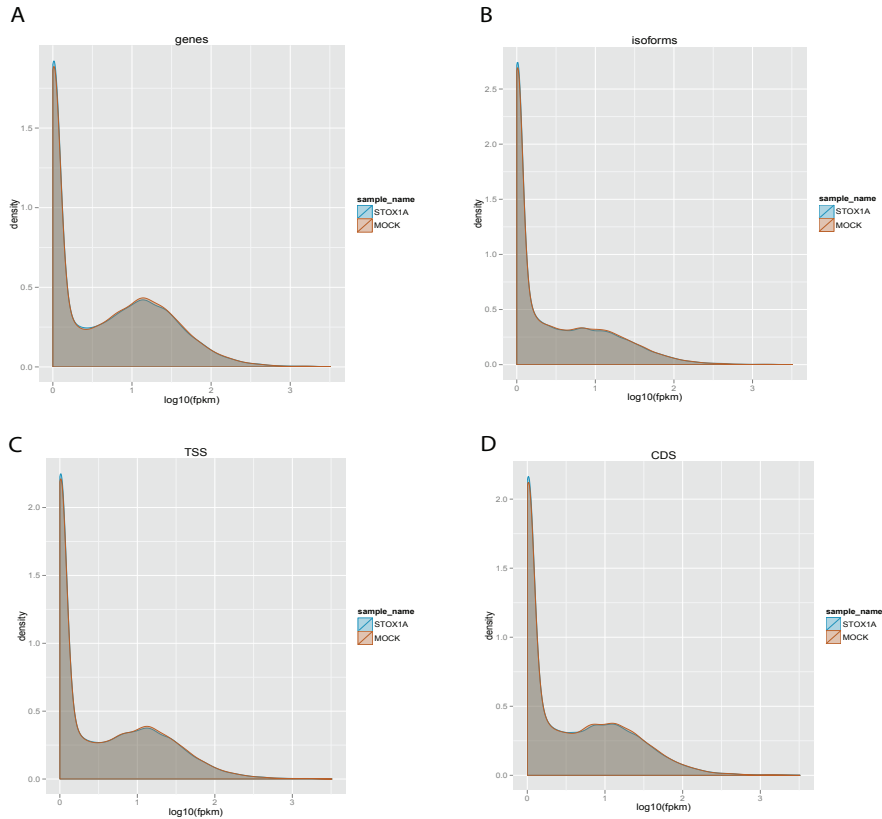


Figure S1. Density plots of expression level distribution of \log_{10} (FPKM) values across all STOX1A and MOCK expressed (A) genes (B) isoforms, (C) TSS groups and (D) CDS.

Supplementary Figure 2

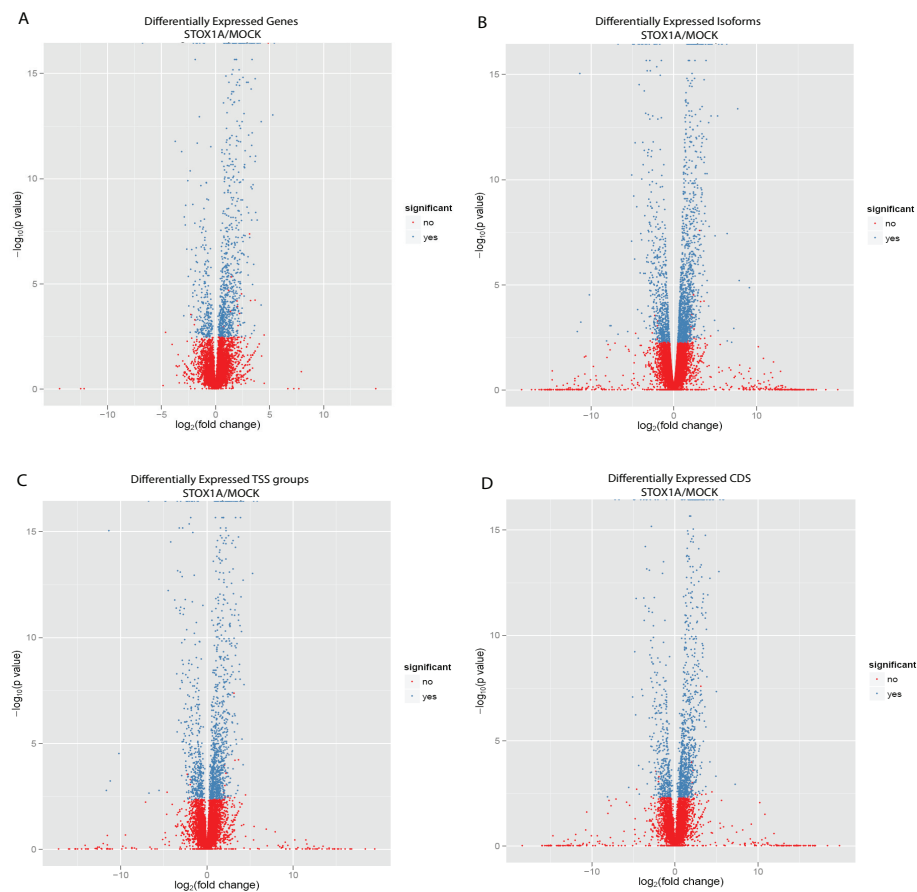


Figure S2. Volcano plots of $-\log_{10}(P\text{-value})$ versus $\log_2\text{-fold changes}$. Blue dots were detected as significant differential expression between STOX1A and MOCK at the 5% false-discovery rate (FDR, $q\text{-value} = 0.05$). Differentially expressed (A) genes (B) isoforms (C) TSS groups and (D) CDS.

Table S1. Genes showing alternative promoter usage.
Appendix Table_S1.pdf

Table S2. Genes showing alternative splicing.
Appendix Table_S2.pdf

Table S3. Significant differential expressed genes in STOX1A compared to MOCK treated cells as calculated by Cuffdiff at the 5% false-discovery rate (FDR, q -value = 0.05). The fold change is the ratio of FPKM between STOX1A and MOCK and converted to Log_2 . The differentially expressed genes were first ranked their q -value and then fold change. The 10 with the highest or lowest fold change are shown here.
Appendix Table_S3.pdf

Table S4. Significant differential expressed isoforms in STOX1A compared to MOCK treated cells as calculated by Cuffdiff at the 5% false-discovery rate (FDR, q -value = 0.05). The fold change is the ratio of FPKM between STOX1A and MOCK and converted to Log_2 . The differentially expressed isoforms were first ranked their q -value and then fold change. The 10 with the highest or lowest fold change are shown here.
Appendix Table_S4.pdf

Table S5. Significant differential expressed TSS groups in STOX1A compared to MOCK treated cells as calculated by Cuffdiff at the 5% false-discovery rate (FDR, q -value = 0.05). The fold change is the ratio of FPKM between STOX1A and MOCK and converted to Log_2 . The differentially expressed TSS groups were first ranked their q -value and then fold change. The 10 with the highest or lowest fold change are shown here.
Appendix Table_S5.pdf

Table S6. Significant differential expressed CDS in STOX1A compared to MOCK treated cells as calculated by Cuffdiff at the 5% false-discovery rate (FDR, q -value = 0.05). The fold change is the ratio of FPKM between STOX1A and MOCK and converted to Log_2 . The differentially expressed CDS were first ranked their q -value and then fold change. The 10 with the highest or lowest fold change are shown here.
Appendix Table_S6.pdf

References

- 1 Brennan RG: The winged-helix DNA-binding motif: another helix-turn-helix takeoff. *Cell* 1993, 74(5):773-776.
- 2 van Dijk M, Mulders J, Poutsma A, Konst AA, Lachmeijer AM, Dekker GA, Blankenstein MA, Oudejans CB: Maternal segregation of the Dutch preeclampsia locus at 10q22 with a new member of the winged helix gene family. *Nature genetics* 2005, 37(5):514-519.
- 3 van Dijk M, van Bezu J, van Abel D, Dunk C, Blankenstein MA, Oudejans CB, Lye SJ: The STOX1 genotype associated with pre-eclampsia leads to a reduction of trophoblast invasion by alpha-T-catenin upregulation. *Human molecular genetics* 2010, 19(13):2658-2667.
- 4 Tuteja G, Kaestner KH: Forkhead transcription factors II. *Cell* 2007, 131(1):192.
- 5 Tuteja G, Kaestner KH: SnapShot: forkhead transcription factors I. *Cell* 2007, 130(6):1160.
- 6 Hannenhalli S, Kaestner KH: The evolution of Fox genes and their role in development and disease. *Nature reviews* 2009, 10(4):233-240.
- 7 Duley L: The global impact of pre-eclampsia and eclampsia. *Seminars in perinatology* 2009, 33(3):130-137.
- 8 van Dijk M, van Bezu J, Poutsma A, Veerhuis R, Rozemuller AJ, Scheper W, Blankenstein MA, Oudejans CB: The pre-eclampsia gene STOX1 controls a conserved pathway in placenta and brain upregulated in late-onset Alzheimer's disease. *J Alzheimers Dis* 2010, 19(2):673-679.
- 9 Hardy J, Allsop D: Amyloid deposition as the central event in the aetiology of Alzheimer's disease. *Trends in pharmacological sciences* 1991, 12(10):383-388.
- 10 Linhoff MW, Lauren J, Cassidy RM, Dobie FA, Takahashi H, Nygaard HB, Airaksinen MS, Strittmatter SM, Craig AM: An unbiased expression screen for synaptogenic proteins identifies the LRRTM protein family as synaptic organizers. *Neuron* 2009, 61(5):734-749.
- 11 Andrews MR, Czvitkovich S, Dassie E, Vogelaar CF, Faissner A, Blits B, Gage FH, French-Constant C, Fawcett JW: Alpha9 integrin promotes neurite outgrowth on tenascin-C and enhances sensory axon regeneration. *J Neurosci* 2009, 29(17):5546-5557.
- 12 Lieberoth A, Splittstoesser F, Katagihallimath N, Jakovcevski I, Loers G, Ranscht B, Karageorgos D, Schachner M, Kleene R: Lewis(x) and alpha2,3-sialyl glycans and their receptors TAG-1, Contactin, and L1 mediate CD24-dependent neurite outgrowth. *J Neurosci* 2009, 29(20):6677-6690.
- 13 van Abel D, Holzel DR, Jain S, Lun FM, Zheng YW, Chen EZ, Sun H, Chiu RW, Lo YM, van Dijk M et al: SFRS7-mediated splicing of tau exon 10 is directly regulated by STOX1A in glial cells. *PloS one* 2011, 6(7):e21994.
- 14 Liu CW, Lee G, Jay DG: Tau is required for neurite outgrowth and growth cone motility of chick sensory neurons. *Cell motility and the cytoskeleton* 1999, 43(3):232-242.
- 15 Sousa I, Clark TG, Holt R, Pagnamenta AT, Mulder EJ, Minderaa RB, Bailey AJ, Battaglia A, Klauck SM, Poustka F et al: Polymorphisms in leucine-rich repeat genes are associated with autism spectrum disorder susceptibility in populations of European ancestry. *Molecular autism* 2010, 1(1):7.
- 16 Wang K, Zhang H, Ma D, Bucan M, Glessner JT, Abrahams BS, Salyakina D, Imielinski M, Bradfield JP, Sleiman PM et al: Common genetic variants on 5p14.1 associate with autism spectrum disorders. *Nature* 2009, 459(7246):528-533.

- 17 Hussman JP, Chung RH, Griswold AJ, Jaworski JM, Salyakina D, Ma D, Konidari I, Whitehead PL, Vance JM, Martin ER et al: A noise-reduction GWAS analysis implicates altered regulation of neurite outgrowth and guidance in autism. *Molecular autism* 2011, 2(1):1.
- 18 Trapnell C, Roberts A, Goff L, Pertea G, Kim D, Kelley DR, Pimentel H, Salzberg SL, Rinn JL, Pachter L: Differential gene and transcript expression analysis of RNA-seq experiments with TopHat and Cufflinks. *Nature protocols* 2012, 7(3):562-578.
- 19 Trapnell C, Pachter L, Salzberg SL: TopHat: discovering splice junctions with RNA-Seq. *Bioinformatics (Oxford, England)* 2009, 25(9):1105-1111.
- 20 Wang Y, Ghaffari N, Johnson CD, Braga-Neto UM, Wang H, Chen R, Zhou H: Evaluation of the coverage and depth of transcriptome by RNA-Seq in chickens. *BMC bioinformatics* 2011, 12 Suppl 10:S5.
- 21 Alderton WK, Cooper CE, Knowles RG: Nitric oxide synthases: structure, function and inhibition. *The Biochemical journal* 2001, 357(Pt 3):593-615.
- 22 Reif A, Grunblatt E, Herterich S, Wichart I, Rainer MK, Jungwirth S, Danielczyk W, Deckert J, Tragl KH, Riederer P et al: Association of a functional NOS1 promoter repeat with Alzheimer's disease in the VITA cohort. *J Alzheimers Dis* 2011, 23(2):327-333.
- 23 Galimberti D, Scarpini E, Venturelli E, Strobel A, Herterich S, Fenoglio C, Guidi I, Scalabrini D, Cortini F, Bresolin N et al: Association of a NOS1 promoter repeat with Alzheimer's disease. *Neurobiology of aging* 2008, 29(9):1359-1365.
- 24 Kim HW, Cho SC, Kim JW, Cho IH, Kim SA, Park M, Cho EJ, Yoo HJ: Family-based association study between NOS-I and -IIA polymorphisms and autism spectrum disorders in Korean trios. *Am J Med Genet B Neuropsychiatr Genet* 2009, 150B(2):300-306.
- 25 Fornasiero EF, Bonanomi D, Benfenati F, Valtorta F: The role of synapsins in neuronal development. *Cell Mol Life Sci* 2010, 67(9):1383-1396.
- 26 Anitha A, Nakamura K, Yamada K, Suda S, Thanseem I, Tsujii M, Iwayama Y, Hattori E, Toyota T, Miyachi T et al: Genetic analyses of roundabout (ROBO) axon guidance receptors in autism. *Am J Med Genet B Neuropsychiatr Genet* 2008, 147B(7):1019-1027.
- 27 Suda S, Iwata K, Shimmura C, Kamenoy Y, Anitha A, Thanseem I, Nakamura K, Matsuzaki H, Tsuchiya KJ, Sugihara G et al: Decreased expression of axon-guidance receptors in the anterior cingulate cortex in autism. *Molecular autism* 2011, 2(1):14.
- 28 Kim M, Roesener AP, Mendonca PR, Mastick GS: Robo1 and Robo2 have distinct roles in pioneer longitudinal axon guidance. *Developmental biology* 2011, 358(1):181-188.
- 29 Aidaraliev N, Kamino K, Kimura R, Yamamoto M, Morihara T, Kazui H, Hashimoto R, Tanaka T, Kudo T, Kida T et al: Dynamin 2 gene is a novel susceptibility gene for late-onset Alzheimer disease in non-APOE-epsilon4 carriers. *Journal of human genetics* 2008, 53(4):296-302.
- 30 Kamagata E, Kudo T, Kimura R, Tanimukai H, Morihara T, Sadik MG, Kamino K, Takeda M: Decrease of dynamin 2 levels in late-onset Alzheimer's disease alters Abeta metabolism. *Biochemical and biophysical research communications* 2009, 379(3):691-695.
- 31 Sever S: Dynamin and endocytosis. *Current opinion in cell biology* 2002, 14(4):463-467.
- 32 Lu Z, Elliott MR, Chen Y, Walsh JT, Klibanov AL, Ravichandran KS, Kipnis J: Phagocytic activity of neuronal progenitors regulates adult neurogenesis. *Nature cell biology* 2011, 13(9):1076-1083.
-

- 33 Kim JY, Oh MH, Bernard LP, Macara IG, Zhang H: The RhoG/ELMO1/Dock180 signaling module is required for spine morphogenesis in hippocampal neurons. *The Journal of biological chemistry* 2011, 286(43):37615-37624.
- 34 De Marco Garcia NV, Karayannis T, Fishell G: Neuronal activity is required for the development of specific cortical interneuron subtypes. *Nature* 2011, 472(7343):351-355.
- 35 Prior M, Shi Q, Hu X, He W, Levey A, Yan R: RTN/Nogo in forming Alzheimer's neuritic plaques. *Neuroscience and biobehavioral reviews* 2010, 34(8):1201-1206.
- 36 Bandtlow CE, Schwab ME: NI-35/250/nogo-a: a neurite growth inhibitor restricting structural plasticity and regeneration of nerve fibers in the adult vertebrate CNS. *Glia* 2000, 29(2):175-181.
- 37 Constancia M, Hemberger M, Hughes J, Dean W, Ferguson-Smith A, Fundele R, Stewart F, Kelsey G, Fowden A, Sibley C et al: Placental-specific IGF-II is a major modulator of placental and fetal growth. *Nature* 2002, 417(6892):945-948.
- 38 Glessner JT, Wang K, Cai G, Korvatska O, Kim CE, Wood S, Zhang H, Estes A, Brune CW, Bradfield JP et al: Autism genome-wide copy number variation reveals ubiquitin and neuronal genes. *Nature* 2009, 459(7246):569-573.
- 39 Pagnamenta AT, Bacchelli E, de Jonge MV, Mirza G, Scerri TS, Minopoli F, Chiocchetti A, Ludwig KU, Hoffmann P, Paracchini S et al: Characterization of a family with rare deletions in CNTNAP5 and DOCK4 suggests novel risk loci for autism and dyslexia. *Biological psychiatry* 2010, 68(4):320-328.
- 40 Gauthier J, Siddiqui TJ, Huashan P, Yokomaku D, Hamdan FF, Champagne N, Lapointe M, Spiegelman D, Noreau A, Lafreniere RG et al: Truncating mutations in NRXN2 and NRXN1 in autism spectrum disorders and schizophrenia. *Human genetics* 2011, 130(4):563-573.
- 41 Leblond CS, Heinrich J, Delorme R, Proepper C, Betancur C, Huguet G, Konyukh M, Chaste P, Ey E, Rastam M et al: Genetic and functional analyses of SHANK2 mutations suggest a multiple hit model of autism spectrum disorders. *PLoS genetics* 2012, 8(2):e1002521.
- 42 Sato D, Lionel AC, Leblond CS, Prasad A, Pinto D, Walker S, O'Connor I, Russell C, Drmic IE, Hamdan FF et al: SHANK1 Deletions in Males with Autism Spectrum Disorder. *American journal of human genetics* 2012.
- 43 van Abel D, Abdul-Hamid O, Dijk M, Oudejans CB: Transcription factor STOX1A promotes mitotic entry by binding to the CCNB1 promoter. *PloS one* 2012, 7(1):e29769.
- 44 Trapnell C, Williams BA, Pertea G, Mortazavi A, Kwan G, van Baren MJ, Salzberg SL, Wold BJ, Pachter L: Transcript assembly and quantification by RNA-Seq reveals unannotated transcripts and isoform switching during cell differentiation. *Nature biotechnology* 2010, 28(5):511-515.
- 45 Roberts A, Pimentel H, Trapnell C, Pachter L: Identification of novel transcripts in annotated genomes using RNA-Seq. *Bioinformatics (Oxford, England)* 2011, 27(17):2325-2329.
- 46 Yang R, Muller C, Huynh V, Fung YK, Yee AS, Koeffler HP: Functions of cyclin A1 in the cell cycle and its interactions with transcription factor E2F-1 and the Rb family of proteins. *Molecular and cellular biology* 1999, 19(3):2400-2407.
- 47 Chedotal A, Richards LJ: Wiring the brain: the biology of neuronal guidance. *Cold Spring Harbor perspectives in biology* 2010, 2(6):a001917.
- 48 Song W, Lahiri DK: Efficient transfection of DNA by mixing cells in suspension with calcium phosphate. *Nucleic acids research* 1995, 23(17):3609-3611.
- 49 Garber M, Grabherr MG, Guttman M, Trapnell C: Computational methods for

- transcriptome annotation and quantification using RNA-seq. *Nature methods* 2011, 8(6):469-477.
- 50 Roberts A, Trapnell C, Donaghey J, Rinn JL, Pachter L: Improving RNA-Seq expression estimates by correcting for fragment bias. *Genome biology* 2011, 12(3):R22.



Chapter 7

**Summarizing Discussion
Directions for future research**

Summarizing discussion

This thesis describes the exploration of STOX1A in neuronal transcriptional networks, a transcription factor previously shown to be associated with late onset Alzheimer's disease (LOAD). Previous studies have shown that over-expression of STOX1A is already detected in early Braak stages i.e. prior to the full blown development of LOAD. This raises the possibility that STOX1A itself or its target genes can be used as potential targets for therapeutic intervention in LOAD. However, although preclinical studies in cell systems and animal models have already supported the concept of directly targeting transcription factors in diseases like cancer [1], these approaches currently remain not yet suitable for therapeutic use. Furthermore, such drugs would block widely-present signalling mechanisms where STOX1A is potentially involved in. Therefore, targeting STOX1A directly without knowing its normal neuronal function could have severe side effects. Alternatively, neuronal STOX1A up- or downstream signalling cascades could be modulated by drugs, and in the future can serve as potential targets for therapeutic drug design to treat diseases like LOAD. It is therefore essential to identify and clarify up- and downstream regulatory mechanisms for STOX1A in neuronal transcriptional signalling. These mechanisms for STOX1A are still largely unknown. Therefore, in this thesis our primary goal was to identify such mechanisms and to find out how STOX1A is operating in neuronal transcriptional networks. This knowledge would be of great importance to give insight in how STOX1A operates in the normal brain but could also explain why STOX1A expression or function is deregulated or disrupted, respectively, in neurodegenerative diseases like LOAD. Furthermore, STOX1A itself or its target genes could also serve as potential biomarkers in LOAD provided they are detectable in spinal fluid and/or reflected in blood.

In this chapter our main findings are summarized and discussed. Furthermore, directions for future research are given.

In addition to the previously discovered STOX1A target genes leucine rich repeat transmembrane neuronal 3 (*LRRTM3*) and Alpha-T-Catenin (*CTNNA3*), our first study (**Chapter 2**) describes the discovery of several potential STOX1A target genes with the use of ChIP-cloning. In this study, potential STOX1A bound DNA fragments were immunoprecipitated, cloned, and subsequently sequenced. Corresponding genes linked to these sequenced fragments, e.g. Contactin-associated protein-like 2 (*CNTNAP2*), a cell-cell adhesion molecule that may play a role in the local differentiation of the axon into distinct functional subdomains [2, 3], were determined. We found that expression of *CNTNAP2* is directly and negatively regulated by STOX1A in neuronal SK-N-SH cells. Interestingly, we found that *CNTNAP2* expression levels are decreased in the hippocampus of LOAD patients where STOX1A expression levels are increased. This suggests that expression of STOX1A and *CNTNAP2* are inversely associated in the hippocampus of LOAD patients.

CNTNAP2 has previously been shown to be linked to autism spectrum disorders

(ASD) but to our knowledge never with LOAD pathology. We therefore show for the first time that *CNTNAP2* is also associated with another brain disorder, Alzheimer's disease.

In **Chapter 3** we extended our search for STOX1A target genes by performing ChIP-seq, a technique to discover fragments of DNA that bind to the experimental protein of interest on a genome wide scale. By applying this technique we discovered several potential STOX1A target genes. One target gene we validated, and found to be directly regulated by STOX1A, is serine/arginine-rich splicing factor 7 (*SFRS7*). While this study was performed in a neuronal cell model, we found that the transcriptional effect of STOX1A on *SFRS7* was only occurring in glial cells. Therefore, the effect of STOX1A on *SFRS7* was found to be cell type specific.

SFRS7 itself also appears to operate in a cell type-dependent manner. While *SFRS7* has previously been shown to inhibit the splicing of tau at exon 10 in neuronal cells [4] we expected to find a similar effect in glial cells. However, STOX1A dependent transactivation of *SFRS7* in glial cells resulted in an increase in tau exon 10 splicing. In concordance, we found that knockdown of *SFRS7* in glial cells inhibits tau exon 10 splicing. Therefore, our results suggest that *SFRS7* acts as a tau exon 10 splicing enhancer in glial cells instead of a tau exon 10 splicing silencer in neuronal cells. Future perspectives of this finding are discussed below.

Besides the systematic search for STOX1A target genes with ChIP-cloning and Chip-seq, we also investigated a previously suggested role for STOX1A: regulation of the cell-cycle. **Chapter 4** describes the results of the direct interaction between STOX1A and the promoter region of the *CCNB1* gene. *CCNB1* is known as an important regulator of the G2/M phase transition of the cell cycle where *CCNB1* binds to CDK1 to form an active kinase necessary for proper G2/M phase progression [5]. The potential relationship between STOX1A, *CCNB1*, and G2/M phase cell cycle progression was therefore investigated. As the results show, the direct interaction between STOX1A and the *CCNB1* promoter transactivated *CCNB1* expression and, as hypothesised, resulted in enhanced progression of cells into mitosis.

Although we primarily focussed on a functional relationship between *CCNB1* and STOX1A, we also found additional cyclins to be differentially expressed. This indicates that STOX1A is important during other phases of the cell cycle as well.

According to the “two hit hypothesis” a combination of both oxidative stress and cell cycle aberration may be necessary for a normal neuron to become a LOAD neuron. The aberrant neuronal cell cycle regulation is possibly one of the underlying mechanism that reflects hyper-phosphorylated tau proteins in neurofibrillary tangles (NFT) by over-activated cell cycle related kinases like CDK1 [6]. Because STOX1A is involved in regulation of the cell cycle (**Chapter 4**), we speculated there might be a correlation between STOX1A, the cell cycle, and tau phosphorylation. This was investigated in **chapter 5**. In this chapter we show that stable overexpression of STOX1A in neuronal SH-SY5Y cells is associated with hyper-phosphorylation of tau proteins at epitopes also found in NFT in LOAD. Furthermore, results show that hyper-phosphorylation of tau epitopes could in part be explained by the increase in CDK1 activity levels specifically induced by STOX1A in these cells. This is also consistent with the findings

of **chapter 4**, where we show that CCNB1, the activating binding partner of CDK1, is a direct target gene transactivated by STOX1A.

In our final chapter (**Chapter 6**) we extended our search to unravel the functional role of STOX1A in neuronal transcriptional signalling using another genome-wide approach. Here, we sequenced (RNA-seq) and determined the entire transcriptome of neuronal SH-SY5Y cells that were stimulated with STOX1A recombinant protein. Although preliminary, these results show some new insights for a potential role for STOX1A in neuronal development e.g. an abundant amount in the top 10 of most significantly STOX1A differentially expressed genes and transcripts are involved in the neurodevelopmental processes neurite outgrowth and axon guidance signalling. Furthermore, canonical pathway analysis with STOX1A differentially expressed genes and transcripts resulted in significant enrichment in axon guidance signalling. These mechanisms have been found to be deregulated in the pathogenesis of autism spectrum disorder (ASD). Speculatively, these results, together with other related findings shown in this thesis (discusses below), imply a potential functional role for STOX1A in the etiology of ASD.

We have also identified additional potential STOX1A target genes which may represent novel candidates for involvement in LOAD, and speculatively, in the future could serve as novel biomarkers.

Directions for future research

CNTNAP2 and STOX1A

The expression of STOX1A is already increased at early Braak stages during the development into LOAD. Secondly, we found that the direct STOX1A target gene CNTNAP2 is downregulated in LOAD, indicating that (besides STOX1A itself) this gene might be used as a potential biomarker for the early diagnosis of LOAD. However, CNTNAP2 expression is significantly downregulated in the final stages (Braak 5/6) of the disease. Therefore, we first have to confirm that CNTNAP2 expression is also changed at early Braak stages as was seen for STOX1A.

It would also be necessary to see if CNTNAP2 proteins can be detected in cerebrospinal fluid (CSF) or blood to serve as a biomarker. If this would be the case, a detection of decreased levels of CNTNAP2 in CSF or blood could be used to predict development into LOAD.

As shown above, discovery of STOX1A target genes can be very helpful to understand underlying transcriptional changes in LOAD which can also potentially serve as novel biomarkers. Interestingly, STOX1A target genes themselves can also serve to predict potential roles for STOX1A in other pathologies. As discussed above, CNTNAP2 has been found to be associated with ASD. This association is also found with other previously characterised STOX1A target genes i.e. polymorphisms in *LRRTM3* have recently been found to be associated with ASD susceptibility in populations of European ancestry [7]. Additionally, *CTNNA3*, has been suggested to be associated with ASD susceptibility [8]. Because *CTNNA3*, *LRRTM3*, and *CNTNAP2* (**Chapter 2**) are validated STOX1A target genes, this strongly suggests that STOX1A operates

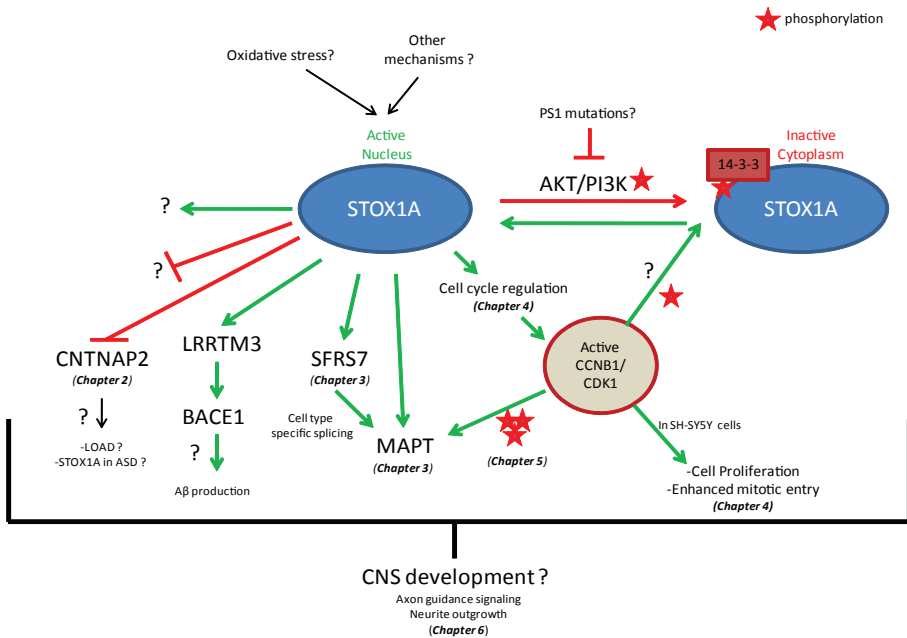


Figure 1. A model for STOX1A which summarizes our findings described in this thesis. Together, as many STOX1A (un)validated target genes have functions in neuronal developmental processes we speculate a potential role for STOX1A in central nervous system (CNS) development. Hypothetically, in LOAD, active CCNB1/CDK1 phosphorylates inactive STOX1A at sites which prevent 14-3-3 molecules from binding to PI3K/AKT phosphorylation sites. STOX1A is then consequently transported into the nucleus where it can perform its transcriptional activity. The resulting transcription of CCNB1 by STOX1A results in an increase in active CCNB1/CDK1 which initiates a positive feedback loop. The resulting accumulating active CCNB1/CDK1 induces phosphorylation of MAPT proteins resulting in NFT formation. Upstream mechanisms influence the expression of STOX1A. Chronic oxidative stress and for instance epigenetic changes in LOAD could possibly cause overexpression of STOX1A. PS1 mutations in familial alzheimer's disease (FAD) results in inhibition of the PI3K/AKT pathway, speculatively this results in translocation of STOX1A to the nucleus. Stars indicate phosphorylation events.

upstream in pathways associated with ASD. This is furthermore supported by our genome-wide transcriptome analysis of STOX1A-induced differential expression. In this study (Chapter 6) we found several additional potential STOX1A target genes associated with ASD. A majority of these genes also operate in pathways associated with neuronal developmental processes, neurite outgrowth and/or axon guidance signalling. This suggests that STOX1A has a potential role in neuronal development. In conclusion, besides the potential implication for the new STOX1A target gene *CNTNAP2* as a novel biomarker for LOAD, it would be very interesting to further investigate the role of STOX1A in neuronal development and its implications in the etiology of ASD.

STOX1A dependent transcription operates in a cell type specific manner

Our findings show that STOX1A is unable to transactivate SFRS7 in neuronal cells. In contrast, we found that in glial cells STOX1A is capable of transactivating SFRS7

thereby changing 3R/4R tau ratios. Several tauopathies show deregulation of 3R-tau and 4R-tau isoform expression altering the 3R/4R tau ratio (increased splicing of tau exon 10 results in more 4R-tau). Corticobasal degeneration and progressive supranuclear palsy (PSP) show mainly 4R-tau pathology [9] which occurs not only in neurons but also in astrocytes, a type of glial cells [10]. The clinical significance of tau accumulation in astrocytes is not clear but a recent study indicated that in a transgenic mouse model of specific astrocytic tau pathology there was mild blood-brain barrier disruption, induction of low-molecular-weight heat shock proteins, and focal neuron degeneration [11]. It would therefore be very interesting to investigate if STOX1A and SFRS7 are associated with astrocytic 4R-tau pathology.

We found cell type-specific effects of STOX1A on SFRS7 expression, suggesting that other factors can influence the transcriptional activation of STOX1A on SFRS7 in a cell type-specific manner. These factors could for instance be co-activators which, in complex with STOX1A, are capable of activating transcription at the SFRS7 promoter in glial cells but are absent in neuronal cells. Another possibility would be that in neuronal cells co-repressors bind to STOX1A thereby inhibiting transcription at the SFRS7 promoter. Gaining knowledge regarding the potential co-factors which are bound to STOX1A in neurons and glial cells will help explain the cell type-specific transactivation of SFRS7. These co-factors could also suppress or activate STOX1A dependent transcription of other genes and are therefore crucial in understanding STOX1A gene regulation. In the future they might also be of great therapeutic relevance as they can modulate the transcriptional activity of STOX1A. For instance, inhibitors targeting STOX1A co-factors could block gene expression of genes like *LRRTM3*, thereby altering the production of A β . Further exploration of these co-factor associated mechanisms would therefore be of great significance.

A potential role for STOX1A in neuronal development

In vitro results described in this thesis show that STOX1A is involved in the regulation of the cell cycle and regulates genes shown to be important in neuronal differentiation and development, like *MAPT* and *CNTNAP2*. Similar functions have been found for several FOX transcription factors which are key players in CNS development; for example, FOXG1 regulates proliferation and differentiation of neuronal progenitor cells of the telencephalon [12].

Although care has to be taken interpreting our *in vitro* results into an actual *in vivo* situation, our results might suggest that STOX1A also has an important function in CNS development. To reveal such association, primary neuronal cell-lines could serve as models to further explore the functional relevance of STOX1A during CNS development. These can be primary cultures of mouse hippocampus and cerebral cortex, which are widely used model systems for molecular and cell biological studies of neuronal development and function. Ideally, STOX1A transgenic or knockout mice would be perfect models to study neuronal developmental roles for STOX1A.

STOX1A and upstream mechanisms in LOAD

Our results have given new insight in the functional roles of STOX1A in neuronal signalling. However, important questions that remain are; why and how is STOX1A

expression deregulated in LOAD? In view of the “two hit hypothesis” it is speculated that the two main causal factors for LOAD are a combination of oxidative stress and cell cycle aberration [6]. Both could also be potential inducers of STOX1A expression and/or activity. For example, oxidative stress has been shown to be capable of inducing the expression of transcription factor SP1 [13] and thereby results in the expression of several AD-related proteins [14]. STOX1A expression could be induced in a similar way. Therefore, investigating STOX1A expression or activity in response to oxidative stress could reveal such upstream mechanisms.

The cell cycle itself, specifically active CDK1, might also induce STOX1A activity. STOX1A can potentially be phosphorylated by CDK1 in a cell cycle dependent manner, a mechanism that has been shown to operate upstream of several forkhead transcription factors including FOXM1 [15], FOXO1 [16], and FOXK2 [17]. For these it has been shown that phosphorylation of residues by active CDK1, takes place near residues phosphorylated by the PI3K/AKT pathway. The residues phosphorylated by active CDK1 may cause conformational changes, which inhibit 14-3-3 proteins from interacting with residues phosphorylated by PI3K/AKT pathway. When 14-3-3 proteins are bound to residues phosphorylated by PI3K/AKT pathway they prevent forkhead transcription factors from entering the nucleus thereby inhibiting their transcriptional activity. In contrast, CDK1 phosphorylation therefore leads to more nuclear localization of the transcription factors thereby increasing their transcriptional activity.

Software tools, which can predict post-translational modifications, might reveal CDK1 target sites on STOX1A, and together with mutagenesis applied on these potential specific CDK1 residues in the STOX1A sequence could mimic CDK1 phosphorylation. The functional effect can be investigated which would reveal the potential upstream regulatory effect of CDK1 on STOX1A activity.

Together, oxidative stress and cell cycle aberrations (like abundantly active CDK1), which appear very early in the disease progression of LOAD and precede formation of A β and NFT's [18], could be responsible for abnormally induced expression and activity of transcription factors like STOX1A. In this scenario, overexpression and overactivated STOX1A subsequently leads to induced expression of cell cycle genes like *CCNB1*. *CCNB1* can then associate with CDK1 forming an active kinase capable of further phosphorylating STOX1A, thus activating STOX1A in a positive feedback loop.

Accumulation of cell cycle kinases can furthermore hyperphosphorylate tau proteins to form NFT until the cell eventually succeeds in apoptosis by mechanisms explained by the “two hit hypothesis”.

Secondly, the resulting overexpression and/or overactivity of STOX1A could suppress or induce expression of *CNTNAP2* and *LRRTM3*, respectively. Suppression of *CNTNAP2* by STOX1A, as shown in chapter 2, could potentially disrupt local differentiation of axons into distinct functional subdomains and therefore aggravate neurodegeneration. Transactivation of *LRRTM3* by STOX1A contributes to abnormal production of A β .

Other upstream regulatory mechanisms most likely exist as well. One of the mechanisms which certainly operates upstream of STOX1A is the PI3K/AKT

pathway [19]. Phosphorylation of STOX1A by the PI3K/AKT pathway inhibits its activity by translocation to the cytoplasm. In LOAD it has been found that AKT activity is decreased [20], which could explain higher activity (nuclear expression) of STOX1A in LOAD.

With the latter notion, STOX1A could also be important in early-onset familial Alzheimer's disease (FAD). It has been shown that wild-type PS1 acts upstream in the regulation of the PI3K/AKT pathway. Mutations in PS1 as found in FAD cause an impairment in its ability to phosphorylate AKT and thereby inhibiting the PI3K/AKT pathway [21]. Speculatively, this suggests that reduced activity of the PI3K/AKT by PS1 mutations in FAD can consequently cause an over-activity of transcription factors which are regulated by the PI3K/AKT pathway, as shown for STOX1A. Therefore it would be very interesting to test if STOX1A is also deregulated in FAD and whether PS1 mutations in a cellular or mouse model can cause an effect on the activity levels of STOX1A through reduced activity of PI3K/AKT.

A consensus binding site for STOX1A

When STOX1A is located in the nucleus it can perform its transcriptional activity through specific binding to DNA elements which in turn regulates transcription of nearby genes. Unfortunately, no such DNA binding consensus sequence has been discovered for STOX1A. One of the goals of our ChIP-seq study was to identify a DNA binding consensus sequence for STOX1A. With the use of our predicted STOX1A binding sequences from our ChIP-seq study we uploaded these sequences into the bioinformatics tool MEMECHIP [22] which predicted several potential binding motifs. However, changes in the number of input sequences seemed to strongly affect the outcome of these results. Possibly, the input sequences included false positive sequences which influenced the outcomes. Therefore, another approach is needed. One possibility would be to validate potential STOX1A binding sites by quantitative PCR and then use these validated binding site sequences for motif analysis. This would exclude false positive sequences which greatly increases reliability in the motif analysis. Furthermore, additional ChIP-seq experiments would reveal binding sites that overlap between individual ChIP-seq experiments and therefore have a greater reliability to identify true STOX1A binding sites.

Concluding remarks

This thesis describes the functional exploration of the transcription factor STOX1A in neuronal signalling. As we have shown, discovery of STOX1A target genes can be useful to reveal underlying mechanisms operating in LOAD which are not previously described in literature, such as CNTNAP2 (**Chapter 2**). Other STOX1A target genes identified by our genome-wide approaches might result in similar findings. STOX1A is therefore an interesting protein, which target genes might be used for future therapeutic drug design. Furthermore, its target genes can potentially serve as novel biomarkers in LOAD.

Secondly, we have shown that the discovery of STOX1A target genes and their associated transcriptional networks suggest the possible implication of STOX1A in other diseases, e.g. glial tau pathologies (**Chapter 3**) and ASD (**Chapter 2 and 6**).

In conclusion, the results presented in this thesis elucidate the emerging biological roles of STOX1A in neuronal signalling and its importance in the development of neurological diseases.

Finally, the findings and hypothesized mechanisms which are presented in this thesis are summarized in figure 1.

References

- 1 Redell MS, Tweardy DJ: Targeting transcription factors for cancer therapy. *Current pharmaceutical design* 2005, 11(22):2873-2887.
- 2 Poliak S, Gollan L, Martinez R, Custer A, Einheber S, Salzer JL, Trimmer JS, Shrager P, Peles E: Caspr2, a new member of the neurexin superfamily, is localized at the juxtaparanodes of myelinated axons and associates with K⁺ channels. *Neuron* 1999, 24(4):1037-1047.
- 3 Rasband MN: It's "juxta" potassium channel! *Journal of neuroscience research* 2004, 76(6):749-757.
- 4 Gao L, Wang J, Wang Y, Andreadis A: SR protein 9G8 modulates splicing of tau exon 10 via its proximal downstream intron, a clustering region for frontotemporal dementia mutations. *Molecular and cellular neurosciences* 2007, 34(1):48-58.
- 5 Porter LA, Donoghue DJ: Cyclin B1 and CDK1: nuclear localization and upstream regulators. *Progress in cell cycle research* 2003, 5:335-347.
- 6 Bonda DJ, Lee HP, Kudo W, Zhu X, Smith MA, Lee HG: Pathological implications of cell cycle re-entry in Alzheimer disease. *Expert reviews in molecular medicine* 2010, 12:e19.
- 7 Sousa I, Clark TG, Holt R, Pagnamenta AT, Mulder EJ, Minderaa RB, Bailey AJ, Battaglia A, Klauck SM, Poustka F et al: Polymorphisms in leucine-rich repeat genes are associated with autism spectrum disorder susceptibility in populations of European ancestry. *Molecular autism* 2010, 1(1):7.
- 8 Wang K, Zhang H, Ma D, Bucan M, Glessner JT, Abrahams BS, Salyakina D, Imielinski M, Bradfield JP, Sleiman PM et al: Common genetic variants on 5p14.1 associate with autism spectrum disorders. *Nature* 2009, 459(7246):528-533.
- 9 Sergeant N, Watzel A, Delacourte A: Neurofibrillary degeneration in progressive supranuclear palsy and corticobasal degeneration: tau pathologies with exclusively "exon 10" isoforms. *Journal of neurochemistry* 1999, 72(3):1243-1249.
- 10 Yoshida M: Cellular tau pathology and immunohistochemical study of tau isoforms in sporadic tauopathies. *Neuropathology* 2006, 26(5):457-470.
- 11 Forman MS, Lal D, Zhang B, Dabir DV, Swanson E, Lee VM, Trojanowski JQ: Transgenic mouse model of tau pathology in astrocytes leading to nervous system degeneration. *J Neurosci* 2005, 25(14):3539-3550.
- 12 Hanashima C, Li SC, Shen L, Lai E, Fishell G: Foxg1 suppresses early cortical cell fate. *Science (New York, NY)* 2004, 303(5654):56-59.
- 13 Santpere G, Nieto M, Puig B, Ferrer I: Abnormal Sp1 transcription factor expression in Alzheimer disease and tauopathies. *Neuroscience letters* 2006, 397(1-2):30-34.
- 14 Citron BA, Dennis JS, Zeitlin RS, Echeverria V: Transcription factor Sp1 dysregulation in Alzheimer's disease. *Journal of neuroscience research* 2008, 86(11):2499-2504.
- 15 Major ML, Lepe R, Costa RH: Forkhead box M1B transcriptional activity requires binding of Cdk-cyclin complexes for phosphorylation-dependent recruitment of p300/CBP coactivators. *Molecular and cellular biology* 2004, 24(7):2649-2661.
- 16 Yuan Z, Becker EB, Merlo P, Yamada T, DiBacco S, Konishi Y, Schaefer EM, Bonni A: Activation of FOXO1 by Cdk1 in cycling cells and postmitotic neurons. *Science (New York, NY)* 2008, 319(5870):1665-1668.
- 17 Marais A, Ji Z, Child ES, Krause E, Mann DJ, Sharrocks AD: Cell cycle-dependent regulation of the forkhead transcription factor FOXK2 by CDK.cyclin complexes. *The Journal of biological chemistry* 2010, 285(46):35728-35739.
- 18 Yang Y, Varvel NH, Lamb BT, Herrup K: Ectopic cell cycle events link human Alzheimer's disease and amyloid precursor protein transgenic mouse models. *J*

- Neurosci 2006, 26(3):775-784.
- 19 van Dijk M, van Bezu J, van Abel D, Dunk C, Blankenstein MA, Oudejans CB, Lye SJ: The STOX1 genotype associated with pre-eclampsia leads to a reduction of trophoblast invasion by alpha-T-catenin upregulation. *Human molecular genetics* 2010, 19(13):2658-2667.
- 20 Lee HK, Kumar P, Fu Q, Rosen KM, Querfurth HW: The insulin/Akt signaling pathway is targeted by intracellular beta-amyloid. *Molecular biology of the cell* 2009, 20(5):1533-1544.
- 21 Baki L, Shioi J, Wen P, Shao Z, Schwarzman A, Gama-Sosa M, Neve R, Robakis NK: PS1 activates PI3K thus inhibiting GSK-3 activity and tau overphosphorylation: effects of FAD mutations. *The EMBO journal* 2004, 23(13):2586-2596.
- 22 Price A, Ramabhadran S, Pevzner PA: Finding subtle motifs by branching from sample strings. *Bioinformatics (Oxford, England)* 2003, 19 Suppl 2:ii149-155.



Appendices

Nederlandse Samenvatting
List of Publications
Curriculum Vitae
Dankwoord

Nederlandse Samenvatting

De rol van transcriptiefactor STOX1A in neurodegeneratieve transcriptionele netwerken.

Dit proefschrift beschrijft de exploratie van STOX1A, een transcriptiefactor die geassocieerd is met Late Onset Alzheimer Disease (LOAD). LOAD is de meest voorkomende vorm van de ziekte van Alzheimer en uit zich na de leeftijd van 65 jaar. De ziekte van Alzheimer is de meest voorkomende vorm van dementie en kenmerkt zich door een algemene achteruitgang in cognitieve functies zoals geheugen en spraak. Pathologisch wordt LOAD gekenmerkt door de zogenaamde plaques bestaande uit het amyloid- β ($A\beta$) eiwit, en de neurofibrillaire “tangles” (NFT). Excessieve ophoping van deze eiwitten in de hersenen resulteert onder andere in afsterving van neuronen (zenuwcellen).

Transcriptiefactoren zoals STOX1A zijn in staat specifiek aan bepaalde stukken DNA te binden en kunnen daardoor over het algemeen vele doelwitgenen reguleren. Transcriptiefactoren zullen deze fragmenten op een specifieke manier binden en daardoor in staat zijn de expressie (uiteindelijke vorming van een eiwit) van hun doelwitgenen te reguleren. Het vinden van deze specifieke stukken DNA is dus belangrijk om inzicht te krijgen over de doelwitgenen die STOX1A reguleert. Transcriptiefactoren zijn door deze eigenschap per definitie betrokken bij belangrijke cellulaire processen. De doelwitgenen en bijbehorende cellulaire processen zijn voor STOX1A grotendeels onbekend. Echter, eerdere studies hebben aangetoond dat STOX1A het Leucine Rich Repeat Transmembrane Neuronal 3 (*LRRTM3*) doelwitgen aanstuurt in neuronale cellen (cellen representatief voor zenuwcellen) en via verhoging van het *LRRTM3* eiwit indirect bijdraagt aan de productie en vorming van het $A\beta$ eiwit. Verder toont deze studie ook aan dat verhoogde expressie van transcriptiefactor STOX1A zelf al te ontdekken is in de eerste stadia van de ziekte, dat wil zeggen vóór de volledige ontwikkelde vorm van LOAD. STOX1A is dus aangetoond betrokken te zijn in het ziekteproces van LOAD. Hierdoor is het in de toekomst potentieel mogelijk om STOX1A als therapeutisch doelwit te gebruiken voor therapeutische interventie in LOAD. Het gebruik van STOX1A als aangrijppunt voor therapeutische interventie zal vanwege zijn brede actieradius op zijn vele doelwitgenen lastig zijn. Dergelijke drugs zouden bijvoorbeeld op grote schaal belangrijke neuronale signaalroutes, waar STOX1A een normale functie in zou kunnen hebben, blokkeren. Andere mogelijkheden behoren tot mechanismen die op een hoger niveau (upstream) in de signaalroutes van STOX1A liggen. Deze kunnen potentieel door drugs gemoduleerd worden en daarmee op een regulerende manier de activiteit en/of expressie van STOX1A beïnvloeden. Dit zou dan een indirect gevolg hebben op expressie van zijn doelwitgenen. Een andere optie zou zijn om STOX1A doelwitgenen zelf (downstream) als drug target te gebruiken. Naast potentiële therapeutische interventie kunnen STOX1A doelwitgenen ook dienen als potentiële biomarkers voor diagnose in LOAD mits ze aantoonbaar zijn in het ruggenmerg vocht en / of in bloed.

Het is daarom van essentieel belang om deze up- en downstream mechanismen te identificeren maar ook hun fundamentele werking in neuronale signaalroutes te

verkennen. Dit proefschrift had het primaire doel om dergelijke mechanismen te identificeren en uit te zoeken hoe STOX1A werkt in neuronale signaalroutes. Deze kennis is van groot belang om zo inzicht te geven in de manier waarop STOX1A werkt in de normale hersenen, maar geeft ook informatie over waarom de functie van STOX1A verstoord is in neurodegeneratieve ziekten zoals LOAD.

In aanvulling op de eerder ontdekte STOX1A doelwitgenen *LRRTM3* en Alpha-T-catenine (*CTNNA3*), beschrijft de eerste studie (**hoofdstuk 2**) de ontdekking van een reeks nieuwe STOX1A doelwitgenen. Hierbij is Contactin Associated Protein Like 2 (*CNTNAP2*) bevestigd als een nieuw STOX1A doelwitgen. *CNTNAP2* is een gen dat een eiwit tot expressie brengt dat mogelijk een rol speelt bij de lokalisatie van kaliumkanalen binnen differentiërende axonen. Axonen zijn uitlopers van zenuwcellen en belangrijk voor de overdracht van elektrische impulsen. Deze studie bewijst dat STOX1A in de neuronale cellijn SK-N-SH, direct bindt aan een DNA fragment dat de expressie van het CNTNAP2 eiwit negatief beïnvloedt.

Interessant is dat de CNTNAP2 expressie niveaus zijn verminderd in de hippocampus van LOAD patiënten waar STOX1A expressie verhoogd is. Dit suggereert dat de expressie van STOX1A en CNTNAP2 omgekeerd geassocieerd zijn in de hippocampus van LOAD patiënten. Studies hebben aangetoond dat CNTNAP2 geassocieerd is met stoornissen in het autisme spectrum (ASD), maar zover bekend nog nooit met LOAD. Deze studie laat daarom voor de eerste keer zien dat CNTNAP2 ook geassocieerd is met een andere stoornis in de hersenen, de ziekte van Alzheimer.

In **hoofdstuk 3** is de zoektocht naar STOX1A doelwitgenen uitgebreid door met behulp van de techniek ChIP-seq op grote schaal (verspreid over het gehele genoom) DNA-fragmenten te identificeren die potentieel aan STOX1A gebonden zijn.

Door het toepassen van deze techniek zijn meerdere potentiële STOX1A doelwitgenen ontdekt. Een van deze doelwitgenen is in onze studie bevestigd en in detail onderzocht. Onze resultaten laten daarbij zien dat het desbetreffende doelwitgen, serine / arginine-rich splicing factor 7 (*SFRS7*), positief wordt gereguleerd door STOX1A. Verder laten de resultaten zien dat dit effect alleen plaatsvindt in een bepaald type cel. Het effect van STOX1A op *SFRS7* bleek daarbij dus celtype specifiek te zijn.

Studies hebben aangetoond dat *SFRS7* in staat is om de vorming van het zogenaamde tau eiwit te beïnvloeden door middel van een proces dat splicing heet. Eenvoudig gezegd kunnen door middel van splicing uit hetzelfde tau gen verschillende vormen van het tau eiwit geproduceerd worden die ook verschillen in eigenschappen. De eerder genoemde NFT vormen, kenmerkend voor de ziekte van Alzheimer (maar ook andere vormen van dementie) bestaan voornamelijk uit abnormaal gefosforyleerd tau eiwit (zie ook later in de tekst). Veranderingen in tau splicing spelen hierbij mogelijk een belangrijke rol. Bepaalde vormen van het tau eiwit kunnen door abnormale splicing in grotere hoeveelheid aanwezig zijn dan normaal en daardoor vatbaar worden voor fosforylatie. Dit zal als gevolg hebben dat er NFT gevormd kunnen worden. Onze bevindingen laten dus zien dat STOX1A door middel van het reguleren van *SFRS7*, met daarbij een indirect effect op tau splicing, een belangrijke functie heeft bij de vorming van NFT.

Naast het systematisch zoeken naar STOX1A doelwitgenen hebben we ook onderzocht of STOX1A betrokken is bij een eerder gesuggereerde functionele rol.



Het ging hierbij om een mogelijke functie voor STOX1A in het regelen van celdeling. Deze suggestie is bevestigd in **Hoofdstuk 4**. De studie in **hoofdstuk 4** beschrijft de directe en positieve regulatie van STOX1A op een gen betrokken bij celdeling. Dit gen, Cyclin B1 (*CCNB1*) is een regulator van de zogenaamde G2 / Mitose fase-overgang belangrijk voor een normale celcyclus. De mogelijke relatie tussen STOX1A, *CCNB1* en de G2 / Mitose fase-overgang zijn daarom in detail onderzocht. Zoals verondersteld zorgt STOX1A, door middel van positieve regulatie van het *CCNB1* gen, voor een versnelde overgang van de G2 naar de Mitose fase. Resultaten laten bovendien ook zien dat STOX1A betrokken is bij de regulatie van andere doelwitgenen die belangrijk zijn voor een juiste celdeling. Deze resultaten geven daarom voor het eerst aan dat STOX1A een belangrijke functie heeft in de regulatie van de celcyclus (celdeling).

In de afgelopen jaren wordt het steeds duidelijker dat celcyclus gerelateerde processen een belangrijke rol spelen in de vroege ontwikkeling van LOAD. Zoals hierboven al beschreven is abnormaal gefosforyleerd tau eiwit het belangrijkste bestandsdeel van NFT. Dit wil zeggen dat er bepaalde chemische groepen in een buitengewoon grote hoeveelheid op het tau eiwit zijn “vastgemaakt”. Onder normale omstandigheden heeft tau een belangrijke rol in de stabilisatie en flexibiliteit van het “skelet” van zenuwcellen. De netwerken bestaande uit dit “skelet” hebben daarnaast onder andere de functie om voedingsstoffen te vervoeren naar plaatsen waar dat in de zenuwcel nodig is. Abnormaal gefosforyleerd tau eiwit belemmert deze normale functies en kan bovendien de vorming van NFT bewerkstelligen. Uiteindelijk zal dit de dood van de zenuwcel tot gevolg hebben. Verschillende studies suggereren dat een afwijkende neuronale celcyclus in LOAD een onderliggend mechanisme is dat bijdraagt aan de abnormale fosforylatie van het tau eiwit en daarbij gezien wordt als een belangrijke oorzaak voor de vorming van NFT in LOAD. Omdat STOX1A betrokken is bij de regulatie van de celcyclus (**hoofdstuk 4**), speculeerden wij dat er misschien een relatie bestaat tussen STOX1A, de celcyclus en tau fosforylatie. Dit is onderzocht in **hoofdstuk 5**. In **hoofdstuk 5** laten we zien dat STOX1A expressie geassocieerd is met de abnormale fosforylatie van tau-eiwitten op plekken zoals die ook gevonden worden in NFT in LOAD. Bovendien suggereren onze resultaten dat dit komt door een toename in de activiteit van het cyclin dependent kinase 1 (CDK1), een ander belangrijk eiwit dat betrokken is bij de G2 / Mitose fase-overgang tijdens de celcyclus (zie hierboven). Onze resultaten laten zien dat CDK1 activiteit hoger is in cellen die gestimuleerd worden door STOX1A eiwit. Recente studies hebben eerder al bevestigd dat CDK1 in staat is tau te fosforyleren. Bovendien is CDK1 in verhoogde hoeveelheid aangetoond in de hersenen van LOAD patiënten. Samen suggereren de resultaten uit **hoofdstuk 4** en **5** daarom dat er een relatie bestaat tussen STOX1A, regulatie van de celcyclus en vorming van NFT in LOAD. STOX1A is dus, zoals we eerder hebben aangetoond, niet alleen betrokken bij de vorming van het A β eiwit, maar ook betrokken bij de vorming van NFT.

In ons laatste hoofdstuk (**hoofdstuk 6**) zijn we een verdere zoektocht gestart om meer duidelijkheid te krijgen over een algemene functionele rol voor STOX1A expressie in zenuwcellen. Hierbij hebben we een relatief nieuwe techniek (RNA-seq) gebruikt die het mogelijk maakt om de totale verzameling van alle zogenoemde messenger

RNA-moleculen (en hun hoeveelheid), die op dat moment onder een bepaalde experimentele conditie in een cel aanwezig zijn, te visualiseren en te meten. Messenger RNA-moleculen zijn in staat een gen te vertalen naar een eiwit. Met andere woorden, de totale verzameling van deze messenger RNA-moleculen weerspiegelt het aantal en de hoeveelheid eiwitten die op dat moment aanwezig zijn in de cel onder een bepaalde experimentele conditie. Deze verzameling (clustering) van messenger RNA-moleculen kan een bepaald patroon weergeven dat gerelateerd kan zijn aan een specifieke biologische functie. Door stimulatie van STOX1A in neuronale cellen en het toepassen van de bovenstaande techniek, laten voorlopige resultaten nieuwe inzichten voor een mogelijke rol voor STOX1A in de ontwikkeling van zenuwcellen zien.

Conclusie

Samenvattend laten de resultaten beschreven in dit proefschrift belangrijke nieuwe inzichten zien in de neuronale signaalroutes die STOX1A reguleert. Hierbij hebben we ook laten zien dat STOX1A niet alleen betrokken is bij de vorming van het A β eiwit, maar ook potentieel betrokken is bij de vorming van NFT. Beide zijn belangrijke pathologische kenmerken die zich uiten in LOAD. Doordat STOX1A expressie al aangetoond kan worden in mensen waar nog geen dementie is geconstateerd maakt dit het in de toekomst wellicht mogelijk om therapeutisch in te grijpen in STOX1A geassocieerde signaalroutes die beschreven zijn in dit proefschrift.

Concluderend, het is zeer belangrijk om de werking van STOX1A in neuronale signaalroutes te verhelderen vanwege de rol van STOX1A in neurologische ziektebeelden.

List of Publications

Daan van Abel, Omar Michel, Rob Veerhuis, Marlies Jacobs, Marie van Dijk, Cees BM Oudejans. Direct downregulation of CNTNAP2 by STOX1A is associated with Alzheimer's disease.

(Journal of Alzheimer's disease, 2012, Accepted for Publication)

Daan van Abel, Omar Abdul-Hamid, Marie van Dijk, Cees BM Oudejans. Transcription factor STOX1A promotes mitotic entry by binding to the CCNB1 promotor.

(PLoS ONE, 2012, Volume 7, Issue 1, Page e29769)

Daan van Abel, Dennis R. Hölzel, Shushant Jain, Fiona M.F. Lun, Yama W.L. Zheng, Eric Z Chen, Hao Sun, Rossa W.K. Chiu, Y.M. Dennis Lo, Marie van Dijk, Cees BM Oudejans. SFRS7 mediated splicing of tau exon 10 is directly regulated by STOX1A in glial cells.

(PLoS ONE, 2011, Volume 6, Issue 7, Page e21994)

Marie van Dijk, Jan van Bezu, **Daan van Abel**, Caroline Dunk, Marinus A Blankenstein, Cees BM Oudejans, Stephen J Lye. The STOX1 genotype associated with pre-eclampsia leads to a reduction of trophoblast invasion by alpha-T-catenin upregulation.

(Hum Mol Genet, 2010, Volume 19, Issue 13, Page 2658-2667)

Conference/abstract

Daan van Abel, Marie van Dijk, Dennis YM Lo, Rossa WK Chiu, Fiona M Lun, Marinus A Blankenstein, Cees BM Oudejans. A genome-wide search for STOX1 target genes, a transcription factor associated with Alzheimer's disease.

(International Conference on Alzheimer's Disease, ICAD 2010. Honolulu, Hawaii, USA. Alzheimer's and Dementia, 2010, Volume 6, Issue 4, Supplement Page S189)

Submitted

Daan van Abel, Omar Michel, Wiep Scheper, Marie van Dijk, Cees BM Oudejans. STOX1A induces phosphorylation of tau proteins at epitopes found in neurofibrillary tangles of Alzheimer's disease.

Daan van Abel, Hari K Thulluru, Omar Michel, Marie van Dijk, Cees BM Oudejans. RNA-seq transcriptome analysis of STOX1A induced differential expression in neuronal cells.

Zhongchun Zhang, Jun Zhao, **Daan van Abel**, Holger Rehmann, Johannes L Bos. Active mutant of Radixin binds Epac1.

Curriculum vitae

Daan van Abel was born on September 9th 1980 in Nijmegen, The Netherlands. After completing his MAVO degree at the Canisius College, he continued high school at the NGS Groenewoud in Nijmegen where he completed his HAVO degree. After graduation in 2000 he started a bachelor in applied sciences at the Hogeschool van Utrecht. His bachelor internship was carried out in the laboratory of Maarten van Lohuizen at the Division of Molecular Genetics, the Netherlands Cancer Institute in 2004. Here he investigated the role of the Histone2A variant macro-Histone2A. In 2005 he successfully completed his bachelor in applied sciences and started a master in biomolecular Sciences at the Vu in Amsterdam. During this master he carried out his first internship in the laboratory of JL Bos at the department Molecular Cancer Research, University Medical Centre (UMC) in 2006. Here he studied the functional properties of radixin, a member of the ERM (ezrin/radixin/moesin) protein family. His second master internship was carried out in the laboratory of JP Medema, department “Laboratory for Experimental Oncology and Radiobiology” (LEXOR) at the Amsterdam Medical Centre (AMC) in 2007. Here he studied the enhanced activation of Gemcitabine by Cyclopentenyl cytosine (CPEC) for the improvement of pancreas carcinoma treatment. After graduation he started in 2008 as a PhD-candidate at the department of Clinical Chemistry, Molecular Biology Laboratory (MBL), VU University Medical Centre (VUmc) in Amsterdam. His four years as a PhD-candidate resulted in this thesis.



Dankwoord

Op het moment dat ik begin met het schrijven van het dankwoord realiseer ik mij pas echt dat mijn proefschrift klaar is en dat mijn vier jaren als PhD-student voorbij zijn. Als PhD-student heb ik met veel tevredenheid mijn ideeën in alle mogelijke vrijheid kunnen uitdenken en uitvoeren. Dit met dank in het bijzonder aan mijn promotor **prof.dr. CBM Oudejans**. Beste Cees! bedankt voor de kans, prettige samenwerking en vrijheid die je mij hebt gegeven om tot deze mijlpaal in mijn leven te zijn gekomen! Bij het schrijven van mijn eerste artikel ging alles nog niet optimaal en legde ik uiteindelijk wel wekelijks een nieuwe versie bij jou en Marie op het bureau. Gelukkig, mede door de vele verbeteringen en jullie kritische blik, heeft dit artikel een mooi eindresultaat opgeleverd. Na het eerste artikel ging het schrijven meteen al een stuk makkelijker.

Een hoogtepunt in onze samenwerking vond ik toch wel het analyseren van de “next generation sequencing data”. Het analyseren bleek uiteindelijk niet zo rap te gaan als verwacht (en nee, zelfs niet op een Apple computer). Gelukkig zijn de vele honderden gigabytes aan data met rokende computers dan toch nog geanalyseerd. Cees! heel erg bedankt voor alle hulp!

Dan wil ik ook mijn copromotor **dr. M. van Dijk**, die het STOX1 gen voor het eerst beschreven heeft in haar PhD-thesis, heel erg bedanken. Beste Marie! naast Cees ben jij gedurende mijn PhD-project eveneens erg belangrijk geweest voor het resultaat dat nu voor ons ligt. Je was altijd bereid om een zoveelste conceptartikel van mij binnen korte tijd kritisch te bekijken en hierop goede feedback te geven. Ook kon ik voor een veelheid aan vragen altijd bij jou terecht. Bedankt voor de prettige samenwerking en al je hulp!

Naast mijn promotor en copromotor wil ik het afdelingshoofd **prof.dr. M.A. Blankenstein** bedanken. Beste Rien, bedankt voor de mogelijkheid dat ik bij jou op de afdeling mijn onderzoek heb mogen uitvoeren! Ik voel mij vereerd dat jij deel uitmaakt van de leescommissie. Bedankt! Ook de andere leden van de leescommissie, **prof.dr. A.J. Rozemuller, dr. W. Scheper, prof.dr. J.C van Swieten, dr. N. Ameziane en dr. R.M.F. Wolthuis**, wil ik hartelijk bedanken voor de interesse, het grondig doorlezen en beoordelen van mijn proefschrift!

Verder wil ik natuurlijk ook mijn directe collega's van het MBL bedanken. **Omar**, speciale dank aan jou voor je directe betrokkenheid bij het STOX1 project. Jij was vooral in het afgelopen jaar mijn redder in nood. Je praktische hulp heeft mij de tijd gegeven om meer te kunnen focussen op het schrijven en afronden van mijn proefschrift. Ik voel me vereerd om jou als paranimf bij de promotie naast mij te hebben staan. Bedankt!

Allerdien, voor technische maar ook inhoudelijke vragen kon ik altijd bij jou terecht. Vooral in het eerste jaar, toen Marie nog in Canada zat, was jij degene die mij wegwijst heeft gemaakt in het laboratorium. Bedankt!

Naast Marie, Omar en Allerdien wil ik natuurlijk ook **Joyce, Ankie, Hari, Argonde** en **Janny** bedanken, niet alleen voor de gezelligheid op het lab, maar ook voor de vele gezamenlijke labuitjes en etentjes! Ik zal ze missen.

Verder wil ik ook de studenten die bij ons in het MBL stage hebben gelopen voor hun hulp bedanken: **Cjala, Ebru, Hulya, Aslihan en Milou**. Ik wens jullie succes met jullie toekomstige carrière!

Ik wil ook mijn (ex)collega AIO's bedanken voor hun gezelligheid. **Martijn**, niet alleen in de gangen bij het metabool lab, maar ook in de trein van en naar Amsterdam-Zuid kwamen wij elkaar regelmatig tegen. Nu kan ik mijn gratitude uiten en jou hier bedanken voor alle gezellige momenten die wij hadden tijdens al weer een van de vele vertraagde intercity's. Bedankt en veel succes met je verdere carrière bij DSM! **Ofir**, ik zal de ontspannende gesprekken over droge humor en films zoals "Old school", "Wedding Crashers" en "the Hangover" missen. Bedankt!

Mariska, ook jij bedankt voor de gezelligheid in de AIO-kamer! Bij jou ligt de promotie ook voor de deur. Ik wens je daarbij veel succes en sterkte toe. **Leonard**, ook jij was een aantal jaren een kamergenoot van mij, en hierbij wil ik ook jou bedanken voor al de gezellige momenten die we hebben gehad. **Joe**, your promotion is also approaching; I wish you good luck with "de laatste loodjes", and thank you for your pleasant company in the AIO kamer. **Monica**, I also had the honor to have you as a pleasant neighbour during my last year in the AIO kamer. Good luck finishing your thesis and Não to preocupes. **Sandra Mulder**, ook jou wil ik bedanken voor alle gezellige momenten op de afdeling maar ook in de trein van en naar Amsterdam-Zuid. Veel succes met je toekomstige postdoc carrière. **Hari**, good luck with your future research and hopefully many publications will follow!

Verder wil ik iedereen van het secretariaat bedanken. **Janny en Magda**, bedankt voor het verwerken van al mijn lastige bestellingen. Het is jullie ondanks mijn slechte handschrift toch telkens gelukt om mijn orderbriefjes te ontcijferen.

Voor de goede werksfeer op de afdeling klinische chemie wil ik ook de mensen van de andere laboratoria bedanken. Vooral de mensen van het metabool laboratorium en het neurologisch laboratorium. **Rob veerhuis en Marlies Jacobs**, bedankt voor jullie vriendelijke hulp en bijdrage aan mijn recente artikel!

Bij promoveren horen helaas ook momenten van stress en frustraties. Gelukkig heb ik deze problemen door vele ontspannende momenten met mijn vrienden en vriendinnen telkens even opzij kunnen zetten.

Beste vrienden en vriendinnen, ik ben erg dankbaar voor jullie luisterend oor. Ik weet dat ik vooral de laatste periode van mijn promotie vaak bij jullie aan kwam met vragen als: ja... maar dan?, en... wat als?, of... maar dat lukt toch nooit.....! Het kwam op die momenten misschien niet zo over, maar jullie adviezen hebben mij erg veel steun geboden (Natuurlijk hadden jullie het weer bij het rechte eind en viel alles achteraf eigenlijk wel weer mee). Bedankt voor jullie fijne en langdurige vriendschap!

Pa en ma! Josje en Joseeke! ik had nooit kunnen bedenken dat toen ik op de basisschool een LBO/MAVO advies kreeg, ik uiteindelijk een PhD-studie zou gaan afronden. Jullie niet aflatend vertrouwen in mijn capaciteiten en jullie motiverende invloed om

door te zetten zijn daarbij erg belangrijk geweest. Zonder jullie als drijvende kracht had ik nooit kunnen bereiken wat ik nu heb gepresteerd. Ik wil hier van de gelegenheid gebruikmaken om met trots tegenover iedereen te uiten dat ik zulke fijne ouders heb. Pa!, ma!, ik kan mij geen betere ouders wensen dan jullie!

Bas, wat ben ik er trots op dat jij mijn broer bent en wat ben ik blij om oom van drie geweldige kinderen, apenkop **Bo**, kale harry **Mila**, en prinsesje **Senne** te zijn. Heel erg bedankt voor het mooie ontwerp van de kaft van mijn proefschrift en wat fijn dat ik jou als paranimf naast mij heb staan bij de promotie. Natuurlijk bedank ik ook mijn geweldige schoonzus **Maike** voor haar support!

Walter van de Laar (Victor Vroomkoning), ik wil jou als dichter, goede kennis, vriend van mijn ouders én vader van een van mijn beste vrienden, bedanken voor het prachtige gedicht dat mijn proefschrift tot een uniek boekje maakt.

En mocht ik onbewust iemand zijn vergeten te bedanken, sorry, en hierbij alsnog bedankt!

